

Factors regulating metamorphosis in  
hemimetabolan insects

Orathai Kamsoi

---

TESI DOCTORAL UPF / 2020

THESIS DIRECTOR

Dr. Xavier Bellés Ros

INSTITUT DE BIOLOGIA EVOLUTIVA  
(CSIC - UNIVERSITAT POMPEU FABRA)





I have no special talent. I am only passionately curious.

**Albert Einstein**



## Acknowledgements

I would like to express my appreciation to my supervisor, Prof. Dr. Xavier Bellés for his supervision, encouragement, guidance and inspiration throughout my Ph.D. study. Also, I would like to express my appreciation to Prof. Dr. Sho Sakurai, who has been a constant source of motivation and inspiration. Thank you both of you for being so creative and passionate about the research, these really encouraged me to continue the research in this field.

I would like to express my grateful to Dr. Dolors Piulachs and Dr. José Luis Maestro, for their advice, comments and encouragement. Also, I am very grateful to the examining committees, for their valuable comments and suggestions to my thesis.

I would like to acknowledge the Royal Thai Government Scholarship and Chiang Mai Rajabhat University for the financial supports.

I would like to thank all present and former members of the Institute of Evolutionary Biology (IBE-CSIC) for enhancing my time as a graduate student and specially the administrative staffs for their support and for helping me.

Thanks to all colleagues and friends from the laboratory P129 (former P64) especially Alba, Ana, and Guillem from whom I learned a lot. Also I would like to thank Cristina Olivella for her hard work in maintaining the cockroach colony and giving me the cockroach samples always at right time.

Many thanks to my Thai friends both in Thailand and in Barcelona, and all of my colleagues in Faculty of Science and Technology, Chiang Mai Rajabhat University for their support and for

being awesome. Thanks for those who inspired me and encouraged me during my study.

I dedicate this work to Dr. Tippawan Singtripop, who guided me to study insect physiology and showed me how to engage with research. Also, I thank her for inspiring me to be a good instructor.

Finally, I would like to express my deepest appreciation to my family for their love and support. Thank you for always having my back.

Orathai Kamsoi

June 2020

Barcelona

## Abstract

In this thesis, we studied different aspects of insect metamorphosis regulation, using the cockroach *Blattella germanica* and the mayfly *Cloeon dipterum*, as models. In *B. germanica*, we found that myoglianin reduces juvenile hormone acid methyl transferase expression in the penultimate nymphal instar, which is a prerequisite for metamorphosis. Myoglianin is also involved in the production of the large ecdysone pulse needed to promote the metamorphic molt. Previous studies have shown that the factor FTZ-F1 induces the death of the prothoracic gland (PG) after the imaginal molt. But we have found that the action of FTZ-F1 is mediated by the adult specifier factor E93. In *C. dipterum*, we observed that metamorphosis occurs in the transition from last nymphal instar to subimago. In this transition, the expression of the antimetamorphic factor Kr-h1 decreases, and that of E93 increases. We also observed that juvenile hormone inhibits metamorphosis and induces the expression of Kr-h1.





## Resum

En aquesta tesi, hem estudiat diferents aspectes de la regulació de la metamorfosi d'insectes, utilitzant com a models la panerola *Blattella germanica* i l'efimera *Cloeon dipterum*. A *B. germanica*, la mioglianina redueix l'expressió de la metil transferasa de la hormona juvenil en el penúltim estadi nimfal, la qual cosa és un requisit per a la metamorfosi. La mioglianina també està implicada en la producció de l'ecdisona necessària per a la muda metamòrfica. Hom sabia que el factor FTZ-F1 induïx la mort de la glàndula protoràcica (PG) després de la muda imaginal. Nosaltres hem trobat que l'acció de FTZ-F1 està mediada pel factor especificador de l'adult E93. A *C. dipterum*, hem observat que la metamorfosi es produeix en la transició de l'últim estadi nimfal a subimago. En ella, l'expressió del factor antimetamòrfic Kr-h1 disminueix i la d'E93 augmenta. També hem vist que l'hormona juvenil inhibeix la metamorfosi i induïx l'expressió de Kr-h1.



## บทคัดย่อ

วิทยานิพนธ์นี้ศึกษาการควบคุมการเปลี่ยนรูปหรือเมตามอร์ฟอซิสของแมลง โดยใช้แมลงสาบ *Blattella germanica* และแมลงชีปะขาว *Cloeon dipterum* เป็นสัตว์ทดลอง ในแมลงสาบพบว่า ไมโอเกลียโนลินลดการแสดงออกของยีนจูวีเนลฮอร์โมนแอกติเมธิลทรานเฟอร์เรสในตัวอ่อนระยะก่อนสุดท้าย ซึ่งจำเป็นสำหรับการเข้าสู่ระยะเต็มวัย โดยไมโอเกลียโนลินยังมีส่วนเกี่ยวข้องในการหลั่งฮอร์โมนเอกไดโชนจำนวนมากสำหรับเมตามอร์ฟอซิส การศึกษาก่อนหน้าพบว่า FTZ-F1 ทำให้เกิดการตายของต่อมโปรทอแรกซิกหลังจากเป็นตัวเต็มวัย แต่ในวิจัยนี้พบว่า E93 เป็นตัวกลางที่ทำให้เกิดการตายของต่อม ในแมลงชีปะขาวพบว่าเมตามอร์ฟอซิสเกิดขึ้นในระหว่างการเปลี่ยนจากตัวอ่อนระยะสุดท้ายเป็นตัวเต็มวัยระยะแรกหรือ subimago โดยเกิดขึ้นหลังจากการแสดงออกของยีน Kr-h1 ลดลง ซึ่งทำให้ E93 เพิ่มขึ้น และยังพบว่าฮอร์โมนจูวีเนลยับยั้งการเปลี่ยนรูป โดยชักนำการแสดงออกของยีน Kr-h1



## Preface

The great diversity of insects is largely the result of the evolutionary innovation of wings and metamorphosis which made them the largest group of animals known today. Therefore, it is not surprising that insect metamorphosis has attracted the interest of entomologists for a long time. Among them, Xavier Belles and his group have been working on insect metamorphosis since the late 1970's, first at the Institute of BioOrganic Chemistry (CSIC, Barcelona), and lately at the Institute of Evolutionary Biology (CSIC-Universitat Pompeu Fabra, Barcelona). Belles's group mainly focused on the action of juvenile hormone and its molecular signaling pathway, framing the results in an evolutionary perspective. Important in their research has been the German cockroach *Blattella germanica* (Polyneoptera), which has been used as the main model insect in Belles' laboratory, as this cockroach follows the ancestral type of hemimetabolan metamorphosis, and thus can serve as a baseline model for evolutionary studies. Moreover, *B. germanica* is highly sensitive to gene transcript depletion by RNA interference (RNAi), which makes this species especially suitable for gene function studies.

The present thesis deals with the mechanisms regulating metamorphosis, particularly in hemimetabolan insects, by using the *B. germanica* as a first model species. We have examined possible candidates to regulate different aspects of metamorphosis, chosen in some cases on the basis of transcriptomic data of *B. germanica* available in our laboratory. Then, we have functionally tested them with RNAi. Moreover, we have also studied the mayfly *Cloeon dipterum*, a species belonging to Palaeoptera, an early-branching insect

group of which very little is known about metamorphosis and its regulatory mechanisms. In this case, we have examined the expression of key genes that are involved in metamorphosis in neopteran insects, and we have approached the functional studies through treatments with a juvenile hormone mimic.

## Table of contents

	Pag.
Acknowledgements.....	v
Abstract.....	vii
Resum.....	ix
บทคัดย่อ.....	xi
Preface.....	xiii
1. GENERAL INTRODUCTION.....	1
1.1. The origin and evolution of insect metamorphosis.....	1
1.2. Types of insect metamorphosis.....	3
1.3. Hormonal regulation of insect metamorphosis.....	5
1.4. The molecular mechanisms underlying the hormonal action: The MEKRE93 pathway.....	6
1.5. <i>Blattella germanica</i> as a model insect.....	12
1.6. <i>Cloeon dipterum</i> (Ephemeroptera) as a new model to study insect metamorphosis.....	14
2. OBJECTIVES.....	17
2.1. The hypotheses of the present thesis.....	17
2.2. The objectives.....	20
3. RESULTS.....	21
3.1. Myoglianin triggers the pre-metamorphosis stage in hemimetabolan insects.....	21
3.2. E93-depleted adult insects preserve the prothoracic gland and molt again.....	35

3.3. Regulation of metamorphosis in mayflies (Insecta, Ephemeroptera).....	75
4. GENERAL DISCUSSION.....	111
4.1. Myoglianin and the reduction of JH titers in the last nymphal instar.....	112
4.2. E93 and the destruction of the PG after the imaginal molt in <i>Blattella germanica</i> .....	114
4.3. The regulatory mechanism of metamorphosis in the mayfly <i>Cloeon dipetrum</i> .....	115
5. CONCLUSIONS.....	119
6. REFERENCES.....	123



# 1. GENERAL INTRODUCTION

Insects are the largest and most diverse group of animals presently known. The great diversity of insects originates from the evolutionary innovations of wings and metamorphosis. The present thesis deals with the mechanisms regulating metamorphosis, particularly in hemimetabolan insects, by using the Blattaria *Blattella germanica* (Polyneoptera) as a main model insect. Moreover, we have also investigated the Ephemeroptera *Cloeon dipterum*, which belong to an early branching insect group (Palaeoptera), about which little is known in relation to metamorphosis and its regulatory mechanisms.

## 1.1. The origin and evolution of insect metamorphosis

The fossil evidence suggests that the first wingless and direct developing true insects (Archaeognatha and Zygentoma) emerged on Earth some 475 million years ago (Mya), during the late Ordovician period (Fig. 1.1). Then, in the Devonian, some 400 Mya, originated the wings and metamorphosis, and shortly after, the Pterygota (winged insects) split into Palaeoptera and Neoptera (Fig. 1.1). Later, the Neoptera diverged to Polyneoptera and Eumetabola, and, finally, the Eumetabola split again into Paraneoptera and Endopterygota, some 370 Mya (Fig. 1.1) (Misof et al., 2014; Wang et al., 2016). In terms of postembryonic development, the direct developing insects (ametabolans) evolved to simple metamorphosis (hemimetaboly), which in turn gave rise to holometaboly (Belles, 2020).

The great radiation of insects took place after the emergence of wings and metamorphosis in the Lower Carboniferous, some 360-350 Mya. Since then, insects have adapted to live in almost every non-marine habitat and to feed on a great variety of resources. Therefore, metamorphosis probably was the key innovation that allowed insects to become the most diverse group of animals on Earth (Belles, 2020).

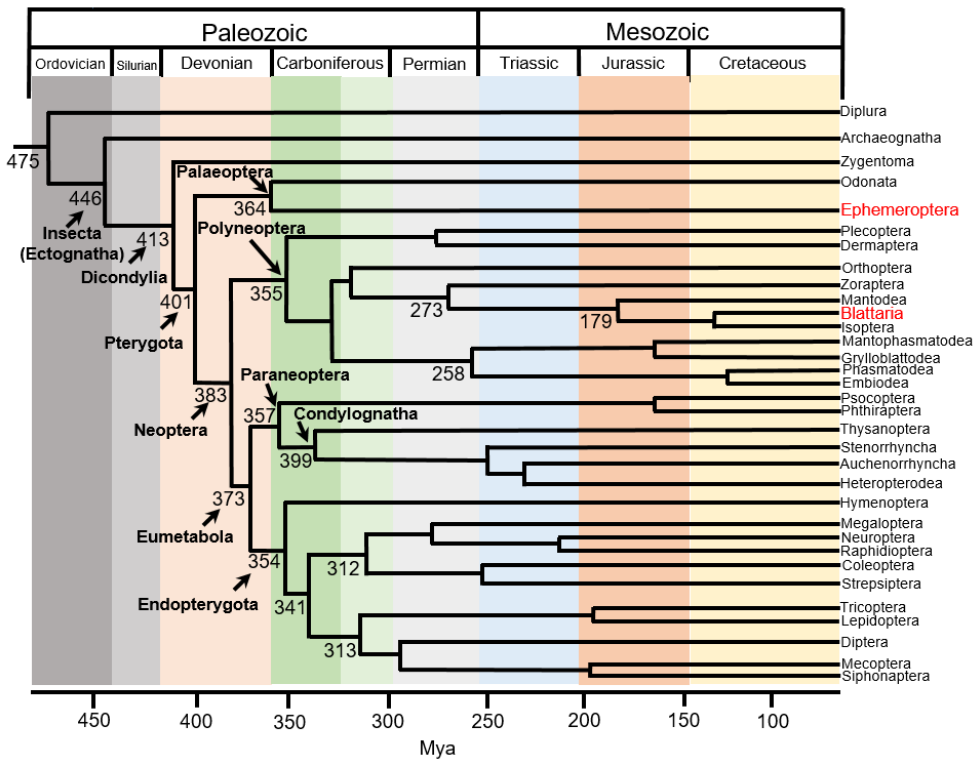


**Figure 1.1. Cladogenesis of the main insect groups**, as proposed by Misof et al. (2014) and Wang et al. (2016). Divergence times are generally similar in both proposals. Those indicated here are based on the average values reported by Wang et al. (2016). The Ephemeroptera and Blattaria branches, which contain *Cloeon dipterum* and *Blattella germanica*, the two species used in this thesis as models, are highlighted in red. Modified from Belles (2020).

## 1.2. Types of insect metamorphosis

Postembryonic development of insects can be classified into three types: ametabolan (practically no changes during development), hemimetabolan (gradual changes and metamorphosis), and holometabolan (dramatic changes and metamorphosis) (Belles, 2020).

1.2.1. The ametabolan type is characteristic of wingless insects (apterygotes) of the orders Archaeognatha (like bristletails) and Zygentoma (like silverfish). There are three main stages of ametabolan development: embryo, nymph, and adult. After hatching, the nymphs, which resemble miniature adults, gradually increase in size through molting, but do not significantly change in form until reaching the reproductive adult stage (Fig. 1.2A), in which they continue molting.

1.2.2. The hemimetabolan type also has three characteristic stages, with the difference with respect to the ametabolans that the nymphs have external wing pads. The nymphs subsequently molt for growing until attaining a threshold size to metamorphose in the last nymphal instar. Then, significant changes occur during metamorphosis to the adult stage, such as fully development of wings and functional genitalia (Fig. 1.2B). After that, the prothoracic gland (PG, which produces the molting hormone) undergoes programmed cell death, which starts just after the adult molt. The degeneration of PG prevents any other further molt in the adult stage. Ephemeropterans, however, are an exception in this sense, as in this group the last nymphal instar molt to a subimaginal instar, with functional wings, which molts one more time to the imago or mature adult instar. The final molt is an important innovation of the

pterygotes, additional to the functional wings. Hemimetabolous metamorphosis is found in the Palaeoptera, Polyneoptera and Paraneoptera, within the exopterygotes (wings developing outside the body).

1.2.3. The holometabolous type has the stages of embryo, larva, pupa and adult. The larva of holometabolous insects is different from the adult, so development requires a pupal stage (normally a non-feeding and immobile stage) as a kind of bridge for the transition from larva to adult (Fig. 1.2C). The holometabolous metamorphosis is characteristic of the Endopterygota, which contains the four more biodiverse insect orders: Hymenoptera, Coleoptera, Lepidoptera, and Diptera.

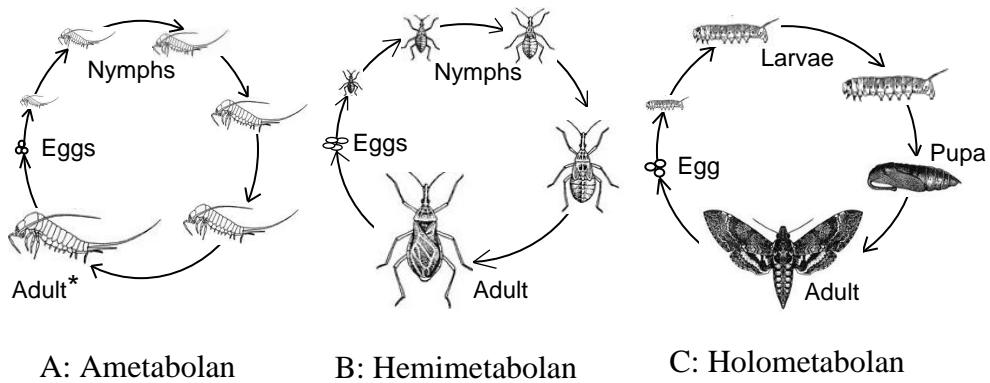


**Figure 1.2. Different types of insect development and metamorphosis.**

(A) Ametabolous, exemplified by bristletails. (B) Hemimetabolous, exemplified by locusts. (C) Holometabolous, exemplified by moths. The asterisk in the ametabolous adult indicates that it continues molting. Modified from Willis J.H. and Willis J.S. (2008).

### 1.3. Hormonal regulation of insect metamorphosis

Research on insect hormones started in 1917, when Kopec demonstrated that the last instar larva of the moth *Lymantria dispar* could not pupate when the brain had been removed. Kopec concluded that there was a brain humoral factor that promoted metamorphosis, a factor that was later identified as the prothoracicotropic hormone (PTTH). In 1934, while investigating molting and metamorphosis in the bug *Rhodnius prolixus*, Wigglesworth discovered that molting occurs after a blood meal, and that molting was inhibited by decapitation. This finding was similar to that of Kopec, but Wigglesworth, using parabiosis experiments, found another factor in the hemolymph of the young insects which inhibited metamorphosis, which was called juvenile hormone (JH). Subsequently, the existence of these and other humoral factors were confirmed in other insects, and between 1940 and 1944, Fukuda demonstrated in the silk moth *Bombyx mori* that molting was promoted by a molting hormone released from the prothoracic gland (PG).

Regarding JH, it was shown in different species that it was released by retrocerebral glands called corpora allata, and had an inhibitory effect on metamorphosis (Karlson, 1996). These initial discoveries led to a general scheme of the hormonal regulation of insect metamorphosis. In brief, molting is induced periodically by molting hormone (ecdysone/20-hydroxyecdysone, 20E), whereas JH inhibits metamorphosis in preadult stages. However, in the last juvenile stage, a pulse of molting hormone in the absence of JH would trigger metamorphosis. In hemimetabolan insects, the last instar nymph metamorphoses directly to the adult stage, whereas in holometabolan

insects the larva metamorphoses first into pupa and then into adult (Fig. 1.3) (Belles, 2020).

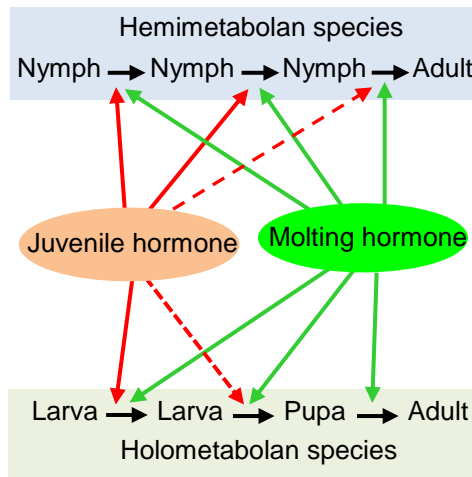


**Figure 1.3. General scheme on endocrine control of development and metamorphosis.** Changes of juvenile hormone and molting hormone in hemimetabolous species and in holometabolous species. From Belles (2020).

#### 1.4. The molecular mechanisms underlying the hormonal action. The MEKRE93 pathway

The molecular action of ecdysone, or its active form, 20E, can be explained by the Ashburner model, which was inferred from the study of chromosome puffing (which corresponds to gene activation) in the salivary glands of the fly *Drosophila melanogaster* after treatment with ecdysone (Ashburner, 1974; Ashburner et al., 1974). When the salivary glands are exposed to 20E, early puffs represent direct ecdysone responses, whereas late puffs, which occur a few hours later, correspond to an indirect response. The effect of 20E at the molecular level starts when the hormone binds to their receptor, the ecdysone

receptor (EcR), which forms a complex with the coreceptor ultraspiracle/retinoid X receptor (USP/RXR), and then initiates a gene expression cascade that regulates biological processes (Hill et al., 2013). After the formation of the ecdysone-receptor complex, it then regulates gene expression by activating the early response genes but repressing the expression of late genes. The products of the early genes would then induce the expression of late genes, and repress the expression of their own genes (Ashburner, 1974; Ashburner et al., 1974).

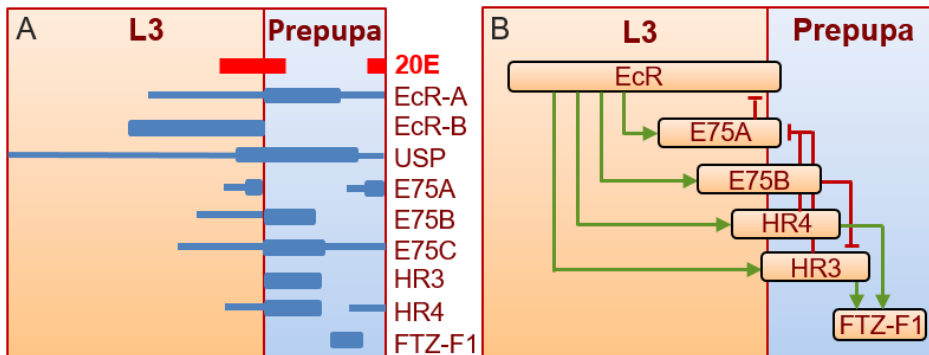
In holometabolan insects, like *D. melanogaster*, the *EcR* gene encodes three protein isoforms: EcR-A, EcR-B1 and EcR-B2 (Talbot et al., 1993). EcR-A and EcR-B1 are mainly produced in larval tissues and regulate metamorphosis. In the target tissues, 20E binds to the receptor and induces the expression of the early response genes: *E74*, *E75*, *BR-C* and *E93* (Sullivan and Thummel, 2003). *E75* gene locates at the 75B early puff, encoding three protein isoforms: E75A, E75B and E75C which is a member of the nuclear receptor superfamily (Segraves and Hogness, 1990). E75A and E74C have a direct function in metamorphosis (Bialecki et al., 2002), whereas E75B inhibits *HR3*, the delayed early response gene whose gene product induces the expression of *ftz-fl* (White et al., 1997). *HR3* and *HR4* are delayed early response genes which are highly expressed at the beginning of prepupal stage, when the expression of early genes becomes reduced. Both contribute to maximal induction of *ftz-fl*, a late response gene, in mid-prepupal stage (Fig. 1.4A) (King-Jones et al., 2005; Lam et al., 1997). The interplay between E75, HR3 and HR4 in regulating the expression of *ftz-fl* is needed to ensure the proper time for metamorphosis (Fig. 1.4B) (Ou and King-Jones, 2013). A recent report by Uyehara and McKay

(2019) in *D. melanogaster* revealed that EcR has many binding sites across the genome. It binds distinct sets of target genes at different developmental times, depending on tissue- and temporal-specific responses in target tissues. During the transition from larva to pupa in developing wings, the majority of EcR binding sites occur in genes that have function in wing formation. These findings indicate that EcR does not control only the expression of genes encoding associated transcription factors, but also plays a widespread role in regulating tissue-specific transcriptional programs during developmental transitions.

In hemimetabolan insects, 20E signaling has been intensively studied in the cockroach *B. germanica*. A group of nuclear receptors, including EcR, RXR/USP, E75, HR3, HR4 and FTZ-F1, has been characterized structurally and functionally (Fig. 1.4C) (Mané-Padrós et al., 2012; Cruz et al., 2008). Furthermore, other transcription factors in this pathway, such as BR-C (Huang et al., 2013; Piulachs et al., 2010) and E93 (Belles and Santos, 2014; Ureña et al., 2014), have also been studied in *B. germanica*. 20E bound to its receptor induces the expression of *E75*, *HR3* and *HR4*. However, the early response gene *E75* inhibits the induction of ecdysone beyond *HR3* and *HR4*. Subsequently, *HR3* induces the expression of the late response gene *ftz-fl* when the ecdysone concentration decreases. In the last nymphal instar *ftz-fl* has a higher expression than in the penultimate nymphal instar, and contributes to metamorphosis, like in the prepupal period of *D. melanogaster* (Fig. 1.4C). FTZ-F1 also plays an important role in the destruction of the PG after the imaginal molt in *B. germanica* (Mané-Padrós et al., 2010).



## *Drosophila melanogaster*



## *Blattella germanica*

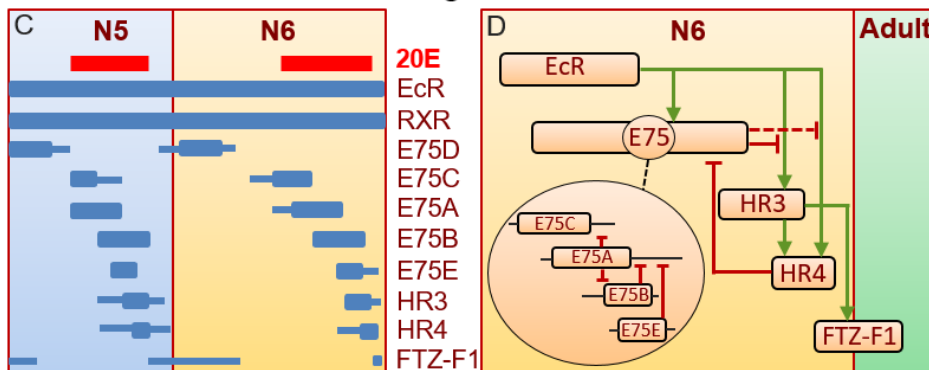


**Figure 1.4. Ecdysone/20E signaling.** (A and B): In the holometabolon *Drosophila melanogaster* in third (last) larval instar (L3) and in prepupa; expression hierarchy of early and late genes (A) and gene interactions (B). (C and D): In the hemimetabolon *Blattella germanica* in penultimate (fifth, N5) and last nymphal instar (sixth, N6), and in the transition to adult; expression hierarchy of early and late genes (C), and gene interactions (D). Original figures with data from different sources compiled by Sullivan and Thummel (2003) (A and B) and Mané-Padrós et al. (2012) (C and D). Modified from Belles (2020).

Although the elements of 20E signaling pathway in *D. melanogaster* and *B. germanica* differ in some details (for example the number of isoforms of E75), the epistatic relationships among them are similar in both species (Fig. 1.4D). Therefore, the 20E signaling

pathway, which is fundamental in insect development and metamorphosis, is essentially conserved at least from cockroaches to flies (Belles, 2020).

Another key hormone that controls metamorphosis is JH. The signal transduction of JH also starts upon binding to its receptor, methoprene-tolerant (Met), a transcription factor belonging to the basic helix-loop-helix Per-ARNT-Sim (bHLH-PAS) family. Subsequently, the JH-Met complex dimerizes with Taiman (Tai), another bHLH-PAS transcription factor. Then, the complex JH-Met + Tai induces the transcription of target genes (Ashok et al., 1998; Jindra et al., 2013).

JH titers are high and inhibit metamorphosis during juvenile stages. However, once the insect molts to the last nymphal instar, the JH titers drop and disappear rapidly, and metamorphosis proceeds. In *B. germanica*, *E93*, whose gene product has been considered an adult specifier (Ureña et al., 2014), starts to be expressed effectively at the beginning of the last nymphal instar, coinciding with the decline of JH production in the CA and the downregulation of *Krüppel-homolog 1* (*Kr-h1*) expression (Belles and Santos, 2014). The molecular mechanisms underlying the action of JH and 20E are based on the MEKRE93 pathway (Fig. 1.5), which starts with the JH-Met + Tai complex, which induces the transcription of the target gene *Kr-h1*. Then, *Kr-h1* represses the expression of *E93*, the factor that triggers metamorphosis (Belles and Santos, 2014).

Transforming growth factor- $\beta$  (TGF- $\beta$ ) signaling pathway, which is fundamental in the control the cell behavior (Massagué and Chen, 2000; Massagué et al., 2000), also affect the production of JH and 20E. In *D. melanogaster*, the TGF- $\beta$  pathway can be divided into

two branches, the TGF- $\beta$ /Activin branch and the bone morphogenetic protein (BMP) branch.

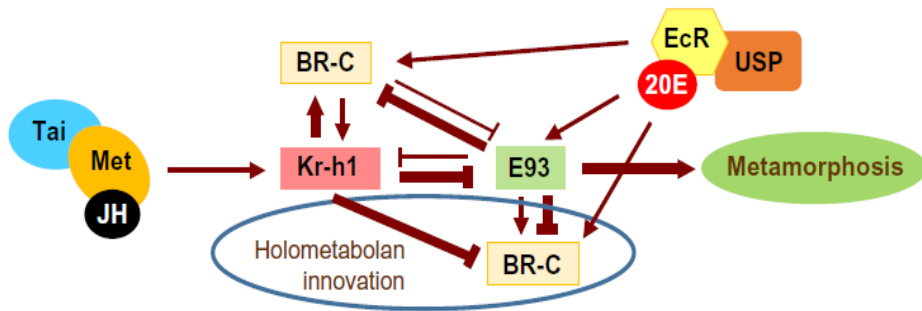


**Figure 1.5. The MEKRE93 pathway in hemimetabolans and holometabolans metamorphosis.** In the nymph-nymph transitions of hemimetabolans, juvenile hormone (JH) (through Methoprene-tolerant, Met, and Taiman, Tai), induces the expression of *Krüppel homolog 1* (*Kr-h1*), whose gene product, in turn, represses the expression of *E93*. In contrast, the fall of JH production in the last juvenile stage interrupts the expression of *Kr-h1* and allows a strong induction of *E93* through ecdysone signaling, which triggers metamorphosis. The main difference between hemimetabolans and holometabolans is the contribution of Broad complex (BR-C), which in hemimetabolans is mainly involved in promoting wing development, whereas in holometabolans determines the formation of the pupa. From Belles (2020).

The TGF- $\beta$ /Activin branch operates through the receptor Baboon (Babo) and signals through a single R-Smad (Smox) and a single Co-Smad (Medea). Whereas the BMP branch has two receptors: Thickveins (Tkv) and Saxophone (Sax), and it operates through a different Smad (Mad) and the Co-Smad Medea, which is common to both branches (Upadhyay et al., 2017). Studies in *D. melanogaster* revealed that the activin signaling is needed for 20E production, as its absence in the PG in the last larval instar reduces the response of the

gland to PTH and insulin (Gibbens et al., 2011). This results from the downregulation of torso (the PTH receptor) and insulin receptor (InR) expression in the PG. Under these conditions, the larvae arrested and could not pupate (Gibbens et al., 2011).

In contrast to the activin signaling, the BMP branch controls JH biosynthesis in the CA through the ligand, Decapentaplegic (Dpp). Using a genetic screen, Huang et al. (2011) identified Tkv and Mad as positive regulators of JH signaling in the larva of *D. melanogaster*. Glutamatergic signals from the brain induce *Dpp* expression in the CA, and Dpp then induces the expression of *jhamt* (which encodes the protein JH acid methyltransferase, a key enzyme that catalyzes the last step of JH biosynthesis), thus stimulating JH biosynthesis (Huang et al., 2011). In hemimetabolan insects, like the cricket *Gryllus bimaculatus*, Myo is a ligand of the Babo receptor of the activin branch of the TGF- $\beta$  pathway, and inhibits JH production in the CA by downregulating the expression of *jhamt* (Ishimaru et al., 2016). Depletion of Myo during the nymphal stages of *G. bimaculatus* upregulates *jhamt* expression, hence JH production increases, and the crickets continue molting to supernumerary nymphs instead of adults (Ishimaru et al., 2016).

## **1.5. *Blattella germanica* as a model insect**

Cockroaches are ideal insects for experimental studies because they are easily and inexpensively reared and maintained in the laboratory. The fossil evidence reveals that cockroaches have been on Earth some 300 million years ago (Grimaldi and Engel, 2005). Therefore, they can serve as a baseline model for evolutionary studies on insect metamorphosis, in particular to study the transition from

hemimetaboly to holometaboly. In our laboratory, the German cockroach, *Blattella germanica*, has been used as a model insect to study the development during embryonic and postembryonic stages, and also to study reproduction. Moreover, a number of hypotheses in the context of insect metamorphosis and evolution have been tested by performing RNA interference (RNAi) experiments, since the German cockroach is very sensitive to this technique (Belles, 2010). The postembryonic development of *B. germanica* at 29°C, from hatching to the adult stage, lasts 25 days as average, and it comprises six nymphal instars, N1-N6. In our studies on the regulation of metamorphosis, we have focused on the three last nymphal instars, antepenultimate (fourth, N4), penultimate (fifth, N5) and last (sixth, N6) (Fig. 1.6).

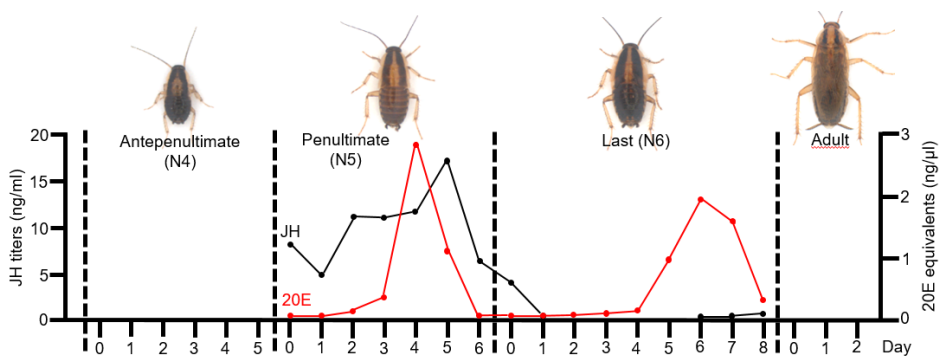


**Figure 1.6.** Length (days) of the antepenultimate (fourth, N4), penultimate (fifth, N5) and last (sixth, N6) nymphal instars of *Blattella germanica*. The hemolymph JH titers (black line) and 20E equivalents (red line) during N5 and N6 are obtained from previous reports (Cruz et al., 2003; Treiblmayr et al., 2006). The dashed lines indicate successive ecdyses.

Previous studies had shown that JH titers in the hemolymph are high in N5, and rapidly decrease at the beginning of N6 (Treiblmayr et al., 2006). At the same time, a peak of 20E occurs towards the last third of N5 and N6 (Cruz et al., 2003) (Fig. 1.6).

## **1.6. *Cloeon dipterum* (Ephemeroptera) as a new model to study insect metamorphosis**

Ephemeroptera (mayflies) are among the most primitive winged insects, which emerged on Earth in late Carboniferous or early Permian, at the same period as Odonata (dragonflies) (Misof et al., 2014). Mayflies are very unique among extant insects since they molt one more time after forming functional wings in the subimago instar, which molts again to become the imago or adult. The nymphs live in freshwater and generally feed on algae. *Cloeon dipterum*, a mayfly species belonging to the family Baetidae, is a tiny insect, with an adult body length measuring between 0.5 and 1 cm. The nymphal period of *C. dipterum*, from freshly hatched nymph to subimago, lasts for 30-40 days (under laboratory conditions at 22°C, Almudi et al., 2019). The mature last instar nymph, which can be recognized for showing black wing pads, goes up to the surface of water and molt to the terrestrial subimago, which, in turn, molts to adult. *C. dipterum* exhibits a conspicuous sexual dimorphism: the female has two sets of eyes, the ocelli and the compound eyes (Fig 1.7A), whereas the male develop an additional pair of turbinate eyes on the mid dorsal part of head (Fig. 1.7B).

In general, mating takes place during the swarming of hundreds adults in the air close to the river or pond, although in the laboratory fertilization can be achieved by artificially forced mating (Almudi et al., 2019). After mating, the females keep the fertilized eggs in the abdomen for 15-18 days, until they are ready to hatch. Then, the female lays the eggs onto the surface of water. The nymph hatches a few seconds after the eggs are laid, and they start feeding (Fig. 1.8).

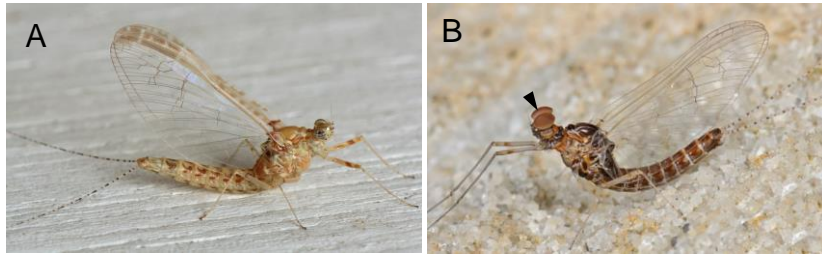


**Figure 1.7. The adult of *Cloeon dipterum*.** (A) Female. (B) Male, arrow head indicates the turbinate eyes. Photos: Barbar Thurlow (A) and Steve Scholnick (B).

The last two stages of mayflies, subimago and imago do not feed and they live for a few days after mating. However, the females that carry the fertilized eggs can live for almost 20 days, until they oviposit (Almudi et al., 2019).

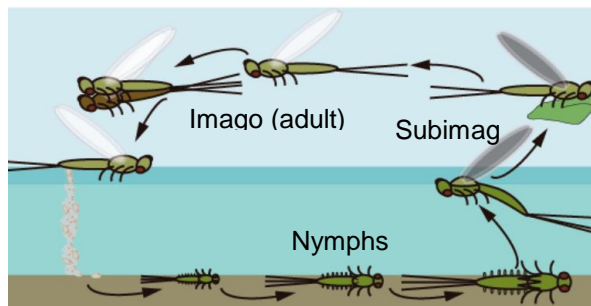


**Figure 1.8. The life cycle of *Cloeon dipterum*.** The female lays fertilized eggs in the water, where they hatch as first instar nymphs. After several molts, the last instar nymph emerges from the water to the land and molt to subimago. Then, the subimago molt again to the adult stage, which can fly and form swarms to mate. From Almudi et al. (2019).





## 2. OBJECTIVES

We previously focused on a number of initial hypotheses, from which the objectives of the present thesis derive.

### 2.1. The hypotheses of the present thesis

This thesis is based on three hypotheses, which are detailed below.

Hypothesis 1. In *Blattella germanica*, Myoglianin (Myo) is involved in the regulation of the decrease of juvenile hormone (JH) production that occurs at the beginning of the last nymphal instar.

Clearance of JH in the last nymphal instar is necessary for the initiation of metamorphosis. The mechanism is condensed in the MEKRE93 pathway (Belles and Santos, 2014), by which a fall of JH production results in a subsequent decrease of Kr-h1 and a concomitant increase of E93, which triggers metamorphosis. These observations led to a subsequent key question: What triggers the decrease of JH at the beginning of the last nymphal instar? We hypothesized that Myo might be a good candidate to play a role in this context. First, because *myo* is one of the most highly expressed genes in the penultimate nymphal instar of *B. germanica* (Ylla et al., 2018), that is, the stage previous to the fall of JH production. Second, because in the cricket *G. bimaculatus* Myo inhibits the expression of *juvenile hormone acid methyl transferase (jhamt)*, a gene coding for the enzyme catalyzing the last step of JH biosynthesis (Ishimaru et al., 2016).

Hypothesis 2. In *Blattella germanica*, E93 is involved in the degradation of the prothoracic gland in the transition from the last nymphal instar to the adult stage.

The final molt is a key process in the context of metamorphosis, which is mediated by the destruction of the prothoracic gland (PG) which takes place after the imaginal molt (Belles, 2019; Belles, 2020). In *B. germanica*, previous studies have revealed that the histolysis of PG is regulated by 20E signaling through a dramatic upregulation of *ftz-fl* expression on the last day of nymphal life (Mané-Adrós et al., 2010). However, given that E93 has a crucial role in insect metamorphosis (Belles and Santos, 2014; Ureña et al., 2014), we wondered whether this factor might have also a role in the destruction of the PG. The fact that E93 has been described as a promoter of cell death in several instances, suggest that it might be a good candidate for such a role. E93 was first discovered as a key player in the histolysis of the salivary glands in *D. melanogaster* during metamorphosis (Woodard et al., 1994; Baehrecke and Thummel, 1995; Lee et al., 2000). Since then, the action of E93 in promoting cell death has also been reported in other tissues, for example in the midgut (Lee and Baehrecke, 2001; Lee et al., 2002) and fat body (Liu et al., 2014) of *D. melanogaster*. Additionally, it has recently been proposed that E93 could have facilitated the evolutionary innovation of metamorphosis and the last molt, by promoting at the same time the maturation of the wings and the destruction of PG (Belles, 2019b). However, nothing is specifically known about the possible role of E93 in PG degeneration. With the above antecedents, we conjectured that the action of FTZ-F1 on PG degeneration (Mané-Adrós et al., 2010) might be mediated by E93.

Hypothesis 3. The MEKRE93 pathway operates in early-branching, paleopteran insects, like mayflies (Ephemeroptera).

In neopterans, the regulation of metamorphosis has been studied intensively, both in hemimetabolans (polyneopterans and paraneopterans) and holometabolans (endopterygotes). The observations suggest that the MEKRE93 pathway is conserved in these insects (Belles, 2019a; Belles and Santos, 2014). However, practically no studies have been carried out on palaeopteran species, probably because it is very difficult to keep them in the laboratory. But the absence of information in paleopterans is unfortunate, giving the interest of the group for the study of the evolution of metamorphosis, because their "primitivism" and because, in ephemeropterans, a subimaginal winged instar molts to another winged (adult) instar, which is a singular phenomenon in insects. Recently, a continuous rearing system of *Cloeon dipterum* has been developed (Almudi et al., 2019), which will allow developmental studies in laboratory conditions. In our case, the *C. dipterum* model will allow us to study the regulation of metamorphosis in mayflies, in particular the main genes involved in the MEKRE93 pathway, to assess whether they have the same function as in neopteran species. If so, then the MEKRE93 pathway could be generalized to all metamorphosing insects.

## 2.2. The objectives

For the present thesis, we have established three objectives that derive directly from the three hypotheses that have been argued in detail above. The three objectives are as follows.

Objective 1. To study the possible role of Myo in regulation of the decrease of juvenile hormone production that occurs at the beginning of the last nymphal instar in *Blattella germanica*.

Objective 2. To study the possible role of the E93 in the destruction of the PG after the imaginal molt in *Blattella germanica*.

Objective 3. To study the mechanisms that regulate metamorphosis in the mayfly *Cloeon dipterum*, particularly during the formation of the subimago, and to compare these mechanisms with those operating in neopteran insects, which are condensed in the MEKRE93 pathway.

## 3. RESULTS

### 3.1. Myoglianin triggers the pre-metamorphosis stage in holometabolan insects

Orathai Kamsoi, Xavier Bellés\*

\* Institute of Evolutionary Biology (CSIC-University of Pompeu Fabra), Passeig Maritim 37, 08003 Barcelona, Spain.

Orathai Kamsoi, Xavier Bellés.

[Myoglianin triggers the pre-metamorphosis stage in holometabolan insects.](#) FASEB J. 2019; 33(3):3659-3669.



## Myoglianin triggers the premetamorphosis stage in hemimetabolan insects

Orathai Kamsoi and Xavier Belles<sup>1</sup>

Institute of Evolutionary Biology, Spanish National Research Council (CSIC)-Universitat Pompeu Fabra, Barcelona, Spain

**ABSTRACT:** Insect metamorphosis is triggered by a decrease in juvenile hormone (JH) in the final juvenile instar. What induces this decrease is therefore a relevant question. Working with the cockroach *Blattella germanica*, we found that myoglianin (Myo), a ligand in the TGF- $\beta$  signaling pathway, is highly expressed in the corpora allata (CA, the JH-producing glands) and the prothoracic gland (PG, which produce ecdysone) during the penultimate (fifth) nymphal instar (N5). In the CA, high Myo levels during N5 repress the expression of juvenile hormone acid methyl transferase, a JH biosynthesis gene. In the PG, decreasing JH levels trigger gland degeneration, regulated by the factors Krüppel homolog 1, FTZ-F1, E93, and inhibitor of apoptosis-1. Also in the PG, a peak of *myo* expression in N5 indirectly stimulates the expression of ecdysone biosynthesis genes, such as *neverland*, enhancing the production of the metamorphic ecdysone pulse in N6. The Myo expression peak in N5 also represses cell proliferation, which can enhance ecdysone production. The data indicate that Myo triggers the premetamorphic nymphal instar in *B. germanica* and possibly in other hemimetabolan insects.—Kamsoi, O., Belles, X. Myoglianin triggers the premetamorphosis stage in hemimetabolan insects. *FASEB J.* 33, 3659–3669 (2019). [www.fasebj.org](http://www.fasebj.org)

**KEY WORDS:** juvenile hormone · ecdysone · corpora allata · prothoracic gland · MEKRE93 pathway

Insect metamorphosis is a fascinating phenomenon, but the master lines of its molecular regulatory mechanisms have only been elucidated recently. The process is controlled by 2 main hormones: ecdysone (where the best-known bioactive form is the derivative 20-hydroxyecdysone), which promotes the successive molts, and juvenile hormone (JH), which prevents the onset of metamorphosis in juvenile stages (1, 2). The molecular mechanisms underlying the action of these hormones are essentially based on the MEKRE93 pathway (3) that starts when JH binds to its receptor, methoprene-tolerant (Met), which belongs to the bHLH-PAS family of transcription factors (4). Upon binding to Met, JH triggers dimerization of Met with another bHLH-PAS protein, Taiman (Tai). The resulting JH-Met + Tai complex induces transcription of the target gene Krüppel-homolog 1 (*Kr-h1*),

whose gene product represses the expression of *E93*, an ecdysone signaling-dependent gene whose gene product triggers metamorphosis (3, 5).

In hemimetabolan metamorphosis, exemplified by the German cockroach *Blattella germanica*, JH titers in the hemolymph rapidly decrease at the beginning of the final (sixth) nymphal instar (N6) (6). This is accompanied by a sudden drop of *Kr-h1* mRNA levels (7) as a result of the decrease in JH and the action of microRNA miR-2, which scavenges *Kr-h1* transcripts (8, 9). Consequently, *E93* becomes de-repressed and its expression increases, which triggers the onset of metamorphosis (3). These observations and knowledge of the MEKRE93 pathway are robust but lead to the following key question: What triggers the decrease in JH at the beginning of N6? Because we believe the answer lies in the penultimate (fifth) nymphal instar (N5), we searched for candidate genes in a series of transcriptomes prepared and sequenced in our laboratory, which covered the entire ontogeny of *B. germanica* (10). The analyses revealed that one of the most highly expressed genes in N5 is myoglianin (*myo*) (10).

Myoglianin (Myo) was discovered in *Drosophila melanogaster* as a new member of the TGF- $\beta$  signaling pathway closely related to the vertebrate muscle differentiation factor myostatin. Expression studies led to the detection of maternally derived *myo* transcripts and of Myo expression in glial cells in midembryogenesis and, subsequently, in the developing somatic and visceral muscles and cardioblasts (11). Myo is a ligand in the activin branch of

**ABBREVIATIONS:** CA, corpora allata; CC-CA, corpora cardiaca-corpora allata complex; Cdk, cyclin-dependent kinase; Cyc, cyclin; Dap, dacapo; dib, disembodied; dsMock, control double stranded RNA; dsMyo, double-stranded RNA targeting myoglianin; dsRNA, double-strand RNA; EdU, 5-ethynyl-2'-deoxyuridine; JH, juvenile hormone; *jlant*, juvenile hormone acid methyl transferase; Kr-h1, Krüppel homolog 1; Met, methoprene-tolerant; Myo, myoglianin; nvd, neverland; PG, prothoracic gland; *plim*, phantom; RNAi, RNA interference; sad, shadow; Smox, Smad on X

<sup>1</sup> Correspondence: Institute of Evolutionary Biology (CSIC-Universitat Pompeu Fabra), Passeig Marítim de la Barceloneta 37, 08003 Barcelona, Spain. E-mail: [xavier.belles@ibe.upf-csic.es](mailto:xavier.belles@ibe.upf-csic.es)

doi: 10.1096/fj.201801511R

This article includes supplemental data. Please visit <http://www.fasebj.org> to obtain this information.

the TGF- $\beta$  signaling pathway (12). In the context of metamorphosis, Myo has been shown to play a crucial role in the remodeling of the mushroom bodies in the larva–pupa transition of *D. melanogaster*, an action mediated by increased expression of the ecdysone receptor B1 (*EcR-B1*) gene in neural tissues (13). Regarding hemimetabolous insects, in the corpora allata (CA, the JH-producing glands) of the cricket *Gryllus bimaculatus*, Ishimaru *et al.* (14) showed that Myo inhibits the expression of juvenile hormone acid methyl transferase (*jhamt*), a gene coding for the last and crucial enzyme in the JH biosynthetic pathway. Reduction of the levels of this enzyme in the final nymphal instar triggers a decrease of JH production and commits the cricket to metamorphose (14). The findings of Ishimaru *et al.* (14) contrast with data reported in *D. melanogaster*, where the bone morphogenetic protein branch of the TGF- $\beta$  signaling pathway promotes JH production by up-regulating the expression of *jhamt* (15).

Using *B. germanica* as a model, we found that Myo has functions beyond repressing the expression of *jhamt* in the CA during the transition from the penultimate to the final nymphal instar. We have also observed that Myo plays significant roles in the prothoracic gland [(PG), the ecdysone-producing gland] that help induce this transition and lead to the onset of metamorphosis. Our data indicate that Myo is an essential factor in terms of triggering the premetamorphosis stage in *B. germanica* and possibly in other hemimetabolous insects because it acts on the CA and the PG, the glands that produce the most important hormones regulating metamorphosis.

## MATERIALS AND METHODS

### Insects

The *B. germanica* cockroaches used in the experiments described herein were obtained from a colony fed Panlab (Harvard Apparatus, Holliston, MA, USA) dog chow and water *ad libitum* and reared in the dark at  $29 \pm 1^\circ\text{C}$  and 60–70% relative humidity. Cockroaches were anesthetized with CO<sub>2</sub> prior to injection treatments, dissections, and tissue sampling.

### RNA extraction and retrotranscription to cDNA

RNA extractions were carried out with the Gen Elute Mammalian Total RNA kit (MilliporeSigma, Madrid, Spain). A sample of 200 ng from each RNA extraction was used for mRNA precursors in the case of fat body, epidermis, and muscle. All the volume extracted of the corpora cardiaca–CA complex (CC–CA), PG, brain, and ovary was lyophilized in a freeze-dryer (ALPHA 1–2 LDplus; Thermo Fisher Scientific, Waltham, MA, USA) and resuspended in 8  $\mu\text{l}$  of milli-Q H<sub>2</sub>O (MilliporeSigma). RNA quantity and quality were estimated by spectrophotometric absorption at 260 nm in a spectrophotometer (ND-1000; NanoDrop Technologies, Wilmington, DE, USA). The RNA samples then were treated with DNase (Promega, Madison, WI, USA) and reverse transcribed with a First Strand cDNA Synthesis Kit (Roche, Basel, Switzerland) and random hexamer primers (Roche).

### Determination of mRNA levels by real-time quantitative PCR

Real-time quantitative PCR was carried out in an iQ5 Real-Time PCR Detection System (Bio-Rad Laboratories, Hercules, CA, USA) using SYBRGreen (iQ Universal SYBR Green Supermix; Applied Biosystems, Foster City, CA, USA). Reactions were performed in triplicate, and a template-free control was included in all batches. Primers used to study the transcripts of interest are detailed in Supplemental Table S1. The efficiency of each set of primers was validated by constructing a standard curve through 3 serial dilutions. Levels of mRNA were calculated relative to BgActin-5c mRNA (accession number AJ862721). Results are given as copies of the mRNA of interest per 1000 copies of BgActin-5c mRNA.

### RNA interference

The detailed procedures for RNA interference (RNAi) assays have been described previously (16). The primers used to prepare the double-strand RNA (dsRNA) targeting *B. germanica* Myo are described in Supplemental Table S1. The sequence corresponding to the dsRNA [i.e., the double-stranded RNA targeting Myo (dsMyo)] was amplified by PCR and then cloned into a pST-Blue-1 vector. A 307 bp sequence from *Autographa californica* nucleopolyhedrovirus (accession number K01149.1) was used as control dsRNA (dsMock). A volume of 1  $\mu\text{l}$  of the dsRNA solution (3  $\mu\text{g}/\mu\text{l}$ ) was injected into the abdomen of freshly emerged fifth instar female nymphs (N5D0) or 1-d-old sixth instar female nymphs (N6D1) with a 5  $\mu\text{l}$  Hamilton microsyringe. Control insects were treated at the same age with the same dose and volume of dsMock.

### Morphologic studies of the PG

The PG was studied in female nymphs at chosen ages and instars. The gland was dissected out of the first thoracic segment of the animal under Ringer's saline, fixed in 4% paraformaldehyde in PBS for 1 h, washed with PBS 0.3% Triton, and incubated for 10 min in 1 mg/ml DAPI in PBS 0.3% Triton. The gland was mounted in Mowiol (Calbiochem, Madison, WI, USA) and observed with a fluorescence microscope (Axio Imager.Z1; Carl Zeiss AG, Oberkochen, Germany).

### Experiments to measure cell proliferation in the PG

5-Ethynyl-2'-deoxyuridine (EdU) is a thymidine analog developed for labeling DNA synthesis and dividing cells *in vitro* (17), which is more sensitive and practical than the commonly used 5-bromo-2'-deoxyuridine. We followed an approach *in vivo*, using the commercial EdU compound Click-it EdU-Alexa Fluor 594 azide (Thermo Fisher Scientific), which was injected into the abdomen of the nymphs at chosen ages and instars with a 5  $\mu\text{l}$  Hamilton microsyringe (1  $\mu\text{l}$  of 20 mM EdU solution in DMSO). The control specimens received 1  $\mu\text{l}$  of DMSO. The PG from treated specimens was dissected 1 h later and processed for EdU visualization according to the manufacturer's protocol.

## RESULTS

### Myo structure and expression in *B. germanica*

We obtained a cDNA of 1611 bp, comprising a complete open reading frame, by combining a Blast (<https://blast.ncbi.nlm.nih.gov/Blast.cgi>) search in *B. germanica* genome,



transcriptomic data, and PCR. Its conceptual translation gave a 537 aa protein (Supplemental Fig. S1) with significant similarity to the Myo sequence of other species, such as the fly *D. melanogaster* and the cricket *G. bimaculatus*, as described by Lo and Frasch (11) and Ishimaru *et al.* (14), respectively (Supplemental Fig. S2). As in other Myo orthologs, the full-length *B. germanica* Myo sequence contained the canonical RXXR processing site and 7 cysteines in the carboxy-terminal portion of the ORF, which correspond to the mature processed protein (Supplemental Figs. S1, 2).

To assess whether Myo was differentially expressed in different tissues, we measured its expression in brain, CC-CA, PG, ovary, fat body, epidermis, and muscle tissues in 3-d-old fifth instar female nymphs (N5D3) of *B. germanica*. PG showed the highest myo mRNA levels; a lower Myo expression was measured in brain, CC-CA, and muscle tissues; and the lowest expression was observed in fat body, ovary, and epidermal tissues (Fig. 1A).

Because we were interested in the main hormones regulating metamorphosis (JH and ecdysone), we focused on the glands producing these hormones (the CC-CA complex and PG, respectively). Therefore, we determined the Myo expression pattern in these 2 glands during the fourth, fifth, and sixth (final) instar female nymphs (N4, N5, and N6). In the CC-CA, the highest expression was observed in N5, in accordance with the pattern we found in our previous transcriptome analyses (10). Within N5, maximal expression was found at the beginning of the instar (N5D0) (~500 mRNA copies per 1000 copies of actin mRNA) and progressively decreased until it practically vanished at the end of the instar (N5D6). During N6, Myo mRNA levels in the CC-CA were relatively low (10–50 mRNA copies per 1000 copies of actin mRNA) (Fig. 1B). In the PG, the highest Myo mRNA levels were also observed in N5, but expression peaked in the mid-late instar (N5D4, ~11,000 mRNA copies per 1000 copies of actin mRNA). The levels progressively decreased throughout the rest of the instar and N6, although they remained relatively high in N6 (~4000 mRNA copies per 1000 copies of actin mRNA) (Fig. 1C).

### Myo depletion prevents metamorphosis

We used systemic RNAi to study the effects of Myo depletion on metamorphosis. We injected a single dose of 3  $\mu$ g of dsMyo into the abdomen of N5D0 cockroaches. Controls were treated equivalently with the same dose of dsMock. In the CC-CA, Myo mRNA levels were significantly reduced in dsMyo-treated cockroaches (Fig. 2A). When monitoring the experimental cockroaches up to the imaginal molt, we observed that all N5 controls ( $n = 44$ ) molted to normal N6 after 6 d on average and then to normal adults 8 d later (Fig. 2B). The N5 dsMyo-treated cockroaches ( $n = 46$ ) molted to N6 after 8 d on average; these N6 cockroaches had an apparently normal morphology but were smaller than the N6 controls (Fig. 2C, D). Of the 46 N6 dsMyo-treated cockroaches, 6 died and 40 molted to a supernumerary nymph (N7). Of the 40 N7 nymphs, 6 molted to the adult stage and 34 molted to a

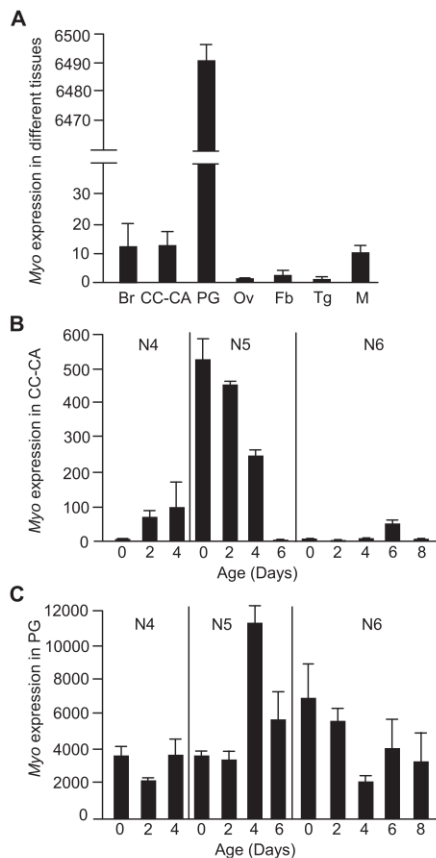
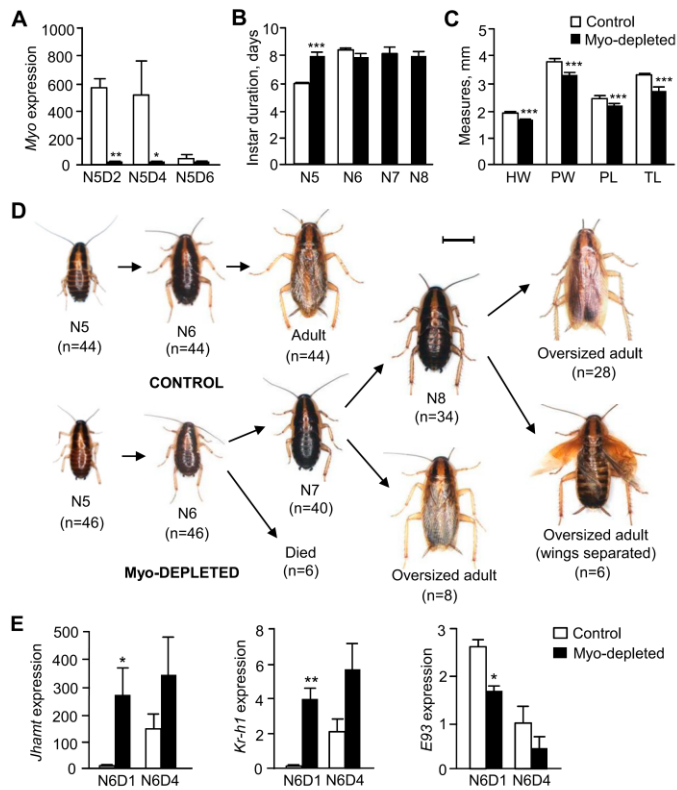


**Figure 1.** Expression of Myo in *B. germanica*. **A**) mRNA levels in brain (Br), CC-CA, PG, ovary (Ov), fat body (Fb), epidermis (tergites 2–7: Tg), and muscle (extensor muscle from the 6 femora pairs: M). Measurements were carried out on 3-d-old fifth-instar female nymphs. **B**) mRNA levels in CC-CA of fourth, fifth, and sixth instar female nymphs. **C**) mRNA levels in PG of fourth, fifth, and sixth instar female nymphs. Results are copies of Myo mRNA per 1000 copies of BgActin-5c mRNA and are expressed as the mean  $\pm$  SEM ( $n = 3–5$ ).

further supernumerary nymph (N8), which then molted to adults. A total of 28 of these adults presented a practically normal morphology (although they were slightly larger than control adults emerging from N6), whereas the wings and tegmina were somewhat separated in the other 6 adults (Fig. 2D). The supernumerary nymphal instars N7 and N8 lasted for ~8 d (Fig. 2B). We then examined the expression of genes involved in JH synthesis and signaling in the CC-CA at the beginning of N6. Results showed that the expression of *jhamt* and *Kr-h1* was significantly

**Figure 2.** Effects of Myo mRNA depletion in the metamorphosis of *B. germanica*. **A**) mRNA levels of Myo in CC-CA of Myo-depleted cockroaches and in controls, measured on 2-, 4-, and 6-d-old fifth instar female nymphs (N5D2, N5D4, and N5D6). **B**) Duration (days) of N5 and N6 (and the supernumerary nymphal instars N7 and N8) in Myo-depleted cockroaches and in controls. **C**) Measures of morphologic parameters in N6 of Myo-depleted cockroaches and in controls. HW, head width; PL, pronotum length; PW, pronotum width; TL, metatibia length. **D**) Dorsal view of control and Myo-depleted cockroaches through successive molts. Freshly emerged fifth instar female nymphs (N5D0) were treated with dsMyo or with dsMock (control), and the morphology after the subsequent molts was examined. The number of specimens at the beginning of the experiments and after every molt is indicated. Scale bar, 4 mm. **E**) mRNA levels of *jhant*, *Kr-h1*, and *E93* in CC-CA from dsMyo-treated cockroaches and controls on N6D1 and N6D4. In **A** and **E**, results are indicated as copies of the given transcript per 1000 copies of BgActin-5c mRNA. In all bar diagrams, results are expressed as the mean  $\pm$  SEM ( $n = 3-5$ ). Asterisks indicate statistically significant differences with respect to controls. \* $P < 0.05$ , \*\* $P < 0.01$ , \*\*\* $P < 0.001$  (Student's *t* test).



up-regulated, whereas that of *E93* was down-regulated (Fig. 2E).

In *D. melanogaster*, decapentaplegic, one of the ligands of the thick vein receptor of the bone morphogenetic branch of the TGF- $\beta$  signaling pathway, which operates through the transcription factor Mothers against decapentaplegic (Mad), promotes JH production in the CA through up-regulating the expression of *jhant* (15). In the cricket *G. bimaculatus*, Myo, which is a ligand of the Baboon receptor of the activin branch of the TGF- $\beta$  signaling pathway that operates through the transcription factor Smad on X (Smox), inhibits JH production in the CA through down-regulating the expression of *jhant* (14). Ishimaru et al. (14) proposed that the inhibitory action of Myo upon the expression of *jhant* is mediated by a repression of the Mad effects. Depletion of Myo in the final nymphal instar of *G. bimaculatus* up-regulated *jhant* expression; hence, JH production increased, and the crickets molted to supernumerary nymphs instead of adults (14). The results obtained in *B. germanica* are similar to those

observed in *G. bimaculatus* in terms of metamorphosis phenotypes and the up-regulation of *jhant* expression after Myo depletion. This is not surprising because both species are hemimetabolans and are closely related phylogenetically, that is, both belong to the "orthopteroid" group of the superorder Polyneoptera (18). Our results unveil the molecular mechanisms preventing metamorphosis, which are based on the MEKRE93 pathway (3). In the final nymphal instar, the *jhant* up-regulation induced by Myo depletion led to an increase in *Kr-h1* expression, a JH-dependent factor that is the main transducer of the anti-metamorphic action of JH (7). Moreover, *Kr-h1* represses *E93* (3), which is the master factor triggering metamorphosis (3, 19). In our Myo-depleted cockroaches, the up-regulation of *Kr-h1* expression explains the down-regulation of *E93* (Fig. 2E), whereas the observed reduction in *E93* expression explains why the cockroaches did not molt to the adult stage.

These observations are consistent with our previous work wherein we reported that the TGF- $\beta$ /activin

signaling pathway contributes to the repression of *Kr-h1* expression and activation of *E93* expression during the metamorphosis of *B. germanica* (20). Because Myo signal is transduced by Smox and represses *ihant* expression and JH production, one would expect that expression of the JH-dependent gene *Kr-h1* would be up-regulated if Smox were repressed, which is what was observed in our experiments (20). In the context of holometabolism metamorphosis, studies in *D. melanogaster* have shown that the TGF- $\beta$ /activin branch is involved in wing disc patterning (21) and neuronal remodeling (22). Moreover, Gibbens *et al.* (23) have shown that the final larval stage of *D. melanogaster* was developmentally arrested when the TGF- $\beta$ /activin pathway was blocked in the PG because the larvae were unable to produce the large pulse of ecdysone needed for metamorphosis. It has been demonstrated that Myo signaling through the TGF- $\beta$ /activin pathway is crucial for mushroom body remodeling in the transition from the final larval stage to the pupa because it up-regulates neuronal *Ecr-B1* expression (13). The same study revealed that myo-defective mutants can molt until the final larval stage and prepupate, but they become arrested before head inversion (13), which is consistent with the results reported by Gibbens *et al.* (23).

#### Myo depletion causes cell hyperproliferation in the PG

The PG of *B. germanica*, like in other cockroaches, has an X-shaped morphology, and its size varies during successive stages. Size variation roughly corresponds to the dynamics of ecdysone production because the most active glands have bigger secretory cells than the inactive glands (24). In the present work, we also studied the dynamics of cell proliferation in the PG during N5 and N6 using EdU labeling. In N5, which lasts for 6 d, we observed intense cell division between d 0 and 3 (the first 50% of the stage). In N6, which lasts for 8 d, intense cell division only occurred over d 0 and 1 (the first 12.5% of the stage) (Fig. 3). During these stages, the ecdysone pulse in N5 peaks sharply at around d 4, whereas in N6 ecdysone production follows a longer, shallower peak over d 5–7 (25). The non-overlapping patterns of cell division and the ecdysone peak indicate that PG cells alternate between periods of cell proliferation and hormone synthesis, as occurs in other secretory glands, such as the CA (26). The form of the ecdysone pulse varies along the different molts; wider pulses appear to be characteristic of metamorphic molts (27). We believe the wide ecdysone pulse in N6, which triggers the metamorphic molt, requires an earlier and radical arrest of cell division, similar to the one observed in our Edu labeling observations (Fig. 3).

We used the same Myo-targeting RNAi experiment described above (3  $\mu$ g of dsMyo injected in N5D0) to examine the effects in the PG. We found that Myo mRNA levels in the PG were significantly reduced in dsMyo-treated cockroaches compared with controls (Fig. 4A). Preliminary dissections of Myo-depleted cockroaches in N5D4 and N6D4 revealed that PG size was greater than in controls (Fig. 4B). Measurement of the PG arm width

during N5 and N6 showed that the PG from Myo-depleted cockroaches grew bigger than in the controls (Fig. 4C). Moreover, microscopic examination of the PG at high magnifications using Edu labeling revealed that Myo-depleted cockroaches exhibited much more active cell division than controls (Fig. 4D).

The transition from G1 into DNA replication (S phase) is crucial in determining whether to enter a new cell cycle, and 4 factors—cyclin (Cyc)E, CycA, dacapo (Dap), and cyclin-dependent kinase (Cdk)2—are key players in this transition. The accumulation of CycE and CycA, which form complexes with Cdk2, promotes the transition to the S phase, whereas Dap negatively regulates this transition, mainly by sequestering the CycE/Cdk2 complexes (28, 29). Moreover, in mouse C2C12 cells, myostatin, which is the Myo homolog in mammals (11), induces CycD degradation, resulting in cell cycle arrest (30). Based on these reports, we measured the expression of *CycE*, *CycA*, *dap*, *Cdk2*, and *CycD* in the PG from Myo-depleted and control cockroaches.

In controls, results indicated low levels of *dap* expression at the beginning of N5, high values in the middle, and low levels again at the end of the stage. *Cdk2*, *CycE*, *CycA*, and *CycD* expression showed an inverse pattern (Fig. 4E), which approximately corresponds to the dynamics of cell proliferation (Fig. 3). *dap* expression in Myo-depleted cockroaches was generally dramatically reduced, whereas *CycA*, *CycD*, and *Cdk2* expression progressively decreased during N5. *CycE* expression was not significantly affected (Fig. 4E). Dap is a member of the mammalian p21 family of cyclin-dependent kinase inhibitors and inhibits the G1-to-S phase transition by sequestering the CycE/Cdk2 complex in a stable but inactive form (31). Induction of *dap* transcription causes a rapid accumulation of Dap protein, which inhibits CycE/Cdk2 activity and leads to G1 cell cycle arrest (32). Conversely, *dap* knockdown leads to tissue hypertrophy and cancer processes (33, 34). We propose that down-regulation of *dap* expression may have maintained cell cycle activity in the PG of Myo-depleted cockroaches, leading to cell hyperproliferation and PG hypertrophy. The *CycE*, *CycA*, and *Cdk2* expression patterns in Myo-depleted cockroaches could be a product of *dap* down-regulation and the complex epistatic relationships between these factors (28, 29). General down-regulation of *CycD* expression in the PG of Myo-depleted cockroaches suggests that Myo has either a direct or indirect stimulatory effect on the expression of this cyclin. This effect differs from phenomena observed in mammals, where myostatin induces CycD degradation (30).

#### Myo depletion reduces the expression of ecdysteroidogenic genes in the PG

Myo depletion increased the duration of N5 (Fig. 2A). To study the reasons for this delay, we measured the expression of the following 4 genes, which code for ecdysone biosynthesis enzymes: neverland (*nvd*), which converts cholesterol to 7-dehydrocholesterol; phantom (*phm*) and disembodied (*dib*), which catalyze the addition of a hydroxyl group to the 25 and 22 carbon of the cholesterol side

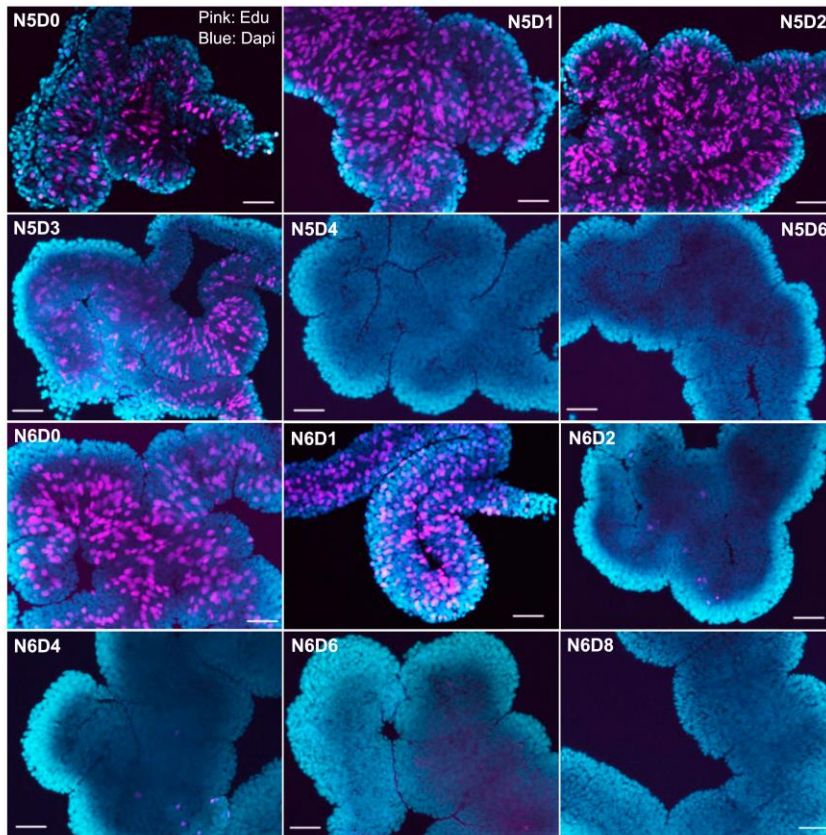


**Figure 3.** Cell proliferation in the PG of *B. germanica*. Double labeling EdU (discrete pink spots) and DAPI (background blue color) of PG tissue of female nymphs along the fifth and the sixth instar (from N5D0 to N5D6 and from N6D0 to N6D8). Scale bars, 50  $\mu$ m.

chain, respectively; and shadow (*sad*), which catalyzes the addition of a hydroxyl group to the 2 carbon of the cholesterol ring (35). Results showed that the expression of *nvd* was dramatically down-regulated in N5D4 Myo-depleted cockroaches. The expression of *phm* and *dib* tended to be down-regulated, whereas that of *sad* was practically unaffected (Fig. 5A).

In *D. melanogaster*, the activin branch of the TGF- $\beta$  pathway promotes the expression of *nvd*, *dib*, and *spookier* (which is involved in catalyzing the conversion of 7-dehydrocholesterol to delta4, diketol), whereas it does not apparently affect *phm* and *sad* expression (23). These genes may be directly affected by the TGF- $\beta$  pathway, or this pathway's influence could be mediated by the PTTH/torso pathway, acting at a transcriptional level, and the insulin pathway, acting post-transcriptionally (23). To

date, there is no evidence that a PTTH/Torso pathway exists in cockroaches. Therefore, we focused on the insulin pathway by measuring insulin receptor (*InR*) expression, which was down-regulated in the PG from Myo-depleted cockroaches (Fig. 5B). If Myo has a systemic stimulatory effect on *InR* expression, it could also explain the small size of the N6 stage emerging from dsMyo-treated N5 cockroaches (Fig. 2C, D).

We propose that Myo indirectly promotes *nvd*, *phm*, and *dib* expression. The stimulatory action on *nvd* and *dib* could be mediated by the insulin pathway, as in *D. melanogaster*. In the case of *B. germanica*, however, the insulin pathway would act at a transcriptional level on these genes, rather than post-transcriptionally, as occurs in *D. melanogaster* (23). Additionally, we cannot rule out the possibility that the apparent stimulation of *phm* and *dib*

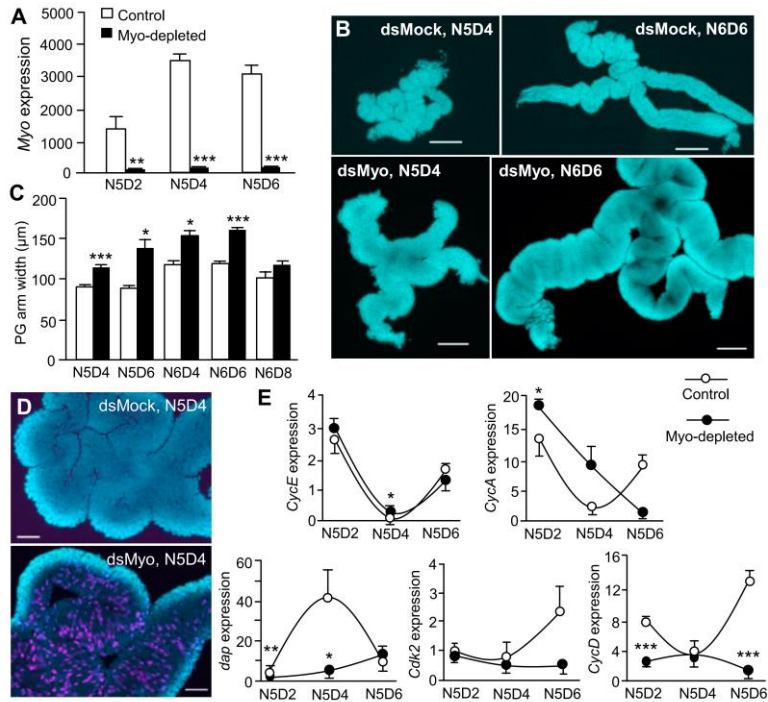


**Figure 4.** Effects of Myo mRNA depletion on PG growth in *B. germanica*. **A)** mRNA levels of Myo in PG of Myo-depleted cockroaches and in controls measured on 2-, 4-, and 6-d-old fifth instar female nymphs (N5D2, N5D4, and N5D6). **B)** DAPI-stained PGs from dsMock and dsMyo specimens in N5D4 at N6D6. Scale bars, 200 µm. **C)** PG arm width along different days of N5 (N5D4 and N5D6) and N6 (N6D4, N6D6, and N6D8), comparing Myo-depleted cockroaches and controls. **D)** Double-labeling EdU (discrete pink spots) and DAPI (gland background bluish color) of PGs of N5D4, comparing Myo-depleted cockroaches and controls. Scale bar, 50 µm. **E)** mRNA levels of *CycE*, *CycA*, *dap*, *Cdk2*, and *CycD* in PG tissues from dsMyo-treated cockroaches and controls on N5D2, N5D4, and N5D6. In **A** and **E**, results are indicated as copies of the given transcript per 1000 copies of BgActin-5c mRNA. In all quantitative diagrams, results are expressed as the mean  $\pm$  SEM ( $n = 3-5$ ). Asterisks indicate statistically significant differences with respect to controls. \* $P < 0.05$ , \*\* $P < 0.01$ , \*\*\* $P < 0.001$  (Student's *t* test).

transcription might also be mediated by fushi tarazu transcription factor 1 (FTZ-F1). Whereas FTZ-F1 enhances *plm* and *dib* expression in the ring gland from late third-stage larva of *D. melanogaster* (36), our measurements revealed that *ftz-fl* expression was delayed and down-regulated in the PG of Myo-depleted cockroaches (Fig. 5C). This supports the hypothesis that FTZ-F1 helps enhance *plm* and *dib* transcription in the PG of *B. germanica*. Finally, decreased expression of ecdysteroidogenic genes in Myo-depleted insects might be mediated by the increased expression of *jhamt* and *Kr-h1* because JH and Kr-h1 inhibit the expression of these genes (37, 38). We explored this possibility through experiments examining Myo in N6.

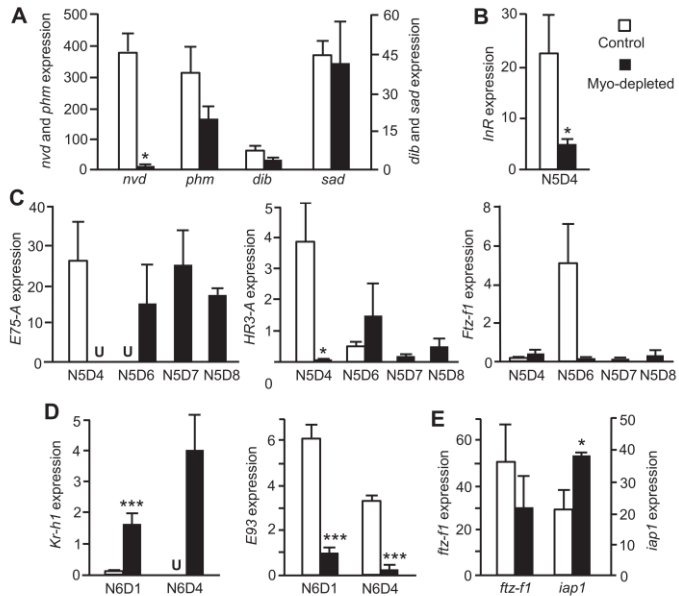
We also studied the expression of the ecdysone-dependent genes *E75-A*, *HR3-A*, and *ftz-fl*, which have previously been characterized in *B. germanica* (39-41). The expression pattern of these genes was conspicuously

reduced (especially that of *ftz-fl*) and delayed in the PG of Myo-depleted cockroaches (Fig. 5C). This is reminiscent of the developmental delay observed in *D. melanogaster* with impaired signaling in the activin branch of the TGF- $\beta$  pathway, which was due to deficient ecdysone production by the PG (23, 42). The same mechanism may explain why N5 lasts longer in Myo-depleted cockroaches (Fig. 2B).

#### Myo depletion prevents the onset of PG degeneration

In the PG of *B. germanica*, ecdysone signaling promotes the degeneration of the gland toward the end of N6 and the beginning of adult life. This is mediated by FTZ-F1, a distal transducer in the ecdysone signaling pathway that is expressed at markedly high levels in the PG in the last day of N6 (N6D8) (43). On the other hand, the inhibitor of

**Figure 5.** Effects of Myo mRNA depletion on the expression of PG factors in *B. germanica*. **A)** mRNA levels of *nvd*, *phm*, *dib*, and *sad* in PG from Myo-depleted cockroaches and controls on 4-d-old fifth instar female nymphs (N5D4). **B)** mRNA levels of *InR* in PG from Myo-depleted cockroaches and controls on N5D4. **C)** mRNA levels of *E75-A*, *HR3-A*, and *ftz-f1* in PG from Myo-depleted cockroaches and controls measured on different days of N5 (N5D4 and N5D6 in controls, and N5D4, N5D6, N5D7, and N5D8 in dsMyo-treated). **D)** mRNA levels of *Kr-h1* and *E93* in PG from Myo-depleted cockroaches and controls on N6D1 and N6D4. **E)** mRNA levels of *iap1* and *ftz-f1* in PG from Myo-depleted cockroaches and controls on N6D8. Results, indicated as copies of the given transcript per 1000 copies of BgActin-5c mRNA, are expressed as mean  $\pm$  SEM ( $n = 3-5$ ). "U" in C and D means that the expression was below the limit of detection. Asterisks indicate statistically significant differences with respect to controls. \* $P < 0.05$ , \*\*\* $P < 0.001$  (Student's *t* test).



apoptosis-1 (IAP1) protects the PG from degeneration in early N6 and earlier nymphal stages. *iap1* shows maximal expression at N6D7 before it starts to decrease at N6D8, coinciding with a sharp peak in *ftz-f1* expression (43). JH also plays a protective role because treating N6 with the JH analog methoprene attenuates the expression of *ftz-f1* in N6D8 and prevents PG degeneration (43).

In our experiments, Myo-depleted N6 cockroaches molted to a supernumerary N7 and, in some cases, successively on to N8 and adult, indicating the PG was functional after N6. To study the mechanisms that prevented PG degeneration, we measured the expression of *Kr-h1* as a key transducer of the JH signal and *ftz-f1*, *iap1*, and *E93* as potential regulators of the onset of PG degeneration. Results showed that *Kr-h1* was up-regulated, whereas *E93* was down-regulated, in N6 Myo-depleted cockroaches (Fig. 5D). This presumably results from the higher production of JH in the CA, where Myo-depleted cockroaches maintained up-regulated *jhamt* expression in N6, with the consequent increase in *Kr-h1* transcription in the CA and peripheral tissues (Fig. 2E). Given that *Kr-h1* represses *E93* expression in metamorphic tissues (3), *E93* was down-regulated in the PG (Fig. 5D). On the last day of N6 (N6D8), *ftz-f1* and *iap1* showed the highest and lowest expression values, respectively, within the stage (43). In the PG of Myo-depleted cockroaches, however, *ftz-f1* expression at N6D8 tended to be lower than in controls (40% on average), whereas *iap1* expression was significantly

up-regulated (73% on average) (Fig. 5E). This is consistent with the notion that IAP1 and JH protect PG from degeneration, whereas FTZ-F1 plays a proapoptotic role (43). *E93* may also be involved in PG degeneration in *B. germanica*, as it is known to have pro-apoptotic functions [for example, in the degeneration of salivary glands during *D. melanogaster* metamorphosis (44–46)], but further work would be necessary to assess this conjecture.

#### Myo depletion in the final nymphal stage produces the same effects as when depleted in the penultimate nymphal stage

Recent reports indicate that JH can inhibit ecdysone production in holometabolous insects, such as the fly *D. melanogaster* and the silkworm *Bombyx mori*. The effect is mediated by *Kr-h1*, which represses the expression of ecdysteroidogenic genes (37, 38). Therefore, it is plausible that the reduced expression of *nvd*, *phm*, and *dib* in dsMyo-treated cockroaches could be due to an increase in *Kr-h1* expression resulting from Myo depletion (Fig. 2E). To study this possibility, we carried out a series of RNAi experiments injecting the dsMyo (3  $\mu$ g) on the first day of the sixth (final) nymphal stage (N6D1) of *B. germanica*, when JH is practically absent (6) and *Kr-h1* expression is very low (7). The dsMyo treatment in N6D1 significantly reduced the Myo mRNA levels in

the PG, as measured on N6D2, N6D4, and N6D6 (Supplemental Fig. S3A). Regarding the ecdysteroidogenic enzymes, results showed that the expression of *nvd*, *phm*, and *dib* was significantly down-regulated in Myo-depleted cockroaches, as measured in N6D6, whereas that of *sad* was practically unaffected (Supplemental Fig. S3B). The dsMyo treatment up-regulated the expression of *Kr-h1*, and, consequently, the expression of *E93* was down-regulated (Supplemental Fig. S3C), as also occurred in the experiments depleting Myo in N5 (Fig. 5D). This could be due to an up-regulation of *jhant* expression in the CA resulting from Myo depletion, which could result in increased production of JH affecting the expression of *Kr-h1* in peripheral tissues, like the PG. To test this conjecture, we measured the expression of *jhant* in N6D6 in the CA of cockroaches treated with dsMyo on N6D1. We found that Myo mRNA in the CA had been significantly reduced by the treatment, and results additionally showed that *jhant* expression was dramatically up-regulated. *Kr-h1* expression tended to be up-regulated, probably due to an increase of JH production, and *E93* tended to be down-regulated, probably as a consequence of the increased *Kr-h1* expression (Supplemental Fig. S3D).

In the cockroaches treated with dsMyo in N6D1, we also studied the dynamics of growth and cell proliferation in the PG using EdU labeling. Dissections of Myo-depleted cockroaches in N6D6 revealed that PG size was greater than in controls (Supplemental Fig. S4A). Measurement of the PG arm width in N6D2, N6D4, and N6D6 showed that, as occurred with the treatment in N5D0, the gland from Myo-depleted cockroaches grew bigger than in the controls, which was well apparent in N6D6 (Supplemental Fig. S4B). In N6, intense cell division in the PG is only observed on d 0 and 1 and is almost undetectable on d 2 (Fig. 3). In the dsMyo treatments on N6D1, controls showed a very faint Edu labeling in N6D2, whereas the PG from Myo-depleted cockroaches showed a very active cell division this day, which vanished 2 d later (Supplemental Fig. S4C).

## DISCUSSION


Transcriptome data indicated that Myo expression is highly up-regulated in N5 of *B. germanica*. This general up-regulation in N5 is consistent with our present results obtained by means of real-time quantitative PCR, which show high levels of Myo expression at the beginning of N5 in the CC-CA and toward the mid-end of N5 in the PG.

Our present results also indicate that high Myo levels in N5 repress *jhant* expression in the CC-CA, which results in a reduction in JH production at the beginning of N6 (Fig. 6). In juvenile stages, JH, acting through Kr-h1, represses the expression of *ftz-f1*, which is a repressor of *iap1* expression in the PG. In N6, low levels of circulating JH result in lower *Kr-h1* expression in the PG, with the concomitant de-repression of *ftz-f1* expression, inhibition of *iap1*, and activation of the caspase-mediated gland degeneration mechanisms (Fig. 6). Because *E93* is a gene activated by ecdysone signaling, is a typical apoptosis-triggering factor and is repressed by Kr-h1, we conjecture that the proapoptotic action of FTZ-F1 might be mediated by *E93* (Fig. 6).

In the PG, Myo is expressed during N5 and N6, but there is a marked peak of expression toward the mid-end of N5. Our data indicate that high expression of *myo* correlates with high expression of ecdysone biosynthesis genes like *nvd*, *phm*, and *dib*. This may be due to the inhibition of Myo on *jhant* expression, and thus on JH production and concomitant *Kr-h1* expression, because Kr-h1 has been shown to repress the expression of ecdysteroidogenic enzyme genes (37, 38). In any case, the high expression of Myo in N5 surely contributes to the production of the large, metamorphic ecdysone pulse in N6. The data also suggest that the peak of Myo expression in N5 helps repress cell proliferation (at least in part by enhancing the expression of *dap*). Control over cell proliferation in N6 may be required to produce the subsequent metamorphic ecdysone pulse (Fig. 6).

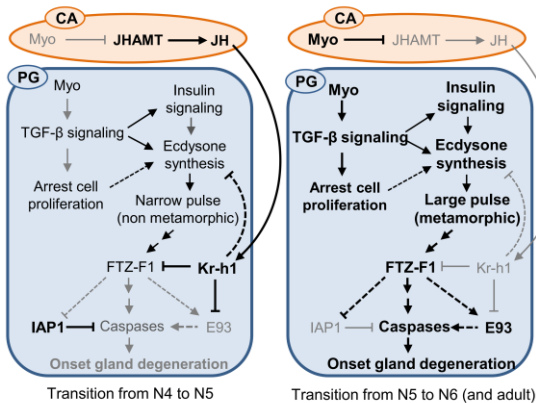


**Figure 6.** Roles of Myo in the CA and the PG in the transition to the premetamorphic stage of *B. germanica*. High levels of the indicated factors and corresponding interactions and final processes are indicated in bold; low levels are indicated in gray. Continuous lines indicate interactions suggested by the experiments. Dashed lines indicate interactions hypothesized.

Our overall findings point to Myo as a key trigger of the transition from penultimate to final (premetamorphic) nymphal stage in *B. germanica*. The repressor role of Myo on *jhamt* expression and JH production has previously been reported in the cricket *G. bimaculatus* (14). Although the functions of Myo in the PG were not examined in this insect, Ishimaru *et al.* (14) reported that Myo expression levels were high in this gland. We presume, therefore, that the trigger role Myo plays in the premetamorphic stage of *B. germanica* may be extended to *G. bimaculatus* and perhaps to other hemimetabolous insects. Myo expression in *D. melanogaster* does not exhibit an especially prominent peak during the larval and pupa stages in the Northern blot analyses published by Lo and Frasch (11) or in the transcriptome profiles reported by us (10). The larva–pupa–adult transition in the holometabolous metamorphosis requires a relatively rapid pattern of decreasing–increasing–decreasing JH production (2, 47). In this context, a dramatic interruption of JH production mediated by the repressive action of Myo on CA *jhamt* expression might not be suited for regulating metamorphosis in holometabolous species. We conclude that the role of Myo as a premetamorphosis trigger, at least in relation to the action in the CA and to JH, might be restricted to hemimetabolous insects, and this mechanism may have been lost in the evolutionary transition from hemimetabolous to holometabolous. 

## ACKNOWLEDGMENTS

The authors thank Guillem Ylla and Jose Carlos Montañes [both from the Institute of Evolutionary Biology (IBE), Spanish National Research Council-Universitat Pompeu Fabra] for helping with transcriptome comparisons and searching for genes in the *B. germanica* genome (available at <https://www.hgsc.bcm.edu/artthropods/german-cockroach-genomeproject>) as provided by the Baylor College of Medicine Human Genome Sequencing Center; Alba Ventos-Alfonso (IBE) for helping with different experiments and image treatment; and Maria-Dolores Pitolachs and Jose-Luis Maestro (IBE) for helpful discussions. This work was supported by Spanish Ministry of Economy and Competitiveness Grants CGL2012-36251 and CGL2015-64727-P (to X.B.), by Catalan Government Grant 2017 SGR 1030 (to X.B.), and by the European Fund for Economic and Regional Development (FEDER funds). O.K. received a Royal Thai Government Scholarship to do a PhD thesis in X.B. laboratory, Barcelona. The authors declare no conflicts of interest.

## AUTHOR CONTRIBUTIONS

X. Belles designed the research; O. Kamsoi performed the RNAi experiments and the real-time quantitative PCR measurements; O. Kamsoi and X. Belles analyzed the data; O. Kamsoi drafted a first version of the manuscript; and X. Belles wrote the final version of the manuscript.

## REFERENCES

1. Nijhout, H. F. (1994) *Insect Hormones*, Princeton University Press, Princeton, NJ, USA

2. Jindra, M., Palli, S. R., and Riddiford, L. M. (2013) The juvenile hormone signaling pathway in insect development. *Annu. Rev. Entomol.* **58**, 181–204

3. Belles, X., and Santos, C. G. (2014) The MEKRE93 (Methoprene tolerant-Krüppel homolog 1-E93) pathway in the regulation of insect metamorphosis, and the homology of the pupal stage. *Insect Biochem. Mol. Biol.* **52**, 60–68

4. Jindra, M., Uhlířová, M., Charles, J.-P., Smykal, V., and Hill, R. J. (2015) Genetic evidence for function of the bHLH-PAS protein Gce/Met as a juvenile hormone receptor. *PLoS Genet.* **11**, e1005394

5. Jindra, M., Bellés, X., and Shinoda, T. (2015) Molecular basis of juvenile hormone signaling. *Curr. Opin. Insect Sci.* **11**, 39–46

6. Treiblmayr, K., Pascual, N., Pitolachs, M.-D., Keller, T., and Belles, X. (2006) Juvenile hormone titer versus juvenile hormone synthesis in female nymphs and adults of the German cockroach, *Blattella germanica*. *J. Insect Sci.* **6**, 1–7

7. Lozano, J., and Belles, X. (2011) Conserved repressive function of Krüppel homolog 1 on insect metamorphosis in hemimetabolous and holometabolous species. *Sci. Rep.* **1**, 163

8. Belles, X. (2017) MicroRNAs and the evolution of insect metamorphosis. *Annu. Rev. Entomol.* **62**, 111–125

9. Lozano, J., Montañes, R., and Belles, X. (2015) MiR-2 family regulates insect metamorphosis by controlling the juvenile hormone signaling pathway. *Proc. Natl. Acad. Sci. USA* **112**, 3740–3745

10. Ylla, G., Pitolachs, M. D., and Belles, X. (2018) Comparative transcriptomics in two extreme neopterans reveals general trends in the evolution of modern insects. *iScience* **4**, 164–179

11. Lo, P. C., and Frasch, M. (1999) Sequence and expression of myoglianin, a novel *Drosophila* gene of the TGF-beta superfamily. *Mech. Dev.* **86**, 171–175

12. Peterson, A. J., and O'Connor, M. B. (2014) Strategies for exploring TGF-β signaling in *Drosophila*. *Methods* **68**, 183–193

13. Awasaki, T., Huang, Y., O'Connor, M. B., and Lee, T. (2011) Glia instruct developmental neuronal remodeling through TGF-β signaling. *Nat. Neurosci.* **14**, 821–823

14. Ishimaru, Y., Tomonari, S., Matsuoka, Y., Watanabe, T., Miyawaki, K., Bando, T., Tomioka, K., Ohuchi, H., Noji, S., and Mito, T. (2016) TGF-β signaling in insects regulates metamorphosis via juvenile hormone biosynthesis. *Proc. Natl. Acad. Sci. USA* **113**, 5634–5639

15. Huang, J., Tian, L., Peng, C., Abdou, M., Wen, D., Wang, Y., Li, S., and Wang, J. (2011) DPP-mediated TGFβ signaling regulates juvenile hormone biosynthesis by activating the expression of juvenile hormone acid methyltransferase. *Development* **138**, 2283–2291

16. Ciudad, L., Pitolachs, M.-D., and Belles, X. (2006) Systemic RNAi of the cockroach vitellogenin receptor results in a phenotype similar to that of the *Drosophila* yolkless mutant. *FEBS J.* **273**, 325–335

17. Chehrehasa, F., Meedeniya, A. C. B., Dwyer, P., Abrahamson, G., and Mackay-Sim, A. (2009) EdU, a new thymidine analogue for labelling proliferating cells in the nervous system. *J. Neurosci. Methods* **177**, 122–130

18. Misof, B., Liu, S., Meusemann, K., Peters, R. S., Donath, A., Mayer, C., Frandsen, P. B., Ware, J., Flouri, T., Beutel, R. G., Niehuis, O., Petersen, M., Izquierdo-Carrasco, F., Wappler, T., Rust, J., Aberer, A. J., Aspöck, U., Aspöck, H., Bartel, D., Blanke, A., Berger, S., Böhm, A., Buckley, T. R., Calcott, B., Chen, J., Friedrich, F., Fukui, M., Fujita, M., Greve, C., Grobe, P., Gu, S., Huang, Y., Jermiin, L. S., Kawahara, A. Y., Krogmann, L., Kubiak, M., Lanfear, R., Letsch, H., Li, Y., Li, Z., Li, J., Liu, H., Machida, R., Mashimo, Y., Kapli, P., McKenna, D. D., Meng, G., Nakagaki, Y., Navarrete-Heredia, J. L., Ott, M., Ou, Y., Pass, G., Podsiadlowski, L., Pohl, H., von Reumont, B. M., Schütte, K., Sekiya, K., Shimizu, S., Slipinski, A., Stamatakis, A., Song, W., Su, X., Szucsich, N. U., Tan, M., Tan, X., Tang, M., Tan, X., Timelthaler, G., Tomizuka, S., Trautwein, M., Tong, X., Uchifume, T., Wabzl, M. G., Wiegmann, B. M., Wilbrandt, J., Wipfler, B., Wong, T. K. F., Wu, Q., Wu, G., Xie, Y., Yang, S., Yang, Q., Yeates, D. K., Yoshizawa, K., Zhang, Q., Zhang, R., Zhang, W., Zhang, Y., Zhao, J., Zhou, C., Zhou, L., Ziesmann, T., Zou, S., Li, Y., Xu, X., Zhang, Y., Yang, H., Wang, J., Wang, J., Kjer, K. M., and Zhou, X. (2014) Phylogenomics resolves the timing and pattern of insect evolution. *Science* **346**, 763–767

19. Ureña, E., Manjón, C., Franch-Marro, X., and Martín, D. (2014) Transcription factor E93 specifies adult metamorphosis in hemimetabolous and holometabolous insects. *Proc. Natl. Acad. Sci. USA* **111**, 7024–7029

20. Santos, C. G., Fernandez-Nicolas, A., and Belles, X. (2016) Smads and insect hemimetabolous metamorphosis. *Dev. Biol.* **417**, 104–113

21. Peterson, A. J., and O'Connor, M. B. (2013) Activin receptor inhibition by Smad2 regulates *Drosophila* wing disc patterning through BMP-response elements. *Development* **140**, 649–659



22. Zheng, X., Wang, J., Haerry, T. E., Wu, A. Y.-H., Martin, J., O'Connor, M. B., Lee, C.-H. J., and Lee, T. (2003) TGF-beta signaling activates steroid hormone receptor expression during neuronal remodeling in the *Drosophila* brain. *Cell* **112**, 303–315
23. Gibbens, Y. Y., Warren, J. T., Gilbert, L. L., and O'Connor, M. B. (2011) Neuroendocrine regulation of *Drosophila* metamorphosis requires TGFbeta/Activin signaling. *Development* **138**, 2693–2703
24. Románá, I., Pascual, N., and Belles, X. (1995) The ovary is a source of circulating ecdysteroids in *Blattella germanica* (Diptera: Dictyoptera: Blattellidae). *Eur. J. Entomol.* **93**, 93–103
25. Cruz, J., Martín, D., Pascual, N., Maestro, J. L., Piulachs, M. D., and Bellés, X. (2003) Quantity does matter. Juvenile hormone and the onset of vitellogenesis in the German cockroach. *Insect Biochem. Mol. Biol.* **33**, 1219–1225
26. Chiang, A.-S., Tsai, W.-H., and Schal, C. (1995) Neural and hormonal regulation of growth of corpora allata in the cockroach, *Diploptera punctata*. *Mol. Cell. Endocrinol.* **115**, 51–57
27. Sakurai, S. (2005) Feedback regulation of prothoracic gland activity. In *Comprehensive Molecular Insect Science* (Gilbert, L. L., Iatrou, K., and Gill, S. S., eds.), pp. 409–431, Elsevier Pergamon, San Diego, CA, USA
28. Barr, A. R., Heldt, F. S., Zhang, T., Bakal, C., and Novák, B. (2016) A dynamical framework for the all-or-none G1/S transition. *Cell Syst.* **2**, 27–37
29. Bertoli, C., Skotheim, J. M., and de Bruin, R. A. M. (2013) Control of cell cycle transcription during G1 and S phases. *Nat. Rev. Mol. Cell Biol.* **14**, 518–528
30. Yang, W., Zhang, Y., Li, Y., Wu, Z., and Zhu, D. (2007) Myostatin induces cyclin D1 degradation to cause cell cycle arrest through a phosphatidylinositol 3-kinase/AKT/GSK-3 beta pathway and is antagonized by insulin-like growth factor 1. *J. Biol. Chem.* **282**, 3799–3808
31. Lane, M. E., Sauer, K., Wallace, K., Jan, Y. N., Lehner, C. F., and Vaessin, H. (1996) Dacapo, a cyclin-dependent kinase inhibitor, stops cell proliferation during *Drosophila* development. *Cell* **87**, 1225–1235
32. Swanson, C. I., Meserve, J. H., McCarter, P. C., Thieme, A., Mathew, T., Elston, T. C., and Duronio, R. J. (2015) Expression of an S phase-stabilized version of the CDK inhibitor Dacapo can alter endoreplication. *Development* **142**, 4288–4298
33. Nakayama, K., Ishida, N., Shirane, M., Inomata, A., Inoue, T., Shishido, N., Horii, I., Loh, D. Y., and Nakayama, K. (1996) Mice lacking p27(Kip1) display increased body size, multiple organ hyperplasia, retinal dysplasia, and pituitary tumors. *Cell* **85**, 707–720
34. Kiyokawa, H., Kineman, R. D., Manova-Todorova, K. O., Soares, V. C., Hoffman, E. S., Ono, M., Khanam, D., Hayday, A. C., Frohman, L. A., and Koffi, A. (1996) Enhanced growth of mice lacking the cyclin-dependent kinase inhibitor function of p27(Kip1). *Cell* **85**, 721–732
35. Niwa, R., and Niwa, Y. S. (2014) Enzymes for ecdysteroid biosynthesis: their biological functions in insects and beyond. *Biosci. Biotechnol. Biochem.* **78**, 1283–1292
36. Pary, J.-P., Blais, C., Bernard, F., Warren, J. T., Petryk, A., Gilbert, L. L., O'Connor, M. B., and Dauphin-Villeman, C. (2005) A role for betaFTZ-F1 in regulating ecdysteroid titers during post-embryonic development in *Drosophila melanogaster*. *Dev. Biol.* **282**, 84–94
37. Liu, S., Li, K., Gao, Y., Liu, X., Chen, W., Ge, W., Feng, Q., Palli, S. R., and Li, S. (2018) Antagonistic actions of juvenile hormone and 20-hydroxyecdysone within the ring gland determine developmental transitions in *Drosophila*. *Proc. Natl. Acad. Sci. USA* **115**, 139–144
38. Zhang, T., Song, W., Li, Z., Qian, W., Wei, L., Yang, Y., Wang, W., Zhou, X., Meng, M., Peng, J., Xia, Q., Perrimon, N., and Cheng, D. (2018) Krüppel homolog 1 represses insect ecdysone biosynthesis by directly inhibiting the transcription of steroidogenic enzymes. *Proc. Natl. Acad. Sci. USA* **115**, 3960–3965
39. Mané-Padrós, D., Cruz, J., Vilaplana, L., Pascual, N., Bellés, X., and Martín, D. (2008) The nuclear hormone receptor BgE75 links molting and developmental progression in the direct-developing insect *Blattella germanica*. *Dev. Biol.* **315**, 147–160
40. Cruz, J., Martín, D., and Bellés, X. (2007) Redundant ecdysis regulatory functions of three nuclear receptor HR3 isoforms in the direct-developing insect *Blattella germanica*. *Mech. Dev.* **124**, 180–189
41. Cruz, J., Nieva, C., Mané-Padrós, D., Martín, D., and Bellés, X. (2008) Nuclear receptor BgFTZ-F1 regulates molting and the timing of ecdysteroid production during nymphal development in the hemimetabolous insect *Blattella germanica*. *Dev. Dyn.* **237**, 3179–3191
42. Brummel, T., Abdollah, S., Haerry, T. E., Shimeil, M. J., Merriam, J., Raftery, L., Wrana, J. L., and O'Connor, M. B. (1999) The *Drosophila* activin receptor baboon signals through dSmad2 and controls cell proliferation but not patterning during larval development. *Genes Dev.* **13**, 98–111
43. Mané-Padrós, D., Cruz, J., Vilaplana, L., Nieva, C., Ureña, E., Bellés, X., and Martín, D. (2010) The hormonal pathway controlling cell death during metamorphosis in a hemimetabolous insect. *Dev. Biol.* **346**, 150–160
44. Baehrecke, E. H., and Thummel, C. S. (1995) The *Drosophila* E93 gene from the 93F early puff displays stage- and tissue-specific regulation by 20-hydroxyecdysone. *Dev. Biol.* **171**, 85–97
45. Lee, C. Y., Wendel, D. P., Reid, P., Lam, G., Thummel, C. S., and Baehrecke, E. H. (2000) E93 directs steroid-triggered programmed cell death in *Drosophila*. *Mol. Cell* **6**, 433–443
46. Lee, C. Y., and Baehrecke, E. H. (2001) Steroid regulation of autophagic programmed cell death during development. *Development* **128**, 1443–1455
47. Belles, X. (2011) Origin and evolution of insect metamorphosis. In *Encyclopedia of Life Sciences (ELS)*, John Wiley & Sons, Ltd, Chichester, United Kingdom

Received for publication July 23, 2018.  
Accepted for publication October 22, 2018.



### **3.2. E93-depleted adult insects preserve the prothoracic gland and molt again.**

Orathai Kamsoi, Xavier Belles\*

\* Institute of Evolutionary Biology (CSIC-University of Pompeu Fabra), Passeig Maritim 37, 08003 Barcelona, Spain.

E93-depleted adult insects preserve the prothoracic gland and molt again. [bioRxiv \(2020\)](#). Publication in progress in *Development* (2020).



## **E93-depleted adult insects preserve the prothoracic gland and molt again**

Orathai Kamsoi, and Xavier Belles<sup>1</sup>

Institute of Evolutionary Biology (CSIC-Universitat Pompeu Fabra),  
Passeig Maritim 37, 08003 Barcelona, Spain

<sup>1</sup> Corresponding author. *E-mail address:* [xavier.belles@ibe.upf-csic.es](mailto:xavier.belles@ibe.upf-csic.es)

### ***Summary statement***

The prothoracic gland disintegrates after insect metamorphosis. It was believed that the factor FTZ-F1 determines this disintegration. This work reveals that FTZ-F1 action is mediated by the factor E93.

### **ABSTRACT**

Insect metamorphosis originated around the middle Devonian, associated with the innovation of the final molt; this occurs after the histolysis of the prothoracic gland (PG; which produces the molting hormone) in the first days of adulthood. We previously hypothesized that transcription factor E93 was crucial in the emergence of metamorphosis, since it triggers metamorphosis in extant insects. This work on the cockroach *Blattella germanica* reveals that E93 also plays a crucial role in the histolysis of PG, which fits the above hypothesis. Previous studies have shown that the transcription factor FTZ-F1 is essential for PG histolysis. We have found that FTZ-F1 depletion, towards the end of the final nymphal instar, downregulates the expression of *E93*, while E93-depleted nymphs molt to adults that retain a functional PG. Interestingly, these adults are able to molt again, which is exceptional in insects. The study of insects able to molt again

in the adult stage may reveal clues as to how nymphal epidermal cells definitively become adult cells, and if it is possible to revert this process.

**KEY WORDS:** Prothoracic gland, E93, FTZ-F1, ecdysone, insect metamorphosis, MEKRE93 pathway

## **INTRODUCTION**

One of the most successful innovations in insect evolution is metamorphosis, as shown by the fact that more than 95% of extant insects develop through this type of postembryonic transformation. The simplest mode of metamorphosis, hemimetaboly, or incomplete metamorphosis, originated with the clade Pterygota (viz. the presence of wings), around the middle Devonian, ca. 400 Mya. Subsequently, during the early Carboniferous, ca. 350 Mya, holometaboly, or complete metamorphosis, evolved from hemimetaboly (Belles, 2020, 2019a). Consubstantial with the emergence of wings and hemimetabolan metamorphosis is the innovation of the final molt, mainly achieved through the histolysis of the prothoracic gland (PG; the gland that produces the molting hormone), which takes place after the winged and reproductively competent adult stage has been reached.

The molecular mechanism that regulates insect metamorphosis is condensed in the MEKRE93 pathway (Belles and Santos, 2014), through which juvenile hormone (JH) bound to its receptor Methoprene tolerant (Met), and induces the expression of Krüppel homolog 1 (Kr-h1); this, in turn, represses the expression of E93. The players most directly involved in regulating metamorphosis are Kr-h1, the transducer of the antimetamorphic signal of JH, and E93, the master trigger of

metamorphosis (see (Belles, 2019b)). *E93* was originally discovered as an ecdysone-induced late prepupal specific gene, during research into the histolysis of the salivary glands in *Drosophila melanogaster* metamorphosis, a process in which *E93* plays a key role (Baehrecke and Thummel, 1995; Lee et al., 2000; C T Woodard et al., 1994). Subsequently, Mou et al. (Mou et al., 2012) found that *E93* is widely expressed in adult cells that form in the pupa of *D. melanogaster*, being required for morphogenesis patterning processes. Further experiments revealed that *E93*-depleted larvae of *D. melanogaster* are able to pupate but die at the end of the pupal stage. Similar results were observed in the beetle *Tribolium castaneum*, where *E93* depletion prevented the pupal-adult transition, resulting in the formation of a supernumerary second pupa (Ureña et al., 2014). Moreover, studies on the cockroach *Blattella germanica* have revealed that *E93* depletion prevents the nymph-adult transition, resulting in reiterated supernumerary nymphal instars (Ureña et al., 2014), and that the expression of *E93* in juvenile nymphs is inhibited by *Kr-h1*, which establishes the MEKRE93 pathway (Belles and Santos, 2014).

Importantly, the MEKRE93 pathway, including the role of *E93* as a metamorphosis trigger, is conserved in extant metamorphosing insects (Belles, 2020). This suggests that it was operative in the pterygote last common ancestor. If this is true, then a single mechanism, the MEKRE93 pathway and *E93* in particular, might have simultaneously promoted metamorphosis, including wing maturation, and PG histolysis (and hence the final molt), at the origin of the Pterygota (Belles, 2019a). The role of *E93* as a promoter of metamorphosis and wing maturation has been thoroughly demonstrated (Belles and Santos, 2014; Mou et al., 2012; Ureña et al., 2014; Uyehara

et al., 2017). In contrast, nothing is known about the possible role of *E93* in PG histolysis. The aim of this work is to explore this possibility using *B. germanica* as a model.

Histolysis of cells and tissues through programmed cell death (PCD) is consubstantial with metamorphosis, especially in holometabolans, as during this process, new structures are generated, while others disappear. In this way, some cells and tissues disintegrate (like the salivary glands), whereas others undergo remodeling, with partial cell replacement (like in the fat body) (Tettamanti and Casartelli, 2019). Intensive studies based on the larva-pupa transition of *D. melanogaster*, have demonstrated the determinant role of ecdysone signaling in PCD processes that affect the salivary glands, midgut and fat body. Ecdysone, or rather its most bioactive derivative, 20-hydroxyecdysone (20E), binds the receptor, EcR, forms a complex with the coreceptor retinoid X receptor (RXR), and initiates a gene expression cascade (Hill et al., 2013) that includes *fushi tarazu-factor 1* (*ftz-f1*) and *E93* among the most important genes in the context of PCD (Baehrecke and Thummel, 1995; Broadus et al., 1999). Next, the corresponding proteins promote the expression of PCD genes, like *reaper* (*rpr*) and *head involution defective* (*hid*), as well as caspases and other direct PCD mediators (Jiang et al., 2000; Lee et al., 2000). Other important players are the inhibitors of apoptosis (IAPs), which protect cells and tissues from PCD by preventing caspase activity (Orme and Meier, 2009), although their inhibitory activity on PCD is counteracted by *Rpr* and *Hid* (Martin, 2002). Therefore, at the larva-pupa transition, downregulation of *iap1* expression provides the competence for PCD triggered by cell death factors (Orme and Meier, 2009; Yin et al., 2007; Yin and Thummel, 2005).



Although E93 had never been related to the PG disintegration, it has been characterized as promoting PCD during metamorphosis in various tissues and species. The most thorough studies have been carried out on the salivary glands of *D. melanogaster*, where stage- and tissue-specific expression of E93 triggers their histolysis (Baehrecke and Thummel, 1995; Berry and Baehrecke, 2007; C.-Y. Lee et al., 2002; Lee et al., 2000; C T Woodard et al., 1994). The action of E93 on PCD during *D. melanogaster* metamorphosis has also been reported to occur in the midgut (C. Y. Lee et al., 2002; Lee and Baehrecke, 2001) and fat body (Liu et al., 2014). More recently, E93 has been shown to play the same PCD role in the fat body of the silkworm *Bombyx mori* (Liu et al., 2015).

In *B. germanica*, our model, previous studies have revealed that *iap1* expression in the PG declines during the nymph-adult transition, which is followed by PG histolysis. In *B. germanica*, PG histolysis is regulated by 20E signaling, which leads to a dramatic upregulation of *ftz-f1* expression, the gene product of this plays a crucial role in the PCD process (D. Mané-Padrós et al., 2010). Given the above antecedents, in this work we conjectured that the PCD action of FTZ-F1 on the PG might be mediated by E93. This presumption has been confirmed, as FTZ-F1 depletion towards the end of the final nymphal instar downregulates *E93* expression, while E93-depletion results in adults that retain a functional PG. It was still more intriguing, however, to observe that the E93-depleted adults were able to molt again. Studying this phenotype could provide important clues as to how nymphal epidermal cells definitively become adult cells, and if it is possible to revert that process.

## RESULTS

### ***E93* expression is tissue-specific**

We studied the expression pattern of *E93* in various tissues involved in metamorphosis, namely the PG, the corpora cardiaca-corpora allata (CC-CA) complex, the epidermal tissue (represented by the abdominal tergites two to seven), and the wing pads. We studied the three most important premetamorphic instars, the fourth (antepenultimate) nymphal instar (N4), the penultimate nymphal instar (N5) and the final nymphal instar (N6). At the same time, we measured *ftz-f1* expression given its relationship with PG histolysis. The PG patterns are clearly differentiated from those of other tissues (Fig. 1). The highest expression levels of *E93* in the CC-CA complex, epidermis, and wing pads are found towards the middle of N6, while in the PG they peak in N6D8. As for *ftz-f1*, there is a single expression peak in N6D8 in the PG (coinciding with that of *E93*), while in the other tissues the expression levels fluctuate as a result of the pulses of 20E that occur around every molt (Fig. 1).

### ***E93* interference late in the final nymphal instar triggers the formation of adults that molt once again**

To maximize the depletion of *E93* transcripts in the PG while only minimally affecting the other metamorphic tissues, we injected dsRNA targeting *E93* (ds*E93*) into N6D6 insects. At this stage, the *E93* expression peak had already occurred in the CC-CA complex, tergites, and wing pads, while it was still to come in the PG. Insects injected in N6D6 with either dsMock (control) (n = 67) or ds*E93* (n = 132) all molted to adults two days later. The insects from control experiments

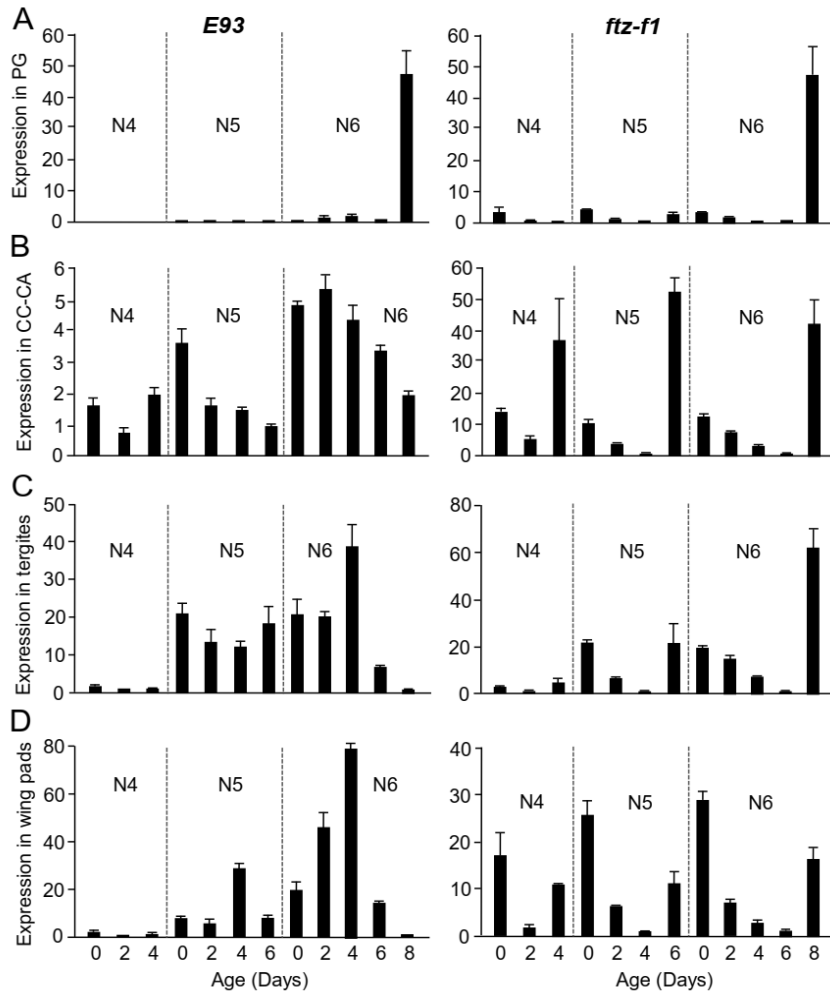


**Figure 1.** *E93* and *ftz-f1* expression in the last nymphal instars of *Blattella germanica*. (A) Expression in the prothoracic gland (PG). (B) Expression in corpora cardiaca-corpora allata (CC-CA) complex. (C) Expression in tergites. (D) Expression in wing pads. The expression was measured during the fourth (antepenultimate) nymphal instar (N4), the fifth (penultimate) nymphal instar (N5) and the sixth (final) nymphal instar (N6) in female insects. The results are indicated as copies of the examined mRNA per 1000 copies of BgActin-5c mRNA, and are expressed as the mean  $\pm$  SEM (n=3).

presented a normal adult external morphology, with well-shaped and completely extended forewings and hindwings (Fig. 2A). As for the dsE93-treated nymphs, 85.6% molted to adults presenting a normal external appearance, with well-shaped and completely extended forewings and hindwings, and 14.4% molted to adults with the wings only partially extended, particularly the hindwings (Fig. 2A).

It has been shown previously that the adult of *B. germanica* start disintegrating the PG after the imaginal molt, and three days later the disintegration is very apparent, since only the axes of muscle, tracheae and nerve of the X-shaped gland, and a few secretory cells, are observed (Romaña et al., 1995). In our RNAi experiments, control adults culminated the histolysis and disintegration process in 3 to 5 days, while the E93-depleted adults retained the integrity of the PG, as observed 8 days after the imaginal molt, when its general morphology resembles that of an N6 PG (Fig. 2B). There is an intriguing difference in cell proliferation: normally, N6 PGs undergo cell division during the first two days of the instar (Kamsoi and Belles, 2019), whereas no cell division was observed in the PG of E93-depleted adults (Fig. S1).

After the imaginal molt, the E93-depleted adults started to molt again, the first symptoms of which were detected 8 days after that molt, when shadows of the new cuticular structures, including new mandibles, could be observed by transparency under the old cuticle. On day 9 the new mandibles were clearly defined (Fig. 2C). One day later, the E93-depleted adults tried to undertake ecdysis, which could not be completed as they were unable to shed the exuvia (Fig. 2D). Even the wings undertook a new apolysis, and a new set of wing veins could be seen by transparency under the veins of the E93-depleted adults, being most clearly visible in the forewings (Fig. 2E).

### **Molting of E93-depleted adults results from the effective depletion of E93 in the PG, which remains functional**

We determined the efficiency of the RNAi treatment by measuring the E93 transcript decrease 48 h after the dsRNA treatment, i.e., in N6D8. Results showed that E93 mRNA levels were significantly depleted (ca. 77%) in the PG (Fig. 3A). E93 transcript depletion was also observed in the other tissues studied (CC-CA, tergites, and wing pads), although the baseline levels were low, as expected from the expression patterns (Fig. 3A).

Simultaneous measurement of *ftz-fl* mRNA levels indicated that E93 depletion did not affect *ftz-fl* expression in the PG, but did trigger a dramatic up-regulation in the CC-CA, tergites and wing pads (Fig. 3A). We also observed that the interference of E93 in the late final nymphal instar did not significantly affect the expression in epidermal tissues of *Kr-h1* and *BR-C*, two important genes in adult morphogenesis (Fig. 3B).

We measured the expression of two genes with opposite functions in PG histolysis, *iap1* and *caspase-1* (*casp-1*), on the last day of the final nymphal instar (N6D8), and the first day of the adult stage (Add1). The results showed that in N6D8 *iap1* expression is significantly higher in E93-depleted insects, although in Add1 this returns to levels similar to those seen in the controls. In contrast, *casp-1* expression in Add1 is significantly lower than that found in the controls (Fig. 3C).

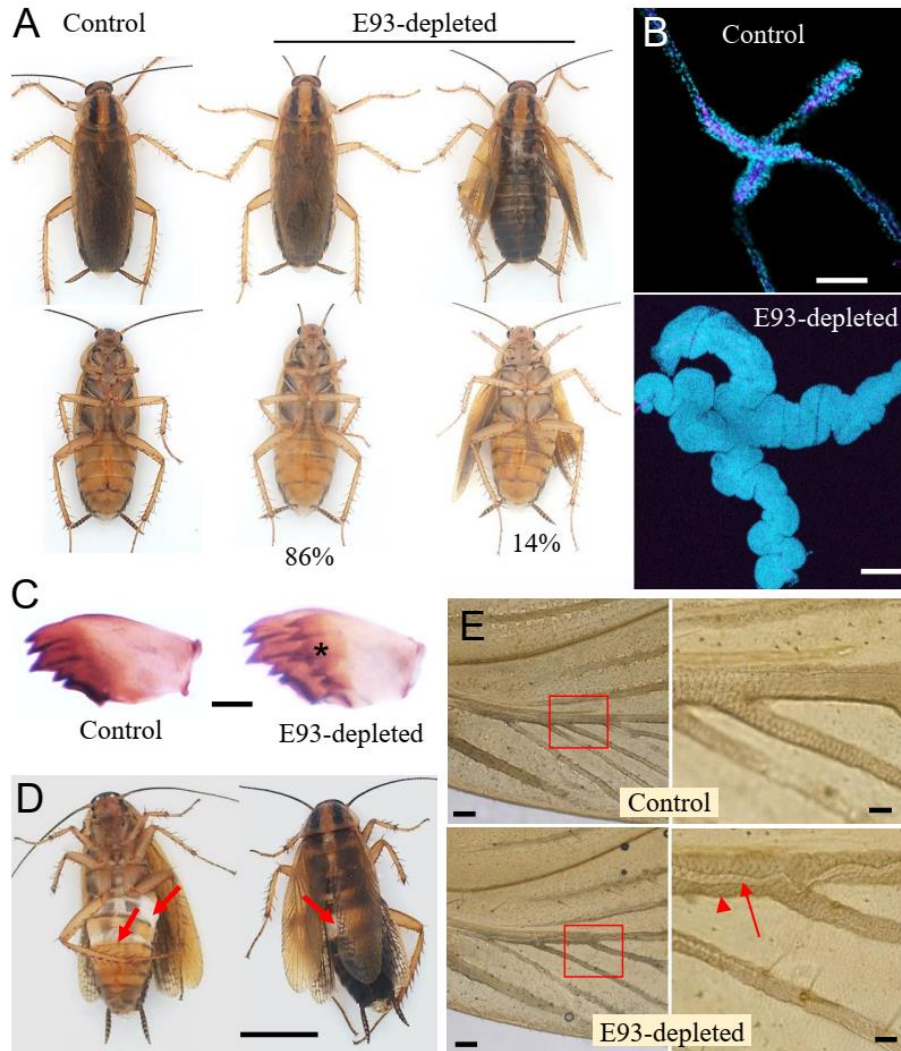


**Figure 2. Effect of *E93* mRNA depletion in the imaginal molt of *Blattella germanica*.** (A) Dorsal and ventral views of control and E93-depleted adults. Sixth instar females nymphs were treated on day 6 with dsMock (control) or dsE93, and the morphology after the imaginal molt was examined; the percentages of E93-depleted adults with extended and unextended wings are indicated; scale bar: 5 mm. (B) Prothoracic gland of control and E93-depleted adults on day 8 of adult life; the glands were stained with Phalloidin (pink) and DAPI (blue); scale bar: 0.1 mm. (C) Right mandible of control and E93-depleted adults on day 9 of adult life; note the new mandible formed under the old one in the E93-depleted adults after apolysis (asterisk); scale bar: 0.2 mm.

In addition, we measured the expression of the steroidogenic genes *neverland* (*nvd*), *phantom* (*phm*), *disembodied* (*dib*) and *shadow* (*sad*) in the PG of control and E93-depleted 8-day-old adults (Add8). All the genes were found to be efficiently expressed in the PG of E93-depleted adults, whereas, as expected, expression was very low or undetectable in the controls (Fig. 3D). Consistently, the ecdysone-dependent genes *E75A* and *HR3A* were significantly expressed in the PG of E93-depleted Add8, suggesting that the gland was producing and was exposed to ecdysteroids, whereas the expression of these two genes was undetectable in the PG of the Add8 controls (Fig. 3E). Indeed, the expression of *E75A* and *HR3A* in the PG of E93-depleted Add8 is relatively comparable to that measured in untreated N6D6 (Fig. 3E), the age of the final nymphal instar at which the ecdysone pulse is produced (Cruz et al., 2003).

### **PG death induced by FTZ-F1 is mediated by E93**

We had previously reported that FTZ-F1 plays a critical role in the histolysis of PG in *B. germanica* (D. Mané-Padrós et al., 2010). Given that E93 depletion in the PG prevented gland histolysis (Fig. 2C), we wondered about the relationships between FTZ-F1 and E93 in the process. As discussed above, E93 appears to repress *ftz-fl* expression in

---

**Figure 2. (Continued)** (D) E93-depleted adults attempting to molt on day 10 of adult life; the arrows show areas where the old cuticle separated, showing the new cuticle formed after the apolysis; scale bar: 5 mm. (E) Basal part of the left forewing of control and E93-depleted adults on day 9 of adult life; the part indicated with the red square is shown at higher magnification in the panels on the right; note the new veins (arrow) formed under the old ones (arrowhead) in the E93-depleted adults after apolysis; scale bar: 0.2 mm (left panels), 0.05 mm (right panels).

CC-CA, tergites and wing pads, but not in the PG (Fig. 3A). A possible explanation for our observations on the action of E93 and FTZ-F1 on PG histolysis is to consider that FTZ-F1 would enhance the expression of E93 in the PG, and that E93 would be the gland histolysis effector.

To test this conjecture, we treated N6D7 female nymphs (i.e., one day before the peak of *ftz-fl* and *E93* in the PG, Fig. 1) with dsFTZ-F1. We then measured the expression of *E93* (and *ftz-fl*) in the PG. The results showed that the RNAi of *ftz-fl* was efficient, as 6 h after the treatment the corresponding mRNA levels became significantly reduced in the PG (as well as in the CC-CA). At 12 h, *ftz-fl* mRNA levels were still decreased in the PG, but the differences with respect to the controls were not statistically significant. Importantly, the mRNA levels of *E93* became significantly down-regulated in the PG at 6 and 12 h, but not in the CC-CA. At 24 h, *ftz-fl* mRNA levels in the PG recovered normal (control) levels, but the significant downregulation of *E93* expression persisted (Fig. 4).

### **E93-depleted adults have transcriptionally active epidermis and wings**

To characterize the type of cuticle synthesized by the E93-depleted adults, we first selected typically nymphal or typically adult cuticular proteins (NCPs and ACPs, respectively) from transcriptomic data covering the life cycle of *B. germanica*, which includes N6D6 and AdD5 (G. Ylla et al., 2018). As NCP genes, we selected *Bg10431*, *Bg10435* and *Bg15257*, which are clearly more expressed in N6 than in adults, whereas *Bg7254* and *Bg16458* were selected as ACP genes, as



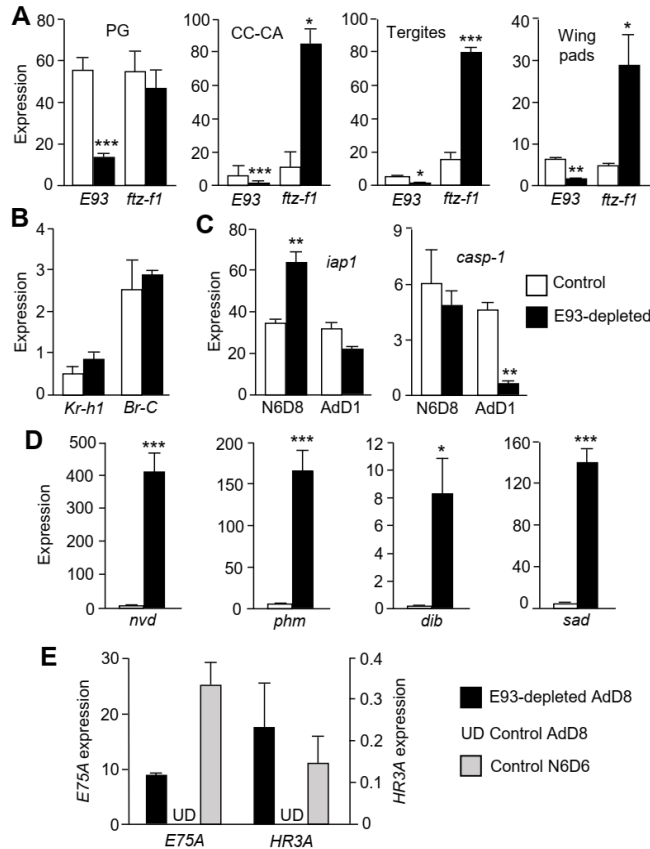


**Figure 3 Effect of E93 depletion on gene expression in *Blattella germanica*.** (A) Expression of *E93* and *ftz-f1* in the prothoracic gland (PG), corpora cardiaca-corpora allata (CC-CA) complex, tergites, and wing pads from E93-depleted insects and controls on day 8 of the sixth nymphal instar (N6D8). (B) Expression of *Kr-h1* and *BR-C* in tergites from E93-depleted insects and controls in N6D8. (C) Expression of *iap1* and *casp-1* in the PG of E93-depleted adults and controls in N6D8 and on the first day of the adult stage (AdD1). (D) Expression of the steroidogenic genes *nvd*, *phm*, *dib*, and *sad*, in the PG from E93-depleted adults and controls in AdD8. (E) Expression of the ecdysteroid signaling genes *E75A* and *HR3A* in the PG from E93-depleted adults and controls in AdD8, and in control nymphs in N6D6. The results are indicated as copies of the examined mRNA per 1000 copies of BgActin-5c mRNA, and expressed as the mean  $\pm$  SEM (n=3); the asterisks indicate statistically significant differences with respect to the controls (\*p<0.05, \*\*p<0.01, \*\*\*p<0.001) according to the student's *t*-test. In panel E "UD" means that mRNA levels were under the detection limit.

they are clearly more expressed in adults than in N6 (Fig. S2). The differences between N6 and adults suggested by these transcriptomic data were validated with quantitative real-time PCR (qRT-PCR) measurements (Fig. 5A). Then, measuring the NPC gene expression in AdD5 tergites showed that the levels of *Bg15257* mRNA were similar in controls and in E93-depleted insects, those of *Bg10435* tended to be higher in E93-depleted insects, whereas those of *Bg10431* were significantly higher in E93-depleted insects. The expression levels of the ACP genes were similar in E93-depleted and in controls (Fig. 5B).

Next, we wondered about the differences in ecdysteroid signaling in tergites, which could explain why E93-depleted adults can molt again, whereas control adults do not. The results showed that the genes of the two components of the ecdysone receptor, *EcR* and *RXR*, are similarly expressed both in E93-depleted and control adults. In contrast, the expression of the ecdysone-dependent genes *E75A* and *HR3A* was undetectable in control adults, whereas it was clearly measurable in E93-depleted adults (Fig. 5C).

Remarkably, wings also showed signs of molting (apolysis) (Fig. 2E). We therefore looked for possible differences in the transcriptional capacity of wings from E93-depleted and control adults. To do this, we measured the expression of the following wing-related genes (Elias-Neto and Belles, 2016) in the hindwings: *blistered* (*bs*), *Notch* (*N*), *Ultrabithorax* (*Ubx*), *scalloped* (*sd*), *nubbin* (*nub*) and *vestigial* (*vg*). For all these genes, the expression was low in the controls, whereas in E93-depleted adults they were four to ten times higher, depending on the gene (Fig. 4). Equivalent measurements carried out on the forewings gave similar results (not shown).

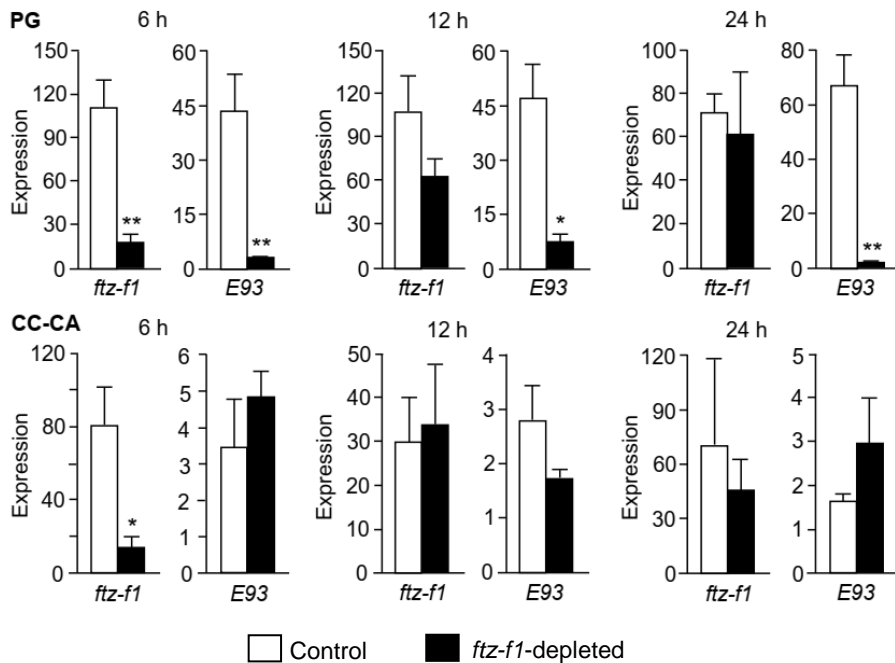


**Figure 4. Effect of FTZ-F1 depletion on *E93* expression in *Blattella germanica*.** Expression was measured in the prothoracic gland (PG), and corpora cardiaca-corpora allata (CC-CA) complex, 6, 12 and 24 h after the dsFTZ-F1 (or control) treatment in 7-day-old final instar nymphs (N6D7). (A) mRNA levels of *ftz-f1* in PG and CC-CA complex. (B) mRNA levels of *E93* in PG and CC-CA complex. The results are indicated as copies of the examined mRNA per 1000 copies of BgActin-5c mRNA, and are expressed as the mean  $\pm$  SEM (n=3); the asterisks indicate statistically significant differences with respect to the controls (\*p<0.05, \*\*p<0.01) according to the student's *t*-test.

### Treatments with 20E do not trigger molting in control adults

Given that molting of the *E93*-depleted adults is associated with the preservation of the PG and active ecdysone signaling in the epidermal cells (Fig. 5C), we wondered whether exogenously administered 20E to untreated adults might trigger molting. The differences in ecdysteroid titers between nymphs and adults are of approximately one order of magnitude. The maximum levels in N6D6 are ca. 2000 pg/ $\mu$ l of

hemolymph, whereas in 8-day-old adult females the levels are ca.125 pg/ $\mu$ l (Romaña et al., 1995). Thus, we injected a 0.5  $\mu$ g dose of 20E in 1  $\mu$ l volume into 8-day-old adult females (i.e., 2500 pg/ $\mu$ l of hemolymph, close to the physiological concentration in N6D6) (n=10). In another equivalent group, we injected the pharmacological dose of 5  $\mu$ g of 20E in 1  $\mu$ l volume (n=10). The controls received the same volume of solvent (n=10). Eight hours after the treatment, three insects of each group were used for qRT-PCR measurements, and the remaining insects were kept under observation for at least two weeks. Expression measurements of *EcR*, *RXR*, *E75A* and *HR3A* in tergites showed that neither 20E treatment increased the expression of *EcR* and *RXR*. In contrast, the expression of *E75A* and *HR3A* was upregulated by 20E in a dose-dependent manner (Fig. 5E). However, even after being treated with 5  $\mu$ g of 20E, the levels were at least an order of magnitude lower than in 8-day-old E93-depleted AdD8 (Fig. 5C). Importantly, none of the treated adults that we left alive showed symptoms of apolysis.

## DISCUSSION

### **The expression pattern of *E93* and *ftz-f1* in the PG is tissue-specific**

The expressions of *E93* and *ftz-f1* in the CC-CA, tergites, and wing pads in the last nymphal instars of *B. germanica* show a regularly fluctuating pattern, whereas in the PG there is a single expression peak of *E93* and *ftz-f1* on the last day of the final nymphal instar (Fig. 1). The characteristic *E93* and *ftz-f1* expression patterns in various tissues have previously been reported in *B. germanica* (D. Mané-Padrós et al., 2010; Ureña et al., 2014), but our results show that there is a very peculiar stage- and tissue-specific up-regulation of these two genes in

the PG, associated with the transition from the final nymphal instar to the adult. This PG-specific regulation of *E93* and *ftz-f1* is also suggested by the epistatic relationships between the two genes, as *E93* does not affect the *ftz-f1* expression in the PG but represses it in the other tissues studied (Fig. 3A), whereas FTZ-F1 enhances the expression of *E93* in the PG but not in other tissues, such as the CC-CA (Fig. 4).

### **E93 depletion in the PG prevents its histolysis after the imaginal molt**

Given the expression patterns in the different tissues (Fig. 1), injecting dsE93 on the penultimate day of the last nymphal instar had an important effect on E93 in the PG. The result was that the insects molted to adults that were morphologically similar to the controls (Fig. 2A), but their PG did not disintegrate (Fig. 2C). The fact that the PG of the E93-depleted adults did not degenerate and were fully active was also shown by their active transcription of the steroidogenic genes (Fig. 3D). The significant expression of the ecdysone-dependent genes *E75A* and *HR3A* in the PG of E93-depleted 8-day-old adults (Fig. 3E) also supports the notion that the glands are actively producing ecdysone. It is worth noting, however, that the long-term fate of the PG in E93-depleted adults is uncertain, since this gland does not present the typical cell proliferation pattern seen in the nymphal instars (Fig. S1), as the PG undergoes cell division during the first days of each instar (Kamsoi and Belles, 2019).

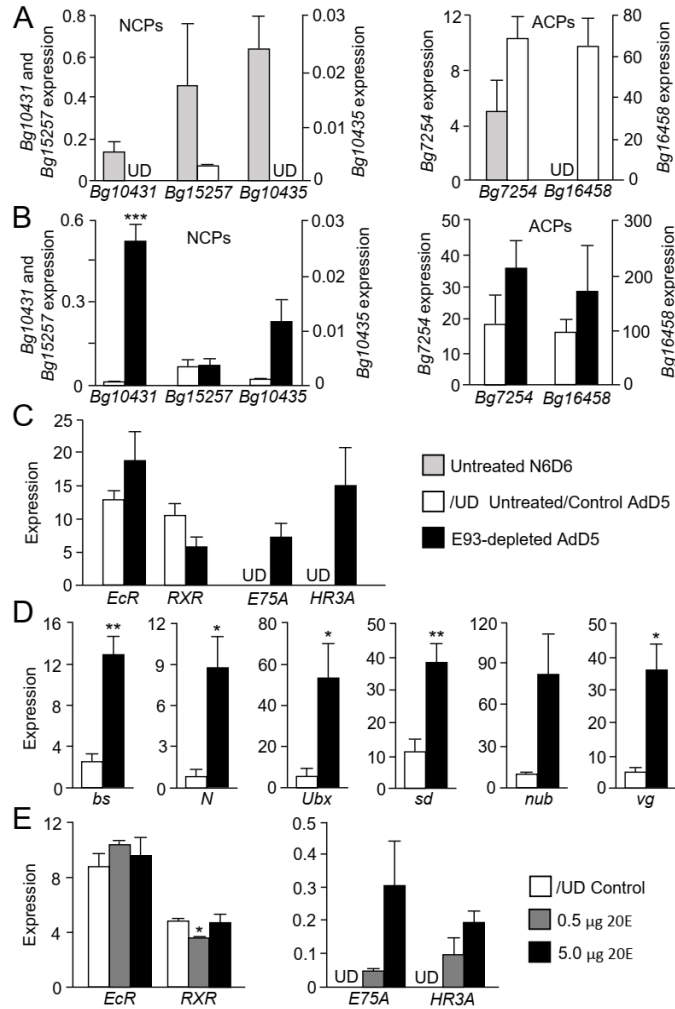


**Figure 5. Effect of *E93* depletion and 20E treatment on gene expression in adult *Blattella germanica* tissues.** (A) Expression of the nymphal cuticular protein (NCP) genes *Bg10431*, *Bg10435*, and *Bg15257*, and the adult cuticular protein (ACP) genes *Bg7254* and *Bg16458* in the epidermis of tergites in nymphs in day 6 of the sixth instar and in day 5 adults. (B) Expression of the same NCP and ACP genes in tergites of *E93*-depleted adults and controls in day 5 adults. (C) Expression of the ecdysteroid signaling genes: *EcR*, *RxR*, *E75A*, *HR3A* in tergites of *E93*-depleted adults and controls at day 8 of adult age. (D) Expression of wing-related genes: *blistered* (*bs*), *notch* (*N*), *nubbin* (*nub*), *scalloped* (*sd*), *ultrabithorax* (*Ubx*), and *vestigial* (*vg*) in the hindwings of *E93*-depleted adults and controls in day 8 adults. (E) Expression of *EcR*, *RXR*, *E75A* and *HR3A* in adults treated with 20E on day 8 of adult life.

Our observations revealed that E93-depletion kept the expression levels of *iap1* in the PG much higher than in the controls, when measured at the end of the final nymphal instar. Correspondingly, the expression of the effector caspase gene *casp-1* was not up-regulated in the PG of E93-depleted insects when measured on the first day of the adult stage (Fig. 3C). These E93 effects on inhibitors and promoters of PCD in the PG provide the mechanistic basis (see (Martin, 2002; Orme and Meier, 2009; Yin et al., 2007; Yin and Thummel, 2005)) for explaining why the gland did not disintegrate after the imaginal molt.

### **E93 triggers PG histolysis**

Previous studies reveal that FTZ-F1 depletion prevents PG histolysis in the context of *B. germanica* metamorphosis (D. Mané-Adrós et al., 2010). Here we show that FTZ-F1 depletion downregulates E93 in the PG (Fig. 4), suggesting that FTZ-F1 enhances the expression of E93 in this gland, which then triggers PG histolysis. This activating role of FTZ-F1 is not observed in other tissues, like the CC-CA (Fig. 4), where E93 expression is declining beyond day 6 of N6 (Fig. 1). The rapid recovery of the FTZ-F1 mRNA levels observed after the injection of dsFTZ-F1 (Fig. 4) is intriguing. Possibly, reaching high levels of FTZ-F1 expression in PG in N6D8 is crucial to undertake metamorphosis, and the gene response mechanisms to a mRNA depletion in this particular tissue and stage are especially efficient.

---

**Figure 5. (Continued)** The results are indicated as copies of the examined mRNA per 1000 copies of BgActin-5c mRNA, and are expressed as the mean  $\pm$  SEM (n=3); the asterisks indicate statistically significant differences with respect to the controls (\*p<0.05, \*\*p<0.01) according to the student's *t*-test. In panels B and D "UD" means that mRNA levels were under the detection limit.

It is known that FTZ-F1 modulates gene expression by interacting with an FTZ-F1 response element (F1RE) located in the target gene promoter (Lavorgna et al., 1991). Interestingly, the promoter region of *B. germanica* *E93* contains a canonical EcR response element (Cherbas et al., 1991; Kayukawa et al., 2017), as expected, but it also contains the sequence TCAAGGCAA that might be compatible with a F1RE (De Mendonça et al., 2002; Ohno et al., 1994) (Fig. S3). This again suggests that FTZ-F1 coactivates the expression of the ecdysone-dependent gene *E93*, although this coactivating effect seems specific of the PG.

Studies on *D. melanogaster* have previously demonstrated that FTZ-F1 acts as a competence factor during prepupal development, promoting the expression of stage-specific genes like *E93* (Broadus et al., 1999; C T Woodard et al., 1994). Moreover, *E93* has been shown to trigger PCD during metamorphosis in various tissues (salivary glands, fat body, and midgut) and species (*D. melanogaster*, and *B. mori*) (Baehrecke and Thummel, 1995; Berry and Baehrecke, 2007; C.-Y. Lee et al., 2002; C. Y. Lee et al., 2002; Lee et al., 2000; Lee and Baehrecke, 2001; Liu et al., 2014, 2015; Wang et al., 2012; C T Woodard et al., 1994). Therefore, although the PCD function of *E93* in the PG in the context of metamorphosis has not previously been reported, this function is not surprising given the above antecedents of *E93* as a PCD effector. The role of *E93* as an effector of PG histolysis after the imaginal molt supports the hypothesis that *E93* may have been a crucial factor underlying the mechanisms that facilitated the evolutionary innovation of insect metamorphosis (Belles, 2020, 2019a).



### **E93-depleted adults molt again**

Depletion of E93 at the end of the final nymphal instar protected the PG from histolysis, but the resulting adults were morphologically normal, in general. Only 14% of them presented partially unextended wings (Fig. 2A), a feature that is not uncommon even in control insects. According to the MEKRE93 pathway (Belles and Santos, 2014), the formation of morphologically normal adults is not surprising as the expression levels of *Kr-h1* (and *BR-C*) in the epidermis at the end of the final nymphal instar of E93-depleted insects are as low as in the controls (Fig. 3B). Interestingly, E93-depleted adults are able to molt again, undertaking apolysis, as shown by the double structures, notably the new mandibles, which can be observed by transparency under the old cuticle.

Even the wings of these E93-depleted adults undertake apolysis, as shown by the double veins observed, particularly in the hindwings (Fig. 2E), and they are transcriptionally active, according to the high expression levels of wing-related genes (Fig. 5C). Wing epidermal cells die and disappear after the imaginal molt, and only remain in the wing veins (Kimura et al., 2004). In E93-depleted adults we observed epidermal cells not only in the veins but also in the intervein regions. Interestingly, the newly formed veins in these adults were bigger than the old ones, thus being folded (Fig. 2E), suggesting that their epidermal cells undertook intensive cell proliferation. The high expression levels of *sd* (Fig. 5D) may have contributed to this proliferation, as this transcription factor acts together with the coactivator Yorkie, regulating Hippo pathway-responsive genes, and cell growth and proliferation (Huang et al., 2005; Zhang et al., 2008).

The cuticle of the E93-depleted adults expresses the ACP genes *Bg7254* and *Bg16458* at normally high levels, and those of the NCP gene *Bg15257* at normally low levels for an adult. However, the typically NCP genes *Bg10435* and, particularly, *Bg10431* are expressed at higher levels than normal (Fig. 5B). Thus, from the point of view of the cuticular proteins expression, the epidermis of the E93-depleted adults can be considered fundamentally adult, but with some nymphal character (Fig. 5B). In the epidermis of Add5 insects, the expression levels of *EcR* and *RXR* were similar in E93-depleted and control insects, but the expression of *E75A* and *HR3A* was undetectable in the latter (Fig. 5C). This might suggest that adult controls cannot molt due to low levels of circulating ecdysteroids.

### **Control adults do not molt even when supplied with 20E**

The above conjecture led us to administer 20E to control adults, at physiological and pharmacological doses. However, even the pharmacological doses resulted only in a modest increase of *E75A* and *HR3A* expression (Fig. 5E), despite there being operative expression of *EcR* and *RXR* (Fig. 5C). Thus, the treatment did not significantly upregulate the *E75A* and *HR3A* expression levels observed in E93-depleted Add8 insects (Fig. 5C), and did not trigger symptoms of molting. This is consistent with classically recorded experiments showing that ecdysteroids very rarely cause molting effects in adult insects, even when injected in doses as high as 3 mg/gr (Schneiderman et al., 1970). Intriguingly, however, a nymphal, active PG implanted into an adult of the Madeira cockroach *Rhyparobia* (= *Leucophaea*) *maderae* can trigger a subsequent molt, even though the insects are unable to undertake the corresponding ecdysis (Engelmann, 2002), just

as in our E93-depleted *B. germanica* adults. A possible explanation for the difference between implanted PG and injected 20E is that the implanted PG releases ecdysone according to a precise pattern of increase and decrease that is crucial for triggering the appropriate cascade of gene expression (Sakurai, 2005), which would not be reproduced by an injection of 20E. Another possibility is the occurrence of a PG factor that makes the epidermal cells competent to respond to ecdysteroids and produce a new cuticle, a putative factor whose production would be interrupted with the histolysis of the PG.

A great deal of work has been done on the pupal commitment of epidermal cells in lepidopterans, including *Manduca sexta* (Hiruma et al., 1991; Riddiford, 1981) and *B. mori* (Muramatsu et al., 2008), which essentially results from the action of ecdysteroids in the absence of JH. However, the possible “adult commitment” of epidermal cells could be due to other factors, among which E93 and/or FTZ-F1 could be involved. Although RNAi targeting E93 was performed at the end of N6, when its expression levels were already declining in the epidermis and wing pads, a certain level of E93-depletion was seen in those tissues, paralleled by a dramatic upregulation of *ftz-f1* expression (Fig. 3A). It is possible therefore, that relatively high levels of E93 and/or low levels of FTZ-F1 trigger the adult commitment of epidermal cells. Whatever the case, these molting adults could represent an interesting model in which to study the mechanisms determining the adult differentiation of insect epidermal cells, and perhaps find ways to revert this process.

## **MATERIALS AND METHODS**

### **Insects and dissections**

The *B. germanica* cockroaches used in the experiments were obtained from a colony fed on Panlab dog chow and water *ad libitum*, and reared in the dark at  $29 \pm 1^\circ\text{C}$  and 60-70% relative humidity. Prior to injection treatments, dissections and tissue sampling (PG, CC-CA complex, abdominal tergites two to seven, and wing pads), the cockroaches were anesthetized with carbon dioxide.

### **RNA extraction and retrotranscription to cDNA**

RNA extractions were carried out with the Gen Elute Mammalian Total RNA kit (Sigma-Aldrich). A sample of 300 ng from each RNA extraction was used for mRNA precursors in the case of wing disc, fat body, ovary and epidermis. All the volume extracted of CC-CA complex, PG and wing was lyophilized in the freeze-dryer FISHER-ALPHA 1-2 LDplus, and then resuspended in 8  $\mu\text{l}$  of milliQ  $\text{H}_2\text{O}$ . RNA quantity and quality were estimated by spectrophotometric absorption at 260 nm in a Nanodrop Spectrophotometer ND-1000® (NanoDrop Technologies). The RNA samples were then treated with DNase (Promega) and reverse transcribed with first Strand cDNA Synthesis Kit (Roche) and random hexamer primers (Roche).

### **Determination of mRNA levels by quantitative real-time PCR**

Measurements with qRT-PCR were carried out in an iQ5 Real-Time PCR Detection System (Bio-Lab Laboratories), using SYBR®Green (iTaq™ Universal SYBR® Green Supermix; Applied Biosystems). Reactions were carried out in triplicate, and a template-free control was included in all batches. Primers used to measure the transcripts of

interest are detailed in Table S1. The efficiency of each set of primers was validated by constructing a standard curve through three serial dilutions. Levels of mRNA were calculated relative to BgActin-5c mRNA (Table S1). Results are given as copies of the examined mRNA per 1000 copies of BgActin-5c mRNA.

### **RNA interference and 20E injections**

The detailed procedures for RNAi assays have been described previously (Ciudad et al., 2006). The primers used to prepare the dsRNA targeting *B. germanica* E93 and FTZ-F1 are described in Table S1. The sequence corresponding to the dsRNAs (dsE93 and dsFTZ-F1) was amplified by PCR and then cloned into a pST-Blue-1 vector. A 307 bp sequence from *Autographa californica* nucleopolyhedrosis virus (Accession number K01149.1) was used as control dsRNA (dsMock). A volume of 1  $\mu$ l of the dsRNA solution (3 $\mu$ g/ $\mu$ l) was injected into the abdomen of sixth instar female nymphs at the chosen ages, with a 5 $\mu$ l Hamilton microsyringe. Control nymphs were equivalently treated with dsMock. To study the possible molting effect of ecdysteroids in normal adults, a volume of 1  $\mu$ l of a 20E solution (0.5  $\mu$ g/ $\mu$ l or 5  $\mu$ g/ $\mu$ l) was injected into the abdomen of 8-day-old adult females with a 5 $\mu$ l Hamilton microsyringe, whereas controls received 1  $\mu$ l of solvent (water with 10% ethanol).

### **Morphological studies of PG**

Dissection of PG in female adults was carried out in Ringer's saline. The PG was fixed in 4% paraformaldehyde for 2 h and permeabilised in PBT (0.3% Triton in PBS), then it was first incubated in 300 ng/ml phalloidin-TRITC (Sigma) for 20 min, and subsequently in 1  $\mu$ g/ml

DAPI (Sigma) in PBT for 5 min. After three washes with PBT, the PG was mounted in Mowiol (Calbiochem) and observed with a fluorescence microscope Carl Zeiss-AXIO IMAGER.Z1. Wings and mandibles were dissected and mounted in Mowiol. Examinations and photographs were made with a stereomicroscope Zeiss DiscoveryV8.

### **Experiments to measure cell proliferation in PG**

For labeling DNA synthesis and dividing cells, we followed an approach *in vivo*, using the commercial EdU compound “Click-it EdU-Alexa Fluor® 594 azide” (Invitrogen, Molecular Probes). EdU was injected into the abdomen of adults at chosen ages with a 5 µl Hamilton microsyringe (1 µl of 20 mM EdU solution in DMSO). Control specimens received 1 µl of DMSO. The PG from treated specimens was dissected 1 h later, and processed for EdU visualization according to the manufacturer's protocol.

### **ACKNOWLEDGEMENTS**

O.K. received a Royal Thai Government Scholarship to do a PhD thesis in X.B. laboratory, in Barcelona. We thank Jose Carlos Montañes for helping with transcriptome comparisons and searching for genes in the *B. germanica* genome, available at <https://www.hgsc.bcm.edu/arthropods/german-cockroach-genomeproject>, as provided by the Baylor College of Medicine Human Genome Sequencing Center. We also thank Alba Ventos-Alfonso for helping in different experiments and image treatment, and Maria-Dolors Piulachs and Jose-Luis Maestro for helpful discussions.

## COMPETING INTERESTS

The authors declare no competing or financial interests.

## AUTHOR CONTRIBUTIONS

Conceptualization: OK, X.B.; Methodology: OK, X.B.; Formal analysis: OK, X.B.; Investigation: OK, X.B.; Resources: X.B.; Writing original draft: X.B., O.K.; Writing, review & editing: X.B.; Supervision: X.B.; Project administration: X.B.; Funding acquisition: X.B.

## FUNDING

This work was supported by Spanish Ministry of Economy and Competitiveness Grants CGL2012–36251 and CGL2015–64727-P (to X.B.), by Catalan Government Grant 2017 SGR 1030 (to X.B.), and by the European Fund for Economic and Regional Development (FEDER funds).

## REFERENCES

- Baehrecke, E. H. and Thummel, C. S. (1995). The *Drosophila* E93 gene from the 93F early puff displays stage- and tissue-specific regulation by 20-hydroxyecdysone. *Dev. Biol.* 171, 85–97.
- Belles, X. (2019a). Krüppel homolog 1 and E93: The doorkeeper and the key to insect metamorphosis. *Arch. Insect Biochem. Physiol.* 103, e21609.
- Belles, X. (2019b). The innovation of the final moult and the origin of insect metamorphosis. *Philos. Trans. R. Soc. B Biol. Sci.* 374, 20180415.
- Belles, X. (2020). *Insect metamorphosis. From natural history to*

- regulation of development and evolution*. Cambridge, MA: Academic Press.
- Belles, X. and Santos, C. G. (2014). The MEKRE93 (Methoprene tolerant-Krüppel homolog 1-E93) pathway in the regulation of insect metamorphosis, and the homology of the pupal stage. *Insect Biochem. Mol. Biol.* 52, 60–68.
- Berry, D. L. and Baehrecke, E. H. (2007). Growth arrest and autophagy are required for salivary gland cell degradation in *Drosophila*. *Cell* 131, 1137–1148.
- Broadus, J., McCabe, J. R., Endrizzi, B., Thummel, C. S. and Woodard, C. T. (1999). The *Drosophila*  $\beta$ FTZ-F1 orphan nuclear receptor provides competence for stage-specific responses to the steroid hormone ecdysone. *Mol. Cell* 3, 143–149.
- Cherbas, L., Lee, K. and Cherbas, P. (1991). Identification of ecdysone response elements by analysis of the *Drosophila* Eip28/29 gene. *Genes Dev.* 5, 121–131.
- Ciudad, L., Piulachs, M.-D. and Belles, X. (2006). Systemic RNAi of the cockroach vitellogenin receptor results in a phenotype similar to that of the *Drosophila* *yolkless* mutant. *FEBS J.* 273, 325–335.
- Cruz, J., Martín, D., Pascual, N., Maestro, J. L., Piulachs, M. D. and Belles, X. (2003). Quantity does matter. Juvenile hormone and the onset of vitellogenesis in the German cockroach. *Insect Biochem. Mol. Biol.* 33, 1219–1225.
- De Mendonça, R. L., Bouton, D., Bertin, B., Escriva, H., Noël, C., Vanacker, J. M., Cornette, J., Laudet, V. and Pierce, R. J. (2002). A functionally conserved member of the FTZ-F1 nuclear receptor family from *Schistosoma mansoni*. *Eur. J. Biochem.* 269, 5700–5711.



- Elias-Neto, M. and Belles, X. (2016). Tergal and pleural structures contribute to the formation of ectopic prothoracic wings in cockroaches. *R. Soc. Open Sci.* 3, 160347.
- Engelmann, F. (2002). Ecdysteroids, juvenile hormone and vitellogenesis in the cockroach *Leucophaea maderae*. *J Insect Sci.* 2, 20.
- Hill, R. J., Billas, I. M. L., Bonneton, F., Graham, L. D. and Lawrence, M. C. (2013). Ecdysone receptors: from the Ashburner model to structural biology. *Annu. Rev. Entomol.* 58, 251–271.
- Hiruma, K., Hardie, J. and Riddiford, L. M. (1991). Hormonal regulation of epidermal metamorphosis in vitro: Control of expression of a larval-specific cuticle gene. *Dev. Biol.* 144, 369–378.
- Huang, J., Wu, S., Barrera, J., Matthews, K. and Pan, D. (2005). The Hippo signaling pathway coordinately regulates cell proliferation and apoptosis by inactivating Yorkie, the *Drosophila* homolog of YAP. *Cell* 122, 421–434.
- Jiang, C., Lamblin, A. F. J., Steller, H. and Thummel, C. S. (2000). A steroid-triggered transcriptional hierarchy controls salivary gland cell death during *Drosophila* metamorphosis. *Mol. Cell* 5, 445–455.
- Kamsoi, O. and Belles, X. (2019). Myoglianin triggers the premetamorphosis stage in hemimetabolan insects. *FASEB J.* 33, 3659–3669.
- Kayukawa, T., Jouraku, A., Ito, Y. and Shinoda, T. (2017). Molecular mechanism underlying juvenile hormone-mediated repression of precocious larval-adult metamorphosis. *Proc. Natl. Acad. Sci. U. S. A.* 114, 1057–1062.

- Kimura, K. I., Kodama, A., Hayasaka, Y. and Ohta, T. (2004). Activation of the cAMP/PKA signaling pathway is required for postecdysial cell death in wing epidermal cells of *Drosophila melanogaster*. *Development* 131, 1597–1606.
- Lavorgna, G., Ueda, H., Clos, J. and Wu, C. (1991). FTZ-F1, a steroid hormone receptor-like protein implicated in the activation of fushi tarazu. *Science* 252, 848–851.
- Lee, C. Y. and Baehrecke, E. H. (2001). Steroid regulation of autophagic programmed cell death during development. *Development* 128, 1443–55.
- Lee, C. Y., Wendel, D. P., Reid, P., Lam, G., Thummel, C. S. and Baehrecke, E. H. (2000). E93 directs steroid-triggered programmed cell death in *Drosophila*. *Mol. Cell* 6, 433–443.
- Lee, C.-Y., Cooksey, B. A. K. and Baehrecke, E. H. (2002a). Steroid regulation of midgut cell death during *Drosophila* development. *Dev. Biol.* 250, 101–111.
- Lee, C.-Y., Simon, C. R., Woodard, C. T. and Baehrecke, E. H. (2002b). Genetic mechanism for the stage- and tissue-specific regulation of steroid triggered programmed cell death in *Drosophila*. *Dev. Biol.* 252, 138–148.
- Liu, H., Wang, J. and Li, S. (2014). E93 predominantly transduces 20-hydroxyecdysone signaling to induce autophagy and caspase activity in *Drosophila* fat body. *Insect Biochem. Mol. Biol.* 45, 30–39.
- Liu, X., Dai, F., Guo, E., Li, K., Ma, L., Tian, L., Cao, Y., Zhang, G., Palli, S. R. and Li, S. (2015). 20-Hydroxyecdysone (20E) primary response gene *E93* modulates 20E signaling to promote *Bombyx* larval-pupal metamorphosis. *J. Biol. Chem.* 290, 27370–27383.

- Mané-Padrós, D., Cruz, J., Vilaplana, L., Nieva, C., Ureña, E., Belles, X. and Martín, D. (2010). The hormonal pathway controlling cell death during metamorphosis in a hemimetabolous insect. *Dev. Biol.* 346, 150–160.
- Martin, S. J. (2002). Destabilizing influences in apoptosis: sowing the seeds of IAP destruction. *Cell* 109, 793–796.
- Mou, X., Duncan, D. M., Baehrecke, E. H. and Duncan, I. (2012). Control of target gene specificity during metamorphosis by the steroid response gene E93. *Proc. Natl. Acad. Sci. U. S. A.* 109, 2949–2954.
- Muramatsu, D., Kinjoh, T., Shinoda, T. and Hiruma, K. (2008). The role of 20-hydroxyecdysone and juvenile hormone in pupal commitment of the epidermis of the silkworm, *Bombyx mori*. *Mech. Dev.* 125, 411–420.
- Ohno, C. K., Ueda, H. and Petkovich, M. (1994). The *Drosophila* nuclear receptors FTZ-F1 alpha and FTZ-F1 beta compete as monomers for binding to a site in the fushi tarazu gene. *Mol. Cell. Biol.* 14, 3166–3175.
- Orme, M. and Meier, P. (2009). Inhibitor of apoptosis proteins in *Drosophila*: gatekeepers of death. *Apoptosis* 14, 950–960.
- Riddiford, L. M. (1981). Hormonal control of epidermal cell development. *Integr. Comp. Biol.* 21, 751–762.
- Romaña, I., Pascual, N. and Belles, X. (1995). The ovary is a source of circulating ecdysteroids in *Blattella germanica*. *Eur. J. Entomol.* 92, 93–103.
- Sakurai, S. (2005). Feedback regulation of prothoracic gland activity. In *Comprehensive Molecular Insect Science* (ed. Gilbert, L. I., Iatrou, K., and Gill, S. S.), pp. 409–431. San Diego, California:

Elsevier Pergamon.

- Schneiderman, H. A., Krishnakumaran, A., Bryant, P. J. and Sehnal, F. (1970). Endocrinological strategies in insect control. *Agric. Sci. Rev.* 8, 13–25.
- Tettamanti, G. and Casartelli, M. (2019). Cell death during complete metamorphosis. *Philos. Trans. R. Soc. B* 374, 20190065.
- Ureña, E., Manjón, C., Franch-Marro, X. and Martín, D. (2014). Transcription factor E93 specifies adult metamorphosis in hemimetabolous and holometabolous insects. *Proc. Natl. Acad. Sci. U. S. A.* 111, 7024–7029.
- Uyehara, C. M., Nystrom, S. L., Niederhuber, M. J., Leatham-Jensen, M., Ma, Y., Buttitta, L. A. and McKay, D. J. (2017). Hormone-dependent control of developmental timing through regulation of chromatin accessibility. *Genes Dev.* 31, 862–875.
- Wang, C. X., Zheng, W. W., Liu, P. C., Wang, J. X. and Zhao, X. F. (2012). The steroid hormone 20-hydroxyecdysone upregulated the protein phosphatase 6 for the programmed cell death in the insect midgut. *Amino Acids* 43, 963–971.
- Woodard, C. T., Baehrecke, E. H. and Thummel, C. S. (1994). A molecular mechanism for the stage specificity of the *Drosophila* prepupal genetic response to ecdysone. *Cell* 79, 607–615.
- Yin, V. P. and Thummel, C. S. (2005). Mechanisms of steroid-triggered programmed cell death in *Drosophila*. *Semin. Cell Dev. Biol.* 16, 237–243.
- Yin, V. P., Thummel, C. S. and Bashirullah, A. (2007). Down-regulation of inhibitor of apoptosis levels provides competence for steroid-triggered cell death. *J. Cell Biol.* 178, 85–92.
- Ylla, G., Piulachs, M. D. and Belles, X. (2018). Comparative

transcriptomics in two extreme neopterans reveals general trends  
in the evolution of modern insects. *iScience* 4, 164–179.

Zhang, L., Ren, F., Zhang, Q., Chen, Y., Wang, B. and Jian, J. (2008).  
*Dev Cell.* 14, 377–387.

## **E93-DEPLETED ADULT INSECTS PRESERVE THE PROTHORACIC GLAND AND MOLT AGAIN**

Orathai Kamsoi and Xavier Belles

Institute of Evolutionary Biology (CSIC-Universitat Pompeu Fabra),  
Passeig Maritim 37, 08003 Barcelona, Spain

### **Supplementary information**

**Fig. S1.** Cell proliferation in the prothoracic gland of *Blattella germanica*.

**Fig. S2.** Transcriptomic expression of typical nymphal cuticular protein (NCP) genes: *Bg10431*, *Bg10435* and *Bg15257* and typical adult cuticular protein (ACP) genes: *Bg7254* and *Bg16458* in *Blattella germanica*.

**Fig. S3.** The nucleotide sequence of the promoter region of the *E93* gene of *Blattella germanica*.

**Table S1.** Primers used to measure gene expression levels with qRT-PCR and to prepare dsRNAs for RNAi experiments.

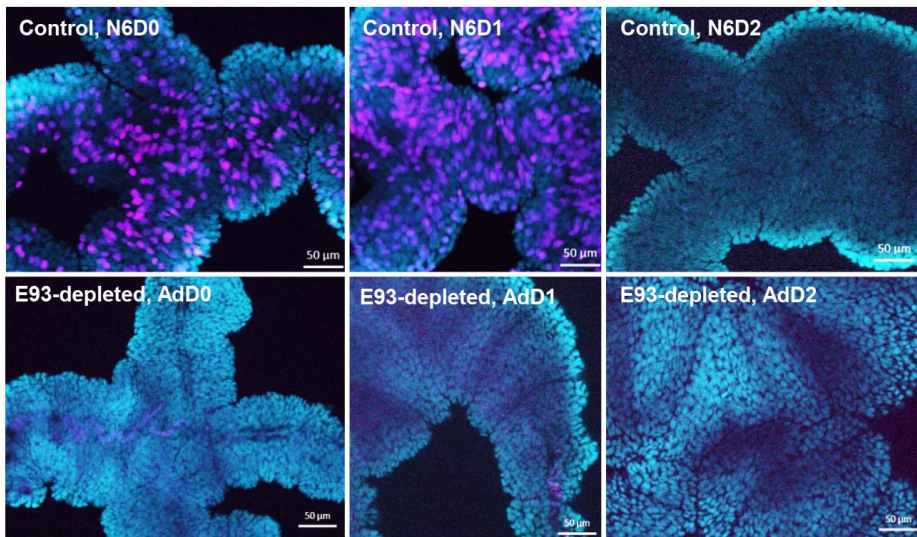


**Fig. S1. Cell proliferation in the prothoracic gland of *Blattella germanica*.** Double labeling EdU (discrete pink spots) and DAPI (background blue color) of prothoracic gland tissue in final instar control nymphs on day 0 (N6D0), day 1 (N6D1) and day 2 (N6D2), and E93-depleted adults in day 0 (AdD0), day 1 (AdD1) and day 2 (AdD2). Scale bars: 50 µm.

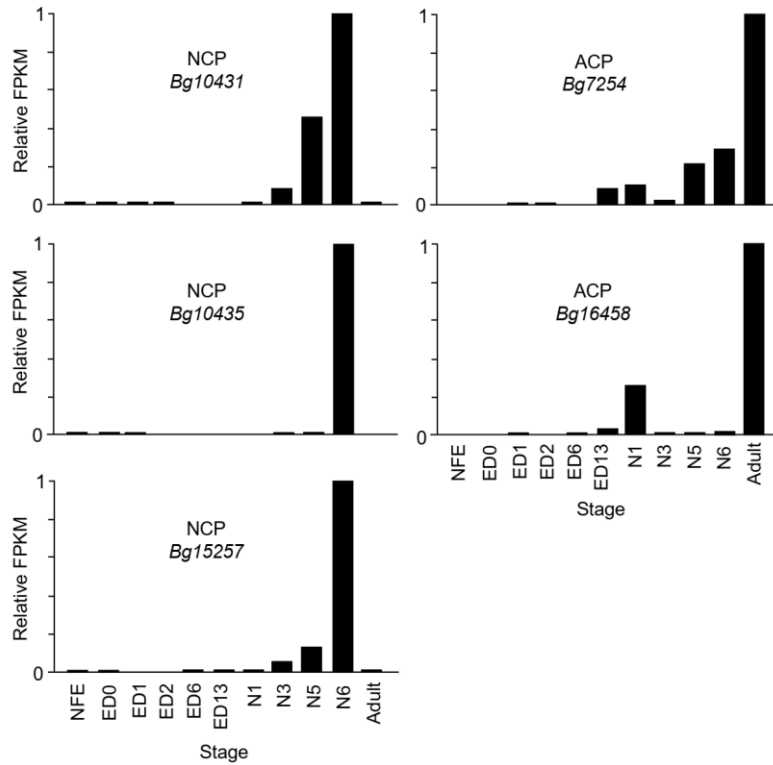


**Fig. S2. Transcriptomic expression of typical nymphal cuticular protein (NCP) genes: *Bg10431*, *Bg10435* and *Bg15257* and typical adult cuticular protein (ACP) genes: *Bg7254* and *Bg16458* in *Blattella germanica*.** Data were obtained from stage-specific transcriptomes that cover the life cycle (Ylla et al., 2018), as follows: non-fertilized egg (NFE); embryo 8, 24, 48, 144, and 312 h after oviposition (ED0, ED1, ED2, ED6, and ED13); first, third, fifth, and sixth (last) nymphal instar (N1, N3, N5, and N6); adult female. Data are expressed as FPKM, and is normalized against the maximum value (= 1) in each gene.



-4010 GGGCCTTCATTACAATAAAATGTTAGACAAATTATTCAGTAATATTACATAAAACAATATTGTGTCATCAGATAAGATTATGATACCA  
-3920 ATGGCTTTACAAAAGCTGCACTAAAGTTGATTTTATTATTATTATTATTATTATTATTCATATCTATTATTATTACAGGTAAGTATTAT  
-3830 TTATATATTTATTTATGTGATATAGAGCTA**AGTCAATTGGACG**CTTCCTCTCCACTCTACCAGCTAAACAAAATTTACAAGATAAATAC  
-3790 ATTATTAATCAAGTAAAAAGAAAATACAAATAAATACAAACGAAGTAAATAAGTTATCATGAATAACTTTTGTATTTCATTGGA  
-3710 ATTTCAAACCTGTTGCTTGAATTTTTTTATTCATACACTCTCTGTGCAGAGCAGAAAACATTTTAAACAGCATCATAAAAATCAAGACC  
-3620 AGAATTAACAATGCAAGATAGTTAAAGATAGTTCTCAAAGGGATGAAACGAAAATATTCCCCTGAAAAAATATTATTTCAGGGATCC  
-3530 CTGTTCAAGTATTTAAATTTTAATCCAGTCTTTGCTCAGTTTCTTTTCTGATGTTTCTACTCTAGGTGTTACTTATGTTACGGAGGTAGA  
-3440 ATGATAGTTGTAATAAAAATAGCCCTACTGCGTTATACCTGTTTATTTTTTAAATAAGATAATGTAATCTCCATCAAAATCCCTAAAAAAG  
-3350 AGCTTTCTGCTCTGAGATGTAGACAGCTAGTTTTCTCTGTAGAATAGTTATCAATAGTACAGTTATATTACCTATATAAATAAATAAAA  
-3260 AACGCTTAATCTCAATAAAGCTCATAATGTCAATTATCATGTGGTTGAATTAATAAGTGTAGATTTTACTGAATCGACACACGAGCAAC  
-3170 ATAGAGTATAGGACAAACCTGCACAGTGTGAATTCACCTCCGACGTTTACAAACGGTCAAAACATTAGTACTTAATGTCACAAACTCTA  
-3080 ACTCTTCAAGATAGTTAACTTTTAAAGACTAGCTCCGATATATCGACACTTTCAAGAAGGTTAAAGGGTAAAGAAATAGGTATCTTGA  
-2990 ATATATAAATAACTATAAATAACTCGGTGGTGAACAGCCAGCTGTAGCATTAGGGTACACATGTCTTAAAAATAGGAGGTGAACCA  
-2900 TCATCCAACTGTGAAGGGGAAATAGTGTTTAGCAGCTAGAGTCACAGAAATTAAGCTGTATCTTGCAATCGCTCACAGAAGGACAG  
-2810 AAGACTTAACTAGACTGTAATAAAGTTAAGCTTTACGCAACTCCCGCTCCGCTAGCATAAATCTCTAATTTATGATCGTCCACAGCA  
-2720 GATTAATCCCGTATTTAAAAGTTAAACAGGGCTATAGCATAAGTCTTCTATGCAAGTAGGCTATGGCATAGGACAAAATTTGGTTGCC  
-2630 AACAG**TCAAGGCCAA**ATGTCTGGATCCTTGTGAATGCTCAACTTTAGAAGCAGATAAAAAGTATAGTCATGTGGAATATTTCGAGAAAAT  
-2540 GAGAACAAATATATCTACGAATTT**CAAGGAAC**CTGGGTAATAGATATAAAGGAATGATGCAAGTGGTGTGCTCTGAAAGCAGAAAT  
-2450 AATAAATGGTAGTTCAACAATTCAGTCTCTTTTTCTGCCGCATAAACCCCGCAATTTTACTGACATACCAAAAATAAAGGAATAATCTGAA  
-2360 AACACACTAATTTATAGTTAGCTGGTTTTGAACAAAATGTAATTAGCCTATTTATTTGCGATGTTTTGTAAATCTATCGATCACAATTA  
-2270 TTACCAACCACTCTAATAACTTAATGAATATGGAATTTAATAATTAATCTGATAAAAAATACCCCTGTCAATAATAATAATAATAA  
-2180 TAATAATAATAATAAACAATGTCCTTTATGGCTAAGCATCTCCTTTGCTTTTCAGATTTAATTTTTCATAAAT**TCAAGGAT**TAGA  
-2090 CTCACACTAGGTATATAGGCAACTTCTCGACTGTTAAATGTGATGTTATCAAAATTTGAAATTTGACCCCGGACTTCAGAAATGGC  
-2000 CGTTTTATTTTTCACAGATACATAAATAATCCATTAATAGCTTTAAGATAAATAGTGGTTAGCTGGTAAATAATTTACTAACAGCTGCTAA  
-1910 GAAATGGTTGGCAGCGCTATACAGATTTTTCAGCATCTCCATCTCAATCTTTGTTATCAGCAAAAGGACTTTCATTTAAAAGCACAA  
-1820 CTCGCACAAATGACTATAATTTAAGACTTTGTCTTGTAACTATGAATACAGAACATAAATAATAATCAGATCAGAAGCCGATGAA  
-1730 CAATTTATTAATGCAATAAATAAATGGAATAACTAGATATCGAAACAAAAGTGTGATGCTCATGAAAGTCAACAATAAAGCAATATATA  
-1640 TCCATTTAGCCCTACATAGATAAATAACAATTTACTAAAATAAGAAAATGCCATCGAATGCAATGCCACGTGGTAAACAATGTCAGCGGG  
-1550 AGCAACAGGCGGATGGGAGCCCCCGCGGTTTTAAGAATGGTGGCATCGGATGCGGCGCTGGGCCCCACCTGGCGACAGAGCG  
-1460 CAGGATTTTGCAACTTCCCTCCCTCCTTTTCAACCCCGCGACTTTTCTGTAGCGAGGAAAACCCGAGGCTCCTGCACAGCAAGTTC  
-1370 CAAATCTCCAGAAAATCTTACATTAATTTCTCATCTCATTTTTTTAATCCCTCAAAAATATTGGAATTTCAATCATCTCTCC  
-1280 GCATAACATTTAACTCTCCGCAATTAATTCGGCAATAAAGCGGTGTTATGATTTAACTTAAGAAACCGGCTACAGTAGACTATATCA  
-1190 ATTTAGAATCAATAGCGCATATGCTACACTCTTTGATGTATCTGATTTGAGTGAACAAATACCTCGGTGATCAAGTGGCTCGCA  
-1100 AACATAGAGCTAGCTCATTATAAATAATTCCTTCAGGACAACAGTGGGAATCGTGGCCTTCCCTCATTATATGAGTGACGACACACCG  
-1010 GAGTTTATAGTGCACGGGTGCATCCGACAGCCAGTGAATCTGACTATTCTTATACGAAGACGGCTGTATGTTGACTTAACTCCCTTT  
-920 TTTCTTAGGAGGATAACGCTAAGGAGTCTACTCTGCACGTGAGTCTAATCTCTGAGGACCCGCAAGACAGCTGACTCGGATCAA  
-830 TACGCCGCTGTCCTCGCCGCGCAGACGTTTGCTATTGATCGACGCCGCGACGCTGCGCCGGGATCGATTCCGAGCTCGGAGACG  
-740 AGCGCCCGTTGCTTGGCCCGCTGTGCGCGCAGAGGACAGGCCGCGACTCGAACCCGGGGCGGAGCTCCCTCCGAAAAAACAAGG  
-650 TTGGCCCTGGCGAAGCGAGCGAGCGCGGAGAAAAGAGTCAAGGTCAGTTTGAAGCAAAATGCGCGGAGTGTCTTATGCTCGTGTGTT  
-560 ACGAGCGACGAGGATCAAAAAGAGCTGCAAAAGTGGACCAAGAACATGGTGTACGTAGTAGTGGTGGTGTGCAAAAGTGTGTGCTGTAG  
-470 GCTCGCGAGGCTGTGCGCTCGGCTTAGTGGGCTCCGCGACTGTGCCCCAAAATAACGTA**AGGAGTTC**CGGGGTCCCTCGTGTGCAT  
-380 CACCCCGCTTTCGTGGCGCCCTGGGTCCTGGGCCCCCTACGCGGGTTCGGGGCTCGCAGTCTTCGCAAGAACCCGCTCGCC  
-290 GAACCCGCTCAAACATTTCTCAAATTTGGGGCGCATTTCTCTTTCGGAGCTACCAAAACATCAGCTGGTGGGGGGTGGCTCGCAGAGCTG  
-200 GAACAGCGGGGACGAAACGTAACAGCCATGCCATGACCCCGCAATACCGAGTAAATACGCGAAATGGAAGATAGTGAATG  
-110 TGACGTGTGAGCAGCGCGGAGCAAGACGCGCTGCAAGTCTTTGGGCCCGAATCCCGATCCGATTCAGCTTTGTTGACGCTGG  
-20 AGCGCGTGGCTGAGGAGTTG**ATG**GGCCGCGAAGATGGAACAGTATCAGGACTCAGTGCTCAGATCTCCGCTCAGATGGACGTTGGAG

**Fig. S3. The nucleotide sequence of the promoter region of the *E93* gene of *Blattella germanica*. The ATG translation initiation codon is indicated in bold blue, a canonical EcRE (Cherbas et al., 1991; Kayukawa et al., 2017) is indicated in bold green, and a sequence (TCAAGGCAA) compatible with a FIRE (Lavogna et al., 1991; Ohno et al., 1994; de Mendonca et al., 2002) is indicated in bold yellow and underlined, except a mismatched nucleotide. Three other potential FIREs are indicated in yellow and underlined, except the mismatched nucleotides.**

**Table S1.** Primers used to measure gene expression levels with qRT-PCR and to prepare dsRNAs for RNAi experiments (highlighted in yellow).

Gene	Forward primer	Reverse primer	Accession code
<i>Actin 5C (Act5C)</i>	AGCTTCCTGATGGTCAGGTGA	TGTCGGCAATCCAGGGTACATGGT	AJ862721
<i>Bg7254</i>	TTGTACGGCTACAGCATCG	ACTGACCCAAAGCGTCTTGT	Scaffold293:1224685-1234782*
<i>Bg10431</i>	CTCATGCCCTCCAGTACTAT	CACGGTAAGACACGACAGGA	Scaffold1062:264085-266425*
<i>Bg10435</i>	CTCTGGTGATGGGCATTTCT	GATTTGCAGAGGACGAGAGG	Scaffold1062:351421-355992*
<i>Bg15257</i>	AGATCCCTCATGCACCAATC	GCGTGATGTTCAACCTCCTT	Scaffold1678:100341-119028*
<i>Bg16458</i>	GATGGGAGAACCTACCAGCA	CTGGATCTGCGCTAACCAACA	Scaffold550:516136-531892*
<i>blistered (bs)</i>	GACGGAGCTCAGTACAACA	CCAGCGGTCTTACTTTCTGC	HF912428.1
<i>Broad-complex (br)</i>	CGGGTCGAGGGGAAAGACA	CTTGGCGCCGAATGCTGCGAT	FN651774
<i>caspase-1 (casp-1)</i>	AAGCGGAAGGATTCATACCA	GATGACTGCCTTGCCTCTTC	LN812812.1
<i>disembodied (dib)</i>	GCAACAGACAATGGACCTCA	AGATCCAATGCAACCTCCTC	Scaffold1245:376847-417309*
<i>E75-A</i>	GTGCTATTGAGTGTGCGACATGAT	TCATGATCCCTGGAGTGGTAGAT	AM238653.1
<i>E93</i>	TCCAATGTTTGATCCTGCAA	TTTGGGATGCAAAGAAATCC	HF536494.1
<i>Ecdysone receptor (EcR)</i>	GACAACTCCTCAGAGAAGATCAAA	CTCCCAATCCTGCCAGACTA	AM039690.1
<i>fushi tarazu factor1 (ftz-f1)</i>	TTGTCACATCGACAAGACGCA	GTACATCGGGCCGAATTTGTTTCT	CAQ57670.1
<i>HR3-A</i>	GATGAGCTGCTCTTAAAGGCGAT	AGGTGACCGAACTCCACATCTC	AM259128.1
<i>inhibitor of apoptosis-1 (iap1)</i>	TCCACCTGTGCATCATCATC	GCGTGATCGTCTAAAACCT	FN668727.1
<i>Kruppel homolog 1 (Kr-h1)</i>	GCGAGTATTGCAGCAAAATCA	GGGACGTTCTTCGTATGGA	HE575250.1
<i>neverland (nvd)</i>	CTGGGGCCAGTCACAATACT	GCAGGGGCTTGTCAATGTAT	Scaffold2003:130463-150129*
<i>Notch (N)</i>	GCTAAGAGGCTGTGGATGC	TGCCAGTGTGTCTGAGAG	HF969255.1
<i>nubbin (nub)</i>	CGTCACCAGAAGAAACAACAGA	CGAGATTGTGGTCTGTGAGAAA	LT216433
<i>phantom (phm)</i>	CTAGGCACCAAGCACCTTC	GCAAGACTGTGTCTTCCAA	Scaffold1282:295424-296920*
<i>Retinoid X receptor (RXR)</i>	ATAATTGACAAGAGGCAGAGGAA	TGAACAGCTCCCTCTTCAT	AJ854489.1
<i>scalloped (sd)</i>	GCCCACAGAGTGCTTTCTCT	CCCTGCCTCATCTTGAATA	HF969263.1
<i>shadow (sad)</i>	ATGAGGAGTTCAGGGTGTG	CTGGCCAGAAGTCATTTGGT	Scaffold189:1562047-1594901*
<i>Ultrathorax (Ubx)</i>	AAGAGGTCGCCAGACGTACA	TTGGAACCAAATTTGATCTGTC	LT216435
<i>vestigial (vg)</i>	AACTGTGTGGTTCACTCACT	AAGGAGGGAAAGTTCGAGC	LN901335
<i>dsE93</i>	AAAGAGTTGTCGGGAGCAGA	CCACTGCTAGAAGCCACTCC	HF536494.1
<i>dsFTZ-F1</i>	GAA TAGTTCA GGGCTTTT TGAAGCT	GCGACGATGTGTAGACCTTCTTG	CAQ57670.1
<i>dsMock</i>	ATCCTTCTCTGGGACCCGGCA	ATGAAGGCTCGACGATCCTA	K01149

\*Genes manually annotated in *Blattella germanica* genome, available as BioProject PRJNA203136.

### 3.3. Regulation of metamorphosis in mayflies (Insecta, Ephemeroptera).

Orathai Kamsoi<sup>1</sup>, Isabel Almudi<sup>2</sup>, Fernando Casares<sup>2</sup>, Xavier Belles<sup>1\*</sup>

<sup>1</sup> Institute of Evolutionary Biology (CSIC-Universitat Pompeu Fabra), Passeig Maritim 37, 08003 Barcelona, Spain.

<sup>2</sup> Centro Andaluz de Biología del Desarrollo (CSIC-UPO-JA), Ctra. de Utrera km 1, 41013 Seville, Spain.

\*Corresponding author. *E-mail address:* [xavier.belles@ibe.upf-csic.es](mailto:xavier.belles@ibe.upf-csic.es)

Regulation of metamorphosis in mayflies (Insecta, Ephemeroptera). Manuscript in preparation.



### 3.3. Regulation of metamorphosis in mayflies (Insecta, Ephemeroptera).

Orathai Kamsoi<sup>1</sup>, Isabel Almudi<sup>2</sup>, Fernando Casares<sup>2</sup>, Xavier Belles<sup>1\*</sup>

<sup>1</sup> Institute of Evolutionary Biology (CSIC-Universitat Pompeu Fabra), Passeig Maritim 37, 08003 Barcelona, Spain.

<sup>2</sup> Centro Andaluz de Biología del Desarrollo (CSIC-UPO-JA), Ctra. de Utrera km 1, 41013 Seville, Spain.

\*Corresponding author. *E-mail address:* [xavier.belles@ibe.upf-csic.es](mailto:xavier.belles@ibe.upf-csic.es)

#### ABSTRACT

Ephemeropterans (mayflies) follow a hemimetabolous development, but they are unique among insects in that they molt one more time after forming functional wings. Thus, the last nymphal molt does not give the definitive adult form, but a winged stage called subimago, which molts again to the adult. Despite this interesting peculiarity, practically nothing is known about how they regulate metamorphosis. We have studied this subject in the species *Cloeon dipterum*. From a morphological point of view, the most radical transformation is between the last nymphal instar and the subimago. It is also in this transition that occur a significant decrease and increase in the expression of factors Kr-h1 (which suppresses metamorphosis) and E93 (which promotes it), respectively. The factor Br-C (which is involved in wing growth) decreased in parallel to the increase of E93. In addition, administration of the juvenile hormone mimic methoprene at the beginning of the last nymphal instar upregulates the expression of Kr-h1 and inhibits the transformation to subimago. However, this treatment did not affect the expression of either E93 or Br-C. Our observations suggest that the metamorphosis of *C. dipterum* occurs

with the formation of the subimago, which would be a first phase of the adult stage. They also suggest that separate pulses of ecdysone are required to promote the respective subimago and adult molts, and that the juvenile hormone inhibits metamorphosis through Kr-h1. New experiments are needed to assess the precise role of E93 and Br-C in *C. dipterum* metamorphosis.

**Key words:** *Cloeon dipterum*, Ephemeroptera, metamorphosis, juvenile hormone, MEKRE93 pathway

## INTRODUCTION

Insect metamorphosis is the process by which an immature form develops into an adult form through distinct morphological transformations. About 70% of the extant species currently known are metamorphosing insects, which inhabit all land habitats, from arid deserts to areas close to the two poles (Belles, 2020; Mora et al., 2011). These data speak for themselves about the evolutionary success of metamorphosis in insects.

Two main modes of insect metamorphosis are currently considered: hemimetaboly and holometaboly. The hemimetabolan development is typical of exopterygotes (Palaeoptera, Polyneoptera and Paraneoptera), and comprises three characteristic stages: the embryo, the juvenile instars (or nymphs), and the adult. The nymphs are morphologically similar to the adult, and develop gradually until the adult stage. In contrast, the Endopterygota follow the holometabolan developmental cycle, which comprises four characteristic stages, the embryo, the juvenile instars (or larvae), the pupa and the adult. The larvae are morphologically more or less divergent with respect to the

adult, and the pupal stage, normally a non-feeding, immobile instar, bridges the morphological gap between the larvae and the adult (Belles, 2020).

In both modes, metamorphosis is regulated by two hormones: the juvenile hormone (JH), which represses metamorphosis, and ecdysone plus its biologically active derivative, 20-hydroxyecdysone (20E), which promotes the successive non-metamorphic and metamorphic molts (Nijhout, 1994). In turn, the transduction mechanisms of the hormonal signals include the transcription factors Krüppel homolog 1 (Kr-h1) and E93, which are JH- and 20E-dependent, respectively. Kr-h1 is the main effector of the antimetamorphic action of JH, while E93 is a key promoter of metamorphosis (Belles, 2019). The interaction of these factors in the MEKRE93 pathway (Belles and Santos, 2014) composes the essential axis regulating insect metamorphosis. Regarding hemimetabolans metamorphosis, in the nymph-to-nymph transitions, JH acts through its receptor Methoprene tolerant to induce the expression of *Kr-h1*, while Kr-h1 represses the expression of *E93*. In turn, the fall of JH production in the last juvenile stage interrupts *Kr-h1* expression, thus allowing a strong induction of *E93*, which triggers adult morphogenesis (Belles, 2019; Belles and Santos, 2014).

The mechanisms regulating metamorphosis have been described in considerable detail in neopterans, both in hemimetabolans (polyneopterans and paraneopterans) and holometabolans (endopterygotes). However, very little is known about paleopterans, particularly about the order Ephemeroptera (mayflies). And this is particularly unfortunate because mayflies are exceptionally interesting from an evolutionary point of view. They are unique among insects in

that they molt one more time after forming functional wings. Thus, the final molt of the nymphal period does not give the definitive adult form, but a winged stage called subimago that morphologically resembles the adult. Moreover, mayfly nymphal stages are aquatic, exhibiting the typical adaptations to this life (like breathing through gills, and generally have herbivore- detritivore regimes. Conversely, subimagos and adults are terrestrial and do not feed, which is consistent with the short duration of these stages, which can last between a few hours and some days or few weeks at most (Berner and Pescador, 1988; Edmunds and McCafferty, 1988; Lancaster and Downes, 2013; Wingfield, 1937)

The developmental cycle of mayflies raises a series of relevant questions, for example, about the transformation from an aquatic organism to a terrestrial one, how is the metamorphosis from nymph to subimago and adult regulated, or what is the functional sense of the subimago. Questions that have not been well resolved using morphological approaches, and that a study on a molecular scale would help to provide clearer answers. However, and largely due to the difficulty of maintaining mayflies in the laboratory, there are very few developmental studies carried out at the molecular scale. An interesting antecedent is the comparative study of the transcriptomes of “young larva”, “mature larva”, subimago, and adult of the mayfly species *Cloeon viridulum* (Si et al., 2017). The expression profiles of various genes involved in the regulation of metamorphosis already provide valuable information. However, the study did not include the analysis of the important factor E93, which specifies metamorphosis (Ureña et al., 2014).



More recently, a new opportunity has emerged with the development of a laboratory rearing system for *Cloeon dipterum* (Almudi et al., 2019). The genome of this species has been described, and gene expression along development and in specific organs has been reported (Almudi et al., 2020). In the present work, we have used *C. dipterum* as model to address some of the questions mentioned above in relation to metamorphosis. We have been particularly interested in the regulatory mechanisms, including those involved in the formation of the subimago, and how do they compare to the mechanisms described in neopteran insects.

## RESULTS

### **The four last nymphal instars are distinguished by the wing pads length**

In order to characterize the developmental stages preceding metamorphosis in *C. dipterum*, we examined the last four last nymphal instars from a morphological point of view, using the wing pads as a diagnostic feature. The wing pads are the hard pockets, or pterothecae, that protect the developing wing primordia, and are easily visible on the dorsal side of the nymph (Fig. 3.3.1). The nymphal instars examined were the pre-antepenultimate (PAN), the antepenultimate (AN), the penultimate (PN), and the last (LN). *C. dipterum* has only a pair of mesothoracic wings, and the wing pad length is the clearest feature to distinguish the above nymphal instars from each other. Thus, in the PAN, the wing pads do not reach the first abdominal segment (A1); they only reach half the length of the metanotum (Fig. 3.3.1A). In the AN, the wing pads just reach the anterior edge of A1 (Fig. 3.3.1B). In the PN, the wing pads go beyond the anterior edge of A1, reaching half

of its length (Fig. 3.3.1C). Finally, in the LN, wing pads are much longer, its length going beyond A2 (Fig. 3.3.1D).

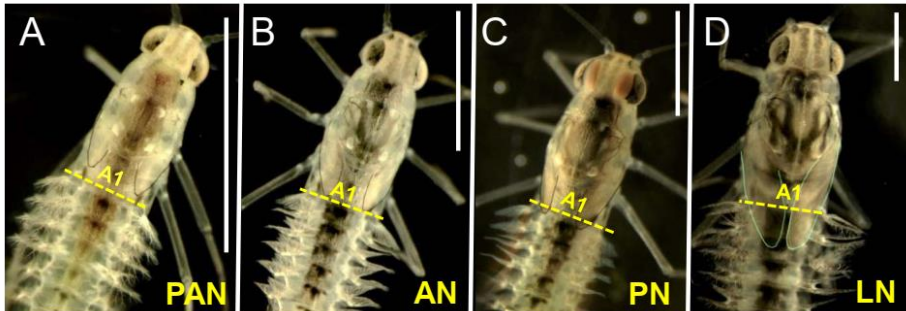


**Figure 3.3.1. The four last nymphal instars of *Cloeon dipterum*.** A: Female nymph in the pre-antepenultimate instar (PAN); the wing pads do not reach the first abdominal segment (A1). B: Female nymph in the antepenultimate instar (AN); the wing pads just reach the anterior edge of A1. C: Male nymph in the penultimate instar (PN); the wing pads go beyond the anterior edge of A1. D: Female nymph in the last instar (LN); the wing pads go beyond A2. In all cases, images were obtained on the first day of the corresponding instar. The perimeter of the wing pads has been indicated with a solid line, and the anterior edge of A1 with a dashed line. Scale bars: 1 mm.

### **The wings mature during the transition from the last nymphal instar to the subimago and the adult**

Within the LN, the wing pads show gradual changes of coloration along the instar, as seen 2 h (LND0), 24 h (LND1), 48 h (LND2), 72 h (LND3) and 84 h (LND4) after molting. The day after LND4, the nymphs molt to the subimago stage. In LND0, LND1 and LND2, the wing pads are thin and semi-transparent, having a pale gray-yellow color, which darkens slightly between those days (Fig. 3.3.1D). In LND3 the wing pads become thicker and the color change to intense yellow (Fig. 3.3.2.A).

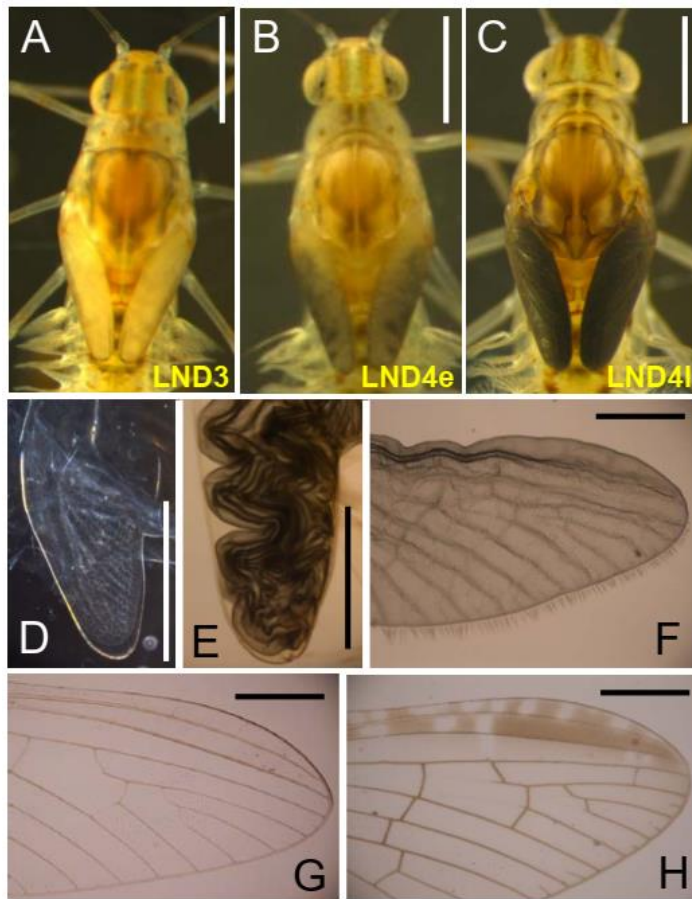


**Figure 3.3.2. Wing maturation in *Cloeon dipterum*.** A-C: Development of the wing pads in the last nymphal instar; shape and color in 3-day-old nymphs (LND3) (A), early 4-day-old (LND4e) (B), and late 4-day-old (LND4l) (C). D: Wing primordia in the penultimate nymphal instar. E: Wing in LND4l, folded within the wing pad. F: Wing in LND4l, artificially removed from the wing pad and extended on a slide. G: Apical part of a subimago wing. K: Apical part of an adult wing. Scale bars: 1 mm.

In LND4, the wing pad color gradually change from partially gray early in day 4 (Fig. 3.3.2.B) to black at the end of the instar (Fig. 3.3.2.C), just before molting to the subimago. The conspicuous changes observed within LN, especially during the last day (LND4), suggest

that the transformation into mature wings occurs towards the end of this instar. Indeed, if the wing pads of the PN contain only wing primordia (Fig. 3.3.2.D), those of LND4 contain folded wings (Fig. 3.3.2.E), which can be artificially taken out of the wing pad and extended on a slide (Fig. 3.3.2.F). In terms of venation and coloration, this wing has the patterning of a normally ecdysed subimago wing (Fig. 3.3.2.G), which shows a row of fine cilia along the edges. In addition, it is dull and translucent, because the adult wing is developing under it. The definitive adults wings (Fig. 3.3.2.H) are shiny and transparent, and lack hairy structures.

**The mouthparts, central filament and leg claws are not formed in the transition from the last nymphal instar to the subimago**

Nymphs of *C. dipterum* are herbivore or detritivore, mostly feeding on algae. Thus, their mouthparts are specialized in chewing, and consist of a pair of quite strong mandibles, a flap-like labrum, maxillae, labium and hypopharynx. In contrast, the subimago and the adult do not feed and practically lack mouthparts. Thus, the mouthparts are newly formed at each nymph-to-nymph molt, and the new structures can be observed by transparency at the end of each nymphal instar (Fig. 3.3.3A), except in the transition to the subimago stage (Fig. 3.3.3B).

After hatching, *C. dipterum* nymphs have only two caudal cerci. The central filament develops after 2 or 3 molts (Fig. 3.3.3C, D), and gradually increases in size at every molt, until LN (Fig. 3.3.3E, F). However, the subimago and the adult only have the cerci (Fig. 3.3.3G, H), as the central filament simply does not form during the transition from LN to subimago. This can be observed in LND4, where after the

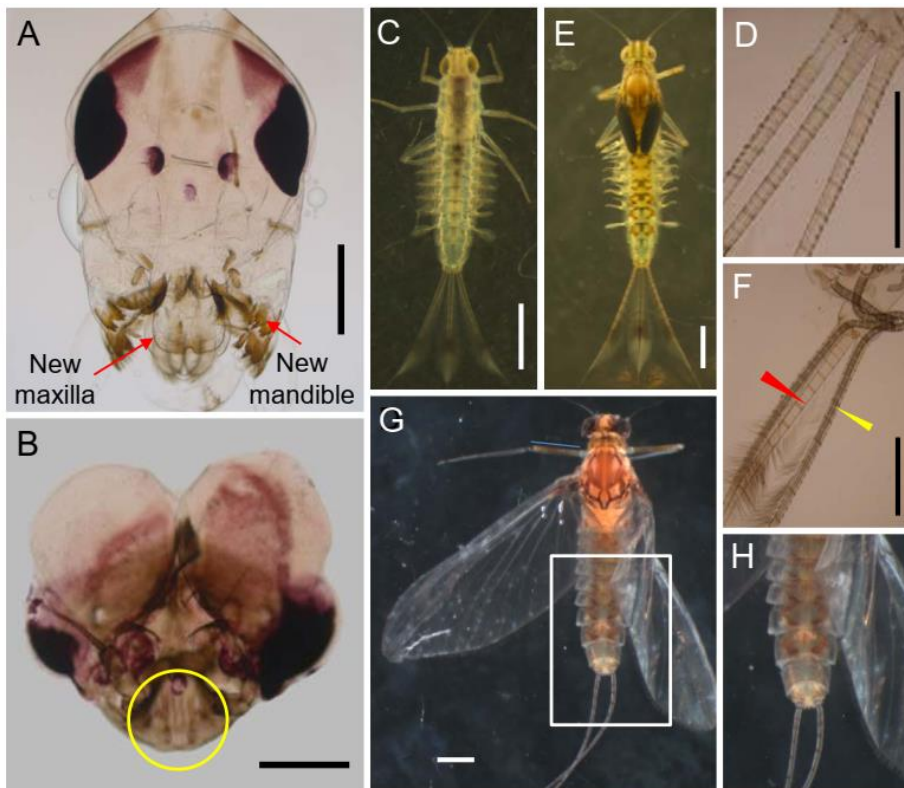


**Figure 3.3.3. The mouthparts and central filament during *Cloeon dipterum* metamorphosis.** A: Head of a female in the last day of the penultimate instar nymph showing the corresponding mouthparts, and a new set of mouthparts (exemplified by a new pair of mandibles and maxillae) forming, which correspond to the last nymphal instar. B: Head of a male subimago showing that mouthparts practically disappeared (circle). C: Fourth instar nymph with two cerci and a central filament. D: Detail of the cerci and filament in fourth instar nymph. E: Late sixth instar nymph (black wing pads stage) showing the two cerci and the central filament. F: Detail of the cerci and filament in a late sixth instar nymph after the apolysis; note that the new cerci formed after the apolysis (yellow arrowhead), whereas the central filament only show the nymphal structure (red arrowhead). G: Habitus of a female subimago. H: Detail of the two cerci of a subimago showed in panel G. Scale bars: 0.5 mm in A and B; 1 mm in C-G.

apolysis and formation of the new cuticle, new respective subimaginal cerci are formed, but not the central filament (Fig. 3.3.3F).

In the legs, a structure that is deeply remodeled during metamorphosis is the apical tarsomere. In the nymphs, it is elongated and claw-shaped (Fig. 3.3.4A), whereas in the subimago and the adult, it takes the form of a short, hook-shaped structure (Fig. 3.3.4B). The formation of this new structure can be observed by examining the apical tarsomere in LND4. It can be seen by transparency that the subimaginal short hook-like structure is formed instead of the long claw characteristic of the nymphs (Fig. 3.3.4C). Furthermore, the legs

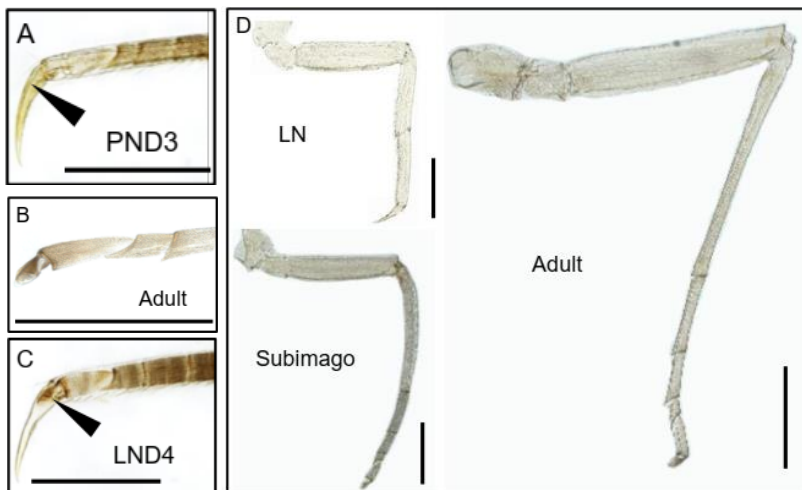


**Figure 3.3.4. Leg development during *Cloeon dipterum* metamorphosis.** A: Detail of the apical tarsomere in 3-day-old penultimate nymphal instar (PND3); note the actual claw and the new claw formed after the apolysis and corresponding to the LN (arrowhead). B: Detail of the apical tarsomere in adult. C: Detail of the apical tarsomere in 4-day-old last nymphal instar (LND4); note the small hook-shaped structure formed after the apolysis and corresponding to the subimago (arrowhead). D: Foreleg of a female last nymphal instar (LN), a female subimago, and an adult female. Scale bars: 0.5 mm.

grow dramatically during metamorphosis, especially the forelegs in the transition from subimago to adult, in which they get to double their length (Fig. 3.3.4D).

### **The expression of key metamorphosis genes changes in the transition from the last nymphal instar to the subimago**

We measured the expression of genes involved in the pathways of JH and 20E. In the JH pathway we examined the following genes: *juvenile hormone acid methyltransferase (jhamt)*, *myoglianin (myo)*, *Methoprene-tolerant (Met)* and *Krüppel homolog 1 (Kr-h1)*. In the 20E pathway we examined *Ecdysone receptor (EcR)*, *Hormone receptor 3 (HR3)*, *ecdysone-induced protein 75B (Eip75B or E75)*, *Broad complex (Br-C)*, measuring all possible isoforms, *Ecdysone-induced protein 93F (Eip93F or E93)*, and *ftz transcription factor 1 (ftz-f1)*. The expression was studied in females of the following nymphal instars: PAN, AN, PN, and LN, as well as the subimago and the adult.

Regarding the JH genes, the results (Fig. 3.3.5) suggest a certain parallelism between *jhamt* and *Kr-h1* expression from PAN to LN. In contrast, the pattern of *myo* expression appears to inversely correlate with those of *jhamt* and *Kr-h1*. The expression of *Met* shows singular high values in the subimago, and appears uncorrelated with those of other JH factors. Regarding the 20E genes, the results (Fig. 3.3.5) indicate that the expression of *EcR* increases along the development, showing the highest values in the subimago and adult.

The pattern of *HR3* and *E75* are fluctuating, but show a relatively similar general pattern, with the highest values in the LN and the subimago. In contrast, *Br-C* expression shows high values in PAN, AN, and PN, a decrease in LN, and a further decrease in the subimago

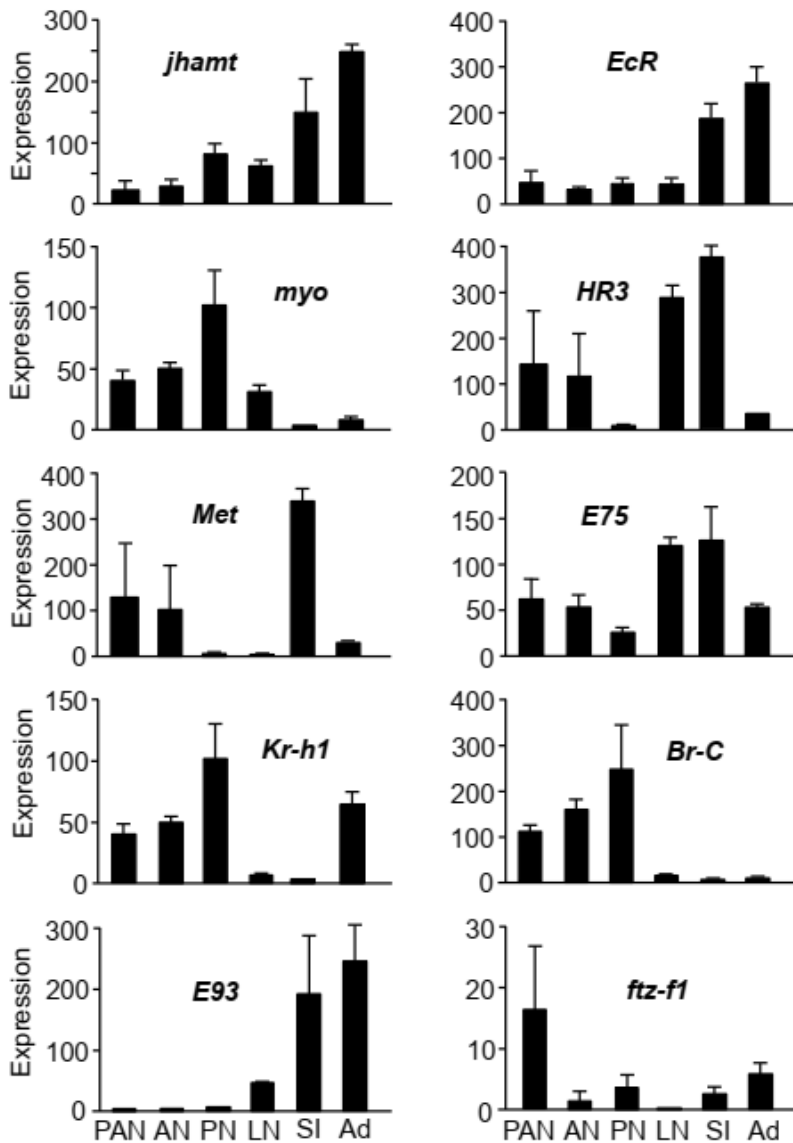


**Figure 3.3.5.** Expression of genes involved in the juvenile hormone and ecdysone pathways in *Cloeon dipterum*. The following genes were examined: *juvenile hormone acid methyltransferase (jhamt)*, *myoglianin (myo)*, *Methoprene-tolerant (Met)*, *Krüppel homolog 1 (Kr-h1)*, *Ecdysone-induced protein 93F (Eip93F or E93)*, *Ecdysone receptor (EcR)*, *Hormone receptor 3 (HR3)*, *ecdysone-induced protein 75B, (Eip75B or E75)*, *Broad complex (Br-C)*, and *ftz transcription factor 1 (ftz-f1)*.



and adult stages, which show very low values. *E93* expression shows a pattern opposite to that of *Br-C*. Finally, *ftz-fl* expression pattern looks uncorrelated with those of other 20E factors. From the point of view of the regulation of metamorphosis, the behavior of *Kr-h1*, which represses it, and of *E93*, which is its main promoter (Belles, 2019b), is crucial, and our pattern shows that *Kr-h1* mRNA levels decrease in LN, while those of *E93* increase in parallel (Fig. 3.3.5). In order to determine more precisely when both patterns intersect, we measured the expression over the 4 days of L4. The results (Fig. 3.3.6) indicate that *Kr-h1* expression abruptly decreases just after molting to LN (LND0), and keeps low values until LND3; then, the expression dramatically increases in LND4 and the subimago, and keep quite high values in the adult (Fig. 3.3.6). In parallel, *E93* expression is very low previous to LN, and start to increase in LND0, keeping quite stable values from LND1 to LND3, and then notably increasing in LND4, and keeping similarly high values in the subimago and the adult (Fig. 3.3.6).

During the 4 days of LN, we also measured the expression of *Br-C* in order to analyze in a more precise way its possible relation with the formation of the subimago, and that of the 20E-dependent early gene *HR3* to determine more precisely the 20E pulses. The expression of *Br-C* decreases progressively along LN, and practically vanishes in the subimago and the adult, whereas the *HR3* pattern shows clear

---

**Figure 3.3.5. (Continued)** The expression was measured in females of the following nymphal instars: pre-antepenultimate (PAN), antepenultimate (AN), penultimate (PN), and last (LN), as well as the subimago (SI) and the adult (Ad). The results are indicated as copies of the examined mRNA per 1000 copies of CdActin-5c mRNA, and are expressed as the mean  $\pm$  SEM (n=3).

expression peaks in LND3 and in the subimago, which suggests that there are respective and discrete 20E pulses in these stages (Fig. 3.3.6). The detailed expression profiles of *Kr-h1*, *E93*, *Br-C*, and *HR3* in males (Fig. S1) are very similar to those in females.

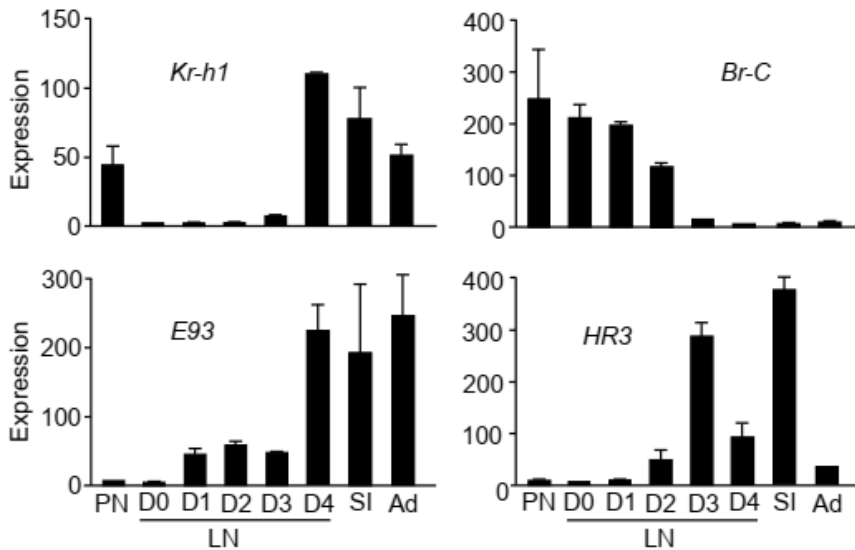


**Figure 3.3.6. Expression of genes relevant for metamorphosis in *Cloeon dipterum*.** The genes *Krüppel homolog 1* (*Kr-h1*), *Ecdysone-induced protein 93F* (*Eip93F* or *E93*), *Broad-complex* (*Br-C*) and *Hormone receptor 3* (*HR3*) were examined. The expression was measured in females of penultimate nymphal instar (PN), all days of the last nymphal instar (LN, from D0 to D4), the subimago (SI) and the adult (Ad). The results are indicated as copies of the examined mRNA per 1000 copies of CdActin-5c mRNA, and are expressed as the mean  $\pm$  SEM (n=3).

### Treatment with a JH mimic inhibits metamorphosis

Next, we wondered whether JH would prevent metamorphosis in *C. dipterum*, as occurs in neopteran insects. Thus, we carried out experiments treating nymphs with the JH mimic methoprene.

Treatments with doses of 0.1 or 1  $\mu\text{g}$  topically applied on freshly ecdysed LN did not produce any apparent effect on development (results not shown). However, a dose 5  $\mu\text{g}$  of methoprene applied in the same conditions produced a clear inhibitory effect on metamorphosis. All control insects ( $n = 13$ ) treated with the same volume (0.5  $\mu\text{L}$ ) of the methoprene solvent (acetone), molted normally to subimago and then to adult. In contrast, the methoprene-treated insects ( $n = 15$ ) reached the last day of the instar (LND4-late, a stage characterized by the black wing pads: Fig. 3.2.2C), but they did not ecdyse to subimago, and died after one or two days.

Detailed examination of these methoprene-treated insects in late LND4 showed that they completed the apolysis and the formation of a new cuticle. Nevertheless, the newly formed cuticle corresponded to a supernumerary nymph rather than a subimago. For example, the examination of head showed that the controls did not form the nymphal mouthparts (Fig. 3.3.7A left panel). In contrast, a new nymphal mouthparts set was developed in methoprene-treated insect, not only a new pair of mandibles, but also a new labrum, hypopharynx, maxillae, and labium were formed again (Fig. 3.3.7A right panel), as would correspond to the formation of a new nymphal instar. Moreover, the controls formed new cerci but they did not form the central filament, which corresponds with the morphology of the subimago (Fig. 3.3.7B left panel). Conversely, methoprene-treated insects formed the two cerci and the central filament, as in the nymphs (Fig. 3.3.7B right panel). In the case of the last tarsomere, the controls developed the short and hook-shaped structure characteristic of the subimago (Fig. 3.3.7C left panel), whereas the methoprene-treated insects formed again the elongated and claw-shaped structure that characterizes the nymphal

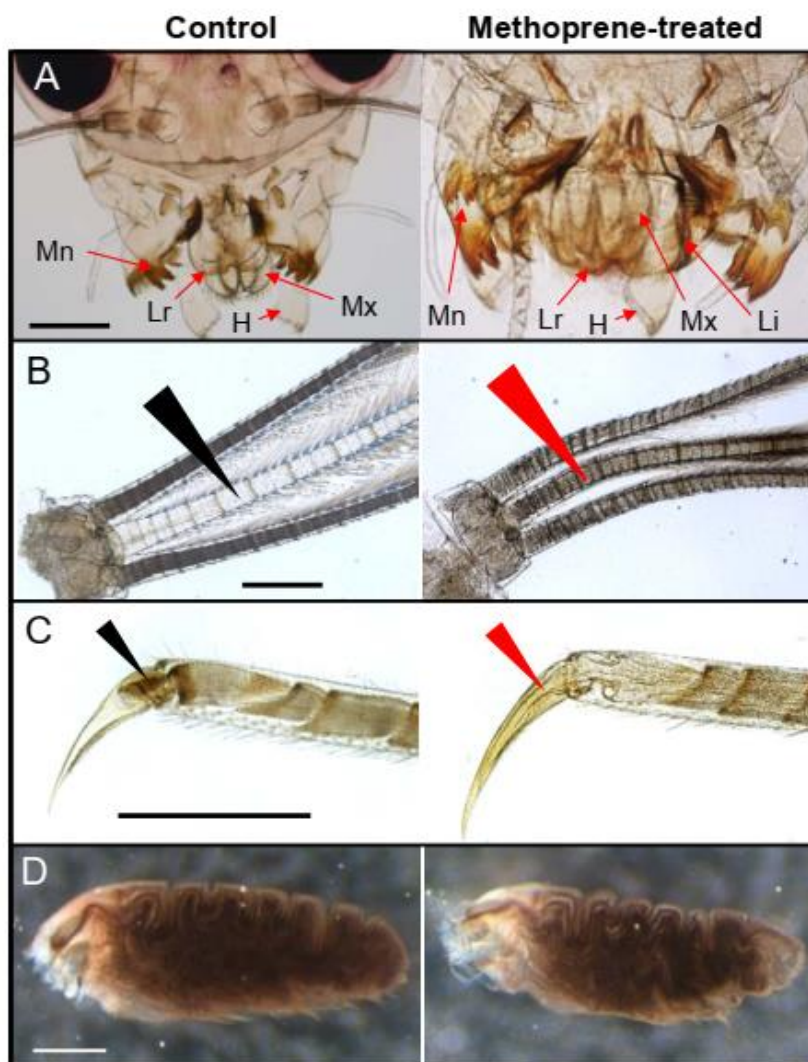


**Figure 3.3.7. Effects of methoprene on metamorphosis in *Cloeon dipterum*.** Methoprene was administered in freshly emerged last instar nymphs (LND0), and morphological features were examined four days later (LND4) in controls and methoprene-treated insects. A: Mouthparts; note that the controls only show the nymphal structures, whereas the methoprene-treated show the nymphal structures and a new set formed after the apolysis; H: hypopharynx, Li: labium; Lr: labrum; Mn: mandible; Mx: maxilla. B: Cerci and central filament; note that the controls form new cerci but they don't form the central filament (black arrowhead), whereas the methoprene-treated insects form the cerci and the central filament (red arrowhead).

instars (Fig. 3.3.7C right panel). Regarding the wing pads, a similarly shaped developing wing was observed by transparency in controls and methoprene-treated insects (Fig. 3.3.7D). In the latter, however, the folded wing structure appeared less compact and with less tissue mass. In this case, both in controls and in methoprene-treated insects, it was impossible to remove the developing wings from the wing pad and extend them on a slide, because they were much more fragile than in untreated insects.

### **Treatment with a JH mimetic enhances the expression of *Kr-h1***

In male and female nymphs treated with methoprene, we measured the expression of those genes most directly involved in regulating metamorphosis. Therefore, two days after the treatment, we quantified the mRNA levels of *Kr-h1*, *E93* and *Br-C* in whole body extracts of controls and methoprene-treated insects. The results (Fig. 3.3.8) showed that methoprene significantly upregulated the expression of *Kr-h1* in males and females. In contrast, the treatment did not apparently affect *E93* and *Br-C* expression, neither in females nor in males.

---

**Figure 3.3.7. (Continued)** C: Last tarsomere exemplified by the hind leg; note that the controls form the new structure, short and hook-shaped, which is characteristic of the subimago (black arrowhead), whereas the methoprene-treated insects form again the elongated and claw-shaped structure that is characteristic of the nymphal instars (red arrowhead). D: Wing pads; note the developing wings seen by transparency; the appearance is similar in controls and in methoprene-treated, although in the latter the wing structure appears less compact and apparently with less tissue mass. Scale bars: 0.5 mm in A and C; 1 mm in B and D.

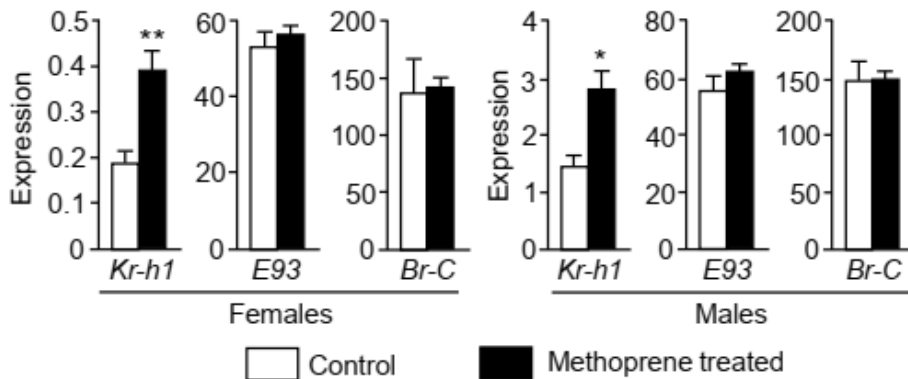


**Figure 3.3.8. Effects of methoprene treatment on the expression of genes involved in metamorphosis.** Methoprene was administered in freshly emerged last instar nymphs, and gene expression was measured in whole body extracts two days later. The genes *Krüppel homolog 1 (Kr-h1)*, *Ecdysone-induced protein 93F (Eip93F or E93)* and *Broad-complex (Br-C)* were examined. The results are indicated as copies of the examined mRNA per 1000 copies of CdActin-5c mRNA, and are expressed as the mean  $\pm$  SEM (n=3); the asterisks indicate statistically significant differences with respect to the controls (\*p<0.05, \*\*p<0.01) according to the student's *t*-test.

## DISCUSSION

### The morphological data

We used the length and color of wing pads as diagnostic features to characterize the nymphal instars that precede metamorphosis. The length of the wing pads allows to distinguish unambiguously the PAN, AN, PN and LN instars, and the wing pad color allows to distinguish between the different stages within the LN, most notoriously the black color acquired in the latest stage that immediately precedes metamorphosis (Fig. 3.3.1 and 3.3.2A-C). The length and color of wing pads has been used in a number of mayfly species to differentiate successive nymphal instars, especially in latest ones, in which the black color generally indicates the immediacy of the subimaginal molt (Alba-

Tercedor, 1983; Bretshko, 1965). Moreover, we also assessed that the maturation of wings just occurs during the last two days of LN (Fig. 3.3.2E).

The mouthparts of *C. dipterum* nymphs are adapted to chew, but practically disappear in the subimago and the adult, which do not feed (Brown, 1963). Our study revealed that the nymphal structures do not form in the transition LN to subimago (Fig. 3.3.3A-B). The subimago and the adult of most mayfly species keep the two caudal cerci and the terminal filament shown by the nymphs, which apparently contributes to stabilize aerodynamically the flight (Wootton and Kukalová-Peck, 2000). However, the subimago and the adult of *C. dipterum* do not possess the central filament, and our observations reveal that it does not form during the molting to subimago (Fig. 3.3.3F). In contrast, metamorphosis involves the formation of new external morphological structures. The most obvious is the pair of membranous wings that develop in the mesothorax in the transition from LN to subimago. Our observations suggest that the subimago wings and adult wings are formed successively, those of the subimago in late LN and those of the adult in the subimaginal stage. Moreover, last tarsomere is conspicuously remodeled. In the nymphs it is claw-shaped, which help the insect cling to its place on the stream bottom, whereas in the subimago and the adult it is hook-shaped, which is more useful for attaching to terrestrial substrates and, in the male, for grasp the female in flight for mating (Fig. 3.3.4A-C) (Lancaster and Downes, 2013). As in the case of the wings, our observations suggest that the hook-shaped tarsomere of the subimago and that of the adult are formed successively. Possibly, the process is different in more derived species with a short longevity pattern, whose subimaginal stage can last only a

few minutes (Edmunds and McCafferty, 1988). In the short longevity species *Palingenia fuliginosa*, for example, both subimaginal and adult structures develop nearly simultaneously, and can be seen overlapping in late last instar nymph (Soldán, 1981). Quantitatively, the general growth between the subimago and the adult, exemplified especially by the cerci and legs, is dramatic. The female's forelegs of *C. dipterum*, for example, are twice as long as those of the subimago (Fig. 3.3.4D). This dramatic leg growth has been observed in other species. For example the foreleg tarsi of the adult male of *Ephoron leukon* are 5-7 times their larval length (Ide, 1937), and those of *Palingenia fuliginosa* are about 8.5 times their larval length (Edmunds and McCafferty, 1988).

### **The patterns of gene expression**

Regarding the general expression data (Fig. 3.3.5), the relatively parallel patterns of *jhamt* and *Kr-h1*, at least in the nymphal stages, is not surprising, as *Kr-h1* expression reflects the JH titers, for example in the cockroach *Blattella germanica* (Lozano and Belles, 2011), and JHAMT is the last and key enzyme of the JH biosynthetic pathway, its expression being correlated with JH production (Dominguez and Maestro, 2018). The high expression of *jhamt* in the SI possibly preludes the high expression achieved by *Kr-h1* in the adult. The inverse correlation of *myo* and *jhamt* patterns would be compatible with an inhibitory effect of Myo on *jhamt* expression and with JH synthesis, as occurs in the cricket *Gryllus bimaculatus* (Ishimaru et al., 2016) and the cockroach *B. germanica* (Kamsoi and Belles, 2019). The expression of *Met*, the gene that codes for the JH receptor (Jindra et al., 2015), appears uncorrelated with other pattern of JH factors, but this lack of correlation is also observed in neopteran species, like *B. germanica*,



where high levels of *Met* expression in the last nymphal instar (Lozano and Belles, 2014) correspond to very low levels of *Kr-h1* mRNA (Lozano and Belles, 2011). With respect to the general expression of the 20E factors, the most suggestive is the pattern of *Br-C*, with high values until the LN, which could be related with the development of wings, as well as the fluctuating patterns of the signal transducers *HR3* and *E75*, which possibly punctuate the successive pulses of 20E production.

The more detailed expression patterns, including daily values in LN (Fig. 3.3.6), in particular that of *HR3*, more clearly suggest that there is a 20E pulse in LND3, and another one in the subimago, which correspond to the respective molt processes to subimago and to adult. This rules out, in this species, that a single 20E pulse could trigger at the same time the formation of the subimago and adult tissues. The daily patterns (Fig. 3.3.6) also indicate that the expression of *Kr-h1* dramatically decreases from the beginning of LN until LND3, which suggest that a *Kr-h1*-free period is crucial for metamorphosis, as it would allow the increase of *E93* expression, according to the MEKRE93 pathway (Belles and Santos, 2014). Regarding *Br-C*, its expression steadily declines in LN, almost completely vanishing in LND4, just when wings mature. In contrast, *E93* continuously expresses during the last nymphal instar particularly in LND4 (Fig.6). In hemimetabolan neopteran insects, *Br-C* plays a crucial role in promoting wing primordia growth and development within the wing pads (Huang et al., 2013; Konopova et al., 2011; Erezyilmaz, 2006), and it is likely that it plays the same role in *C. dipterum*.

### **The methoprene experiments**

The treatment with methoprene in LND0 prevented the formation of the subimago. The methoprene-treated insects could not ecdyse, but they were able to apolyse, forming a new set of mouthparts and the central filament, which are not formed in the subimago. Moreover, they developed a claw-shaped apical tarsomere, which is characteristic of nymphs, instead of the hook-shaped structure of the subimago (Fig. 3.3.7A-C). Despite the treatment, the methoprene-treated insects were still able to develop the wings, although they were extremely fragile, thus we were unable to extend them for detailed examination (Fig. 3.3.7D). It is worth noting, however, that the formation of membranous wings, although malformed and wrinkled, is not uncommon in supernumerary nymphs obtained after treatment with JH or JH mimics (Slama et al., 1974).

At molecular scale, the methoprene treatment in LND0 triggered a significant increase of *Kr-h1* mRNA levels, as measured in LND2 (Fig. 3.3.8). This is not surprising since JH induces *Kr-h1* expression, as demonstrated in polyneopteran and paraneopteran insects (Konopova et al., 2011; Lozano and Belles, 2011). Intriguingly, the increase of *Kr-h1* expression was not accompanied by a parallel decrease of *E93* expression, as the MEKRE93 pathway would predict. This is especially surprising because methoprene-treated insects, despite having *E93* expression levels similar to those of the controls (Fig. 3.3.8), did not metamorphose, although *E93* determines insect metamorphosis, as demonstrated in different neopteran insects (Belles, 2020; Ureña et al., 2014). Moreover, even in the paleopteran *Ischnura senegalensis* (Odonata), electroporation-mediated RNA interference experiments (Okude et al., 2017) have revealed that *Kr-h1* represses

*E93* expression, and that *E93* is essential for adult morphogenesis (Okude et al., 2019).

A possibility to explain the high levels of *Kr-h1* expression associated with normal levels of *E93* expression in methoprene-treated insects (Fig. 3.3.8) is that both genes are expressed in different tissues and their gene products do not interact. Thus, the expression of *E93* could concentrate in epidermal tissues and wing pads, playing its typical morphogenetic functions (Ureña et al., 2014), whereas the expression of *Kr-h1* might concentrate in reproductive organs, in males and females. It is worth noting that *C. dipterum* must start sexual maturation towards the end of the last nymphal instar, as it is an ovoviviparous species (Gaino and Reborá, 2005). Also, it has been reported that JH has gonadotropic functions in early branching insects, not only in Polyneoptera and Paraneoptera (Raikhel et al., 2005), but also in *Zygentoma* (Hagedorn, 1989). Since the RNA extracts were obtained from the whole body, the results of *Kr-h1* might reflect the expression in the reproductive system, whereas those of *E93* could come from the epidermis. The absence of inhibition of *E93* expression in the epidermis could be due to the fact that *Kr-h1* expression was not upregulated, due to the absence of JH signaling in this tissue, perhaps because *Met*, which codes the JH receptor, might not be expressed in the epidermis from late LN. Indeed, the absence of JH signaling in the epidermis in late nymphs would be an effective solution for an ovoviviparous and short lived species that requires JH gonadotropic functions before metamorphosis, but at the same time it needs to suppress JH signaling in metamorphic tissues.

Another intriguing issue is that methoprene treatment in LND0 *C. dipterum* did not stimulate *Br-C* expression (Fig. 3.3.8), while this

stimulatory effect is typical of hemimetabolan insects (Huang et al., 2013). In this case, the most reasonable hypothesis is that *E93*, in the epidermal tissue including the wings, is repressing the *BR-C* expression at metamorphosis, as occurs in other hemimetabolan insects (Belles, 2019; Ureña et al., 2014).

### **The homology and the functional sense of the subimago**

The intersection of *Kr-h1* and *E93* expression patterns in LN (Fig. 3.3.6) indicates that metamorphosis takes place in the transition from the LN to subimago. In neopterans, this intersection generally occurs in the last nymphal instar (hemimetabolans) or in the pupa (holometabolans), and marks the activation of adult morphogenesis (data reviewed by Belles, 2020). Therefore, the subimago should be considered as a kind of first instar of the adult stage, being the “adult” a second and final instar. Si et al. (2017) reached this same conclusion by comparing the transcriptomes of young larva, mature larva, subimago, and adult of the mayfly *C. viridulum*.

The functional sense of the subimago has been extensively discussed (see Edmunds and McCafferty, 1988). Paleontological data indicates that immature stages of fossil Ephemeroptera possess freely articulated developing wings, and that wing development proceeded gradually through successive molts (Kukalová-Peck, 1983, 1978). This suggests that the subimago of extant mayflies is a kind of relic of one or more subadult winged instars of ancestral mayflies. This is the opinion held by Snodgrass (1954) and Schafer (1975), who do not consider that the subimago has any other selective sense. Ide (1937) considered that the hydrofuge properties of the hairy surface of the body, legs, and wings of the subimago would allow the insect to

overcome the hazards of a metamorphic transition from an aquatic nymph to a winged terrestrial form at the water-air interface. In this line, Edmunds and McCafferty (1988) speculated that the hydrofuge structures may have been selected to prevent the membrane of the wing from sticking to itself in the folded, furled, or convoluted position, and may thus facilitate unfolding at emergence. It is also plausible that the hairy surface of the subimago, particularly on wings, have a function during the delicate ecdysis and exuvia removal in the wings, within the molting process of subimago to adult (Belles, 2020). Finally, Maiorana (1979) proposed that the function of the subimago is to allow necessary growth from the nymphal to the adult morphology, which could not otherwise be accomplished in a single molt. In support of this notion are the data indicating that full expansion of body structures, notably legs and caudal cerci, is completed in the transition from subimago to adult (Edmunds and McCafferty, 1988).

Comparison of the information from the fossils with that obtained from the study of the extant mayflies indicates that the present subimago stage would be a relic of one or more subadult winged instars of ancestral mayflies, as previously conjectured (Schaefer, 1975; Snodgrass, 1954). However, contrary to the opinion of these authors, we do believe that it has a selective sense. Our results, especially the dramatic growth of the appendages observed between the subimago and the adult, suggest that the main functional sense of the subimago would be to allow enough growing to reach the size for optimal flying and mating, as previously proposed by Maiorana (1979). Importantly, our results also suggest that the mayfly subimago would be a phase of the adult stage, rather than a stage homologous to the holometabolan pupa, as suggested by this last author (Maiorana, 1979). This leads to the

conclusion that the metamorphosis mode of mayflies should be considered simply as hemimetabolan, since juveniles are morphologically similar to adults, and do not undergo a pupal stage. Thus, other names proposed to designate ephemeropteran metamorphosis, such as paurometaboly (Berlese, 1913) or prometaboly (Weber, 1949), are unnecessary and should be discouraged.

## **MATERIALS AND METHODS**

### ***Cloeon dipterum* rearing in the laboratory**

The *C. dipterum* mayflies used in the experiments were obtained from a colony starting from gravid females by forced mating in the laboratory at Centro Andaluz de Biología del Desarrollo (Sevilla, Spain). The nymphs were reared in unchlorinated and oxygenated water at  $22 \pm 1^\circ\text{C}$ , 60% relative humidity, and under 12:12 h (light: dark) photoperiod, feeding them on filamentous algae (*Chara* sp.). A detailed description of the rearing methods is provided by Almudi et al. (2019).

### **RNA extraction and retrotranscription to cDNA**

Total RNA was extracted from whole bodies of *C. dipterum* nymphs, subimago and adult by using Gen Elute Mammalian Total RNA kit (Sigma-Aldrich) method according to the manufacturer's instructions. A sample of 400 ng from each RNA extraction was used for mRNA precursors. RNA quantity and quality were estimated by spectrophotometric absorption at 260 nm in a Nanodrop Spectrophotometer ND-1000® (NanoDrop Technologies). The RNA samples were then treated with DNase (Promega) and reverse

transcribed with first Strand cDNA Synthesis Kit (Roche) and random hexamer primers (Roche).

### **Determination of mRNA levels by quantitative real-time PCR**

Measurements with qRT-PCR were carried out in an iQ5 Real-Time PCR Detection System (Bio-Lab Laboratories), using SYBR<sup>®</sup>Green (iTaq<sup>™</sup> Universal SYBR<sup>®</sup> Green Supermix; Applied Biosystems). Reactions were carried out in triplicate, and a template-free control was included in all batches. Primers used to measure the transcripts of interest are detailed in Table S1. The efficiency of each set of primers was validated by constructing a standard curve through three serial dilutions. Levels of mRNA were quantified relative to CdActin-5c mRNA (Table S1). Results are given as copies of the examined mRNA per 1000 copies of CdActin-5c mRNA.

### **Treatments with methoprene**

To study the effect of juvenile hormone on metamorphosis, newly ecdysed last instar nymphs of *C. dipterum* were treated with methoprene (Sigma-Aldrich) at a dose of 5 µg. Nymphs were immobilized on ice, and a volume of 0.25 µl of an acetone solution of methoprene (20 µg/µl) was topically applied on the mesonotum with a 5µl Hamilton microsyringe. Controls received 0.25 µl of acetone.

### **Morphological studies and imaging**

The nymphs, subimago and adults were examined and photographed using a stereomicroscope Zeiss DiscoveryV8 and a bright field microscope Carl Zeiss-AXIO IMAGER.Z1.

## ACKNOWLEDGEMENTS

Work supported by Spanish Ministries of Economy and Competitiveness, and Science, Innovation and Universities (Grants CGL2012–36251 and CGL2015–64727-P, to X.B., and BFU2015-66040-P, PGC2018-093704-B-I00 and MDM-2016-0687, to F.C.), by Catalan Government (Grant 2017 SGR 1030 to X.B.), by European Union’s Horizon 2020 research and innovation program (Marie Skłodowska-Curie Grant Agreement 657732 to I.A.), and by the European Fund for Economic and Regional Development, FEDER funds (to X.B. and F.C.). O.K. received a Royal Thai Government Scholarship to do a PhD thesis in X.B. laboratory.

## REFERENCES

- Alba-Tercedor, J., 1983. Ecología, distribución y ciclos de desarrollo de efemerópteros de Sierra Nevada. I: *Baetis maurus* Kimmins, 1938 (Ephemeroptera, Baetidae)., in: Actas Del Primer Congreso Español de Limnología. pp. 179–187.
- Almudi, I., Martín-Blanco, C.A., García-Fernandez, I.M., López-Catalina, A., Davie, K., Aerts, S., Casares, F., 2019. Establishment of the mayfly *Cloeon dipterum* as a new model system to investigate insect evolution. *Evodevo* 10, 6.  
<https://doi.org/10.1186/s13227-019-0120-y>
- Almudi, I., Vizueta, J., de Mendoza, A., Wyatt, C., Marletaz, F., Firbas, P., Feuda, R., Masiero, G., Medina, P., Alcaina, A., Cruz, F., Gómez-Garrido, J., Gut, M., Alioto, T.S., Vargas-Chavez, C., Davie, K., Misof, B., González, J., Aerts, S., Lister, R., Paps, J., Rozas, J., Sánchez-Gracia, A., Irimia, M., Maeso, I., Casares, F., 2020. Genomic adaptations to aquatic and aerial life in mayflies



- and the origin of wings in insects. *Nat. Commun.* 11: 2631.
- Belles, X., 2020. Insect metamorphosis. From natural history to regulation of development and evolution. Academic Press, Cambridge, MA.
- Belles, X., 2019. Krüppel homolog 1 and E93: The doorkeeper and the key to insect metamorphosis. *Arch. Insect Biochem. Physiol.* 103, e21609. <https://doi.org/10.1002/arch.21609>
- Belles, X., Santos, C.G., 2014. The MEKRE93 (Methoprene tolerant-Krüppel homolog 1-E93) pathway in the regulation of insect metamorphosis, and the homology of the pupal stage. *Insect Biochem. Mol. Biol.* 52, 60–68. <https://doi.org/10.1016/j.ibmb.2014.06.009>
- Berlese, A., 1913. Intorno alle metamorfosi degli insetti. *Redia* 9, 121–136.
- Berner, L., Pescador, M.L., 1988. The Mayflies of Florida. University Press of Florida, Gainesville.
- Bretshko, G., 1965. Zur larvenentwicklung von *Cloeon dipterum*, *Cloeon simile*, *Centroptilum luzeolum* und *Betis rhodani*. *Z. Wiss. Zool.* 17–36.
- Brown, D.S., 1963. The morphology and function of the mouthparts of *Cloeon dipterum* L. and *Baetis rhodani* (Pictet) (Insecta, Ephemeroptera). *Proc. Zool. Soc. Lond.* 136, 147–176.
- Dominguez, C.V., Maestro, J.L., 2018. Expression of juvenile hormone acid O-methyltransferase and juvenile hormone synthesis in *Blattella germanica*. *Insect Sci.* 25, 787–796.
- Edmunds, G.F., McCafferty, W.P., 1988. The mayfly subimago. *Annu. Rev. Entomol.* 33, 509–527. <https://doi.org/10.1146/annurev.en.33.010188.002453>

- Gaino, E., Reborá, M., 2005. Egg envelopes of *Baetis rhodani* and *Cloeon dipterum* (Ephemeroptera, Baetidae): a comparative analysis between an oviparous and an ovoviviparous species. *Acta Zool.* 86, 63–69.
- Hagedorn, H., 1989. Physiological roles of hemolymph ecdysteroids in the adult insect, in: Koolman, J. (Ed.), *Ecdysone. From Chemistry to Mode of Action*. Georg Thieme Verlag, Stuttgart-New York, pp. 279–289.
- Huang, J.-H., Lozano, J., Belles, X., 2013. Broad-complex functions in postembryonic development of the cockroach *Blattella germanica* shed new light on the evolution of insect metamorphosis. *Biochim. Biophys. Acta - Gen. Subj.* 1830, 2178–2187.  
<https://doi.org/10.1016/j.bbagen.2012.09.025>
- Ide, F.P., 1937. The subimago of *Ephoron leukon* Will., and a discussion of the imago instar (Ephem.). *Can. Entomol.* 69, 25–29.  
<https://doi.org/10.4039/Ent6925-2>
- Ishimaru, Y., Tomonari, S., Matsuoka, Y., Watanabe, T., Miyawaki, K., Bando, T., Tomioka, K., Ohuchi, H., Noji, S., Mito, T., 2016. TGF- $\beta$  signaling in insects regulates metamorphosis via juvenile hormone biosynthesis. *Proc. Natl. Acad. Sci. U. S. A.* 113, 5634–5639. <https://doi.org/10.1073/pnas.1600612113>
- Jindra, M., Uhlirova, M., Charles, J.-P., Smykal, V., Hill, R.J., 2015. Genetic evidence for function of the bHLH-PAS protein Gce/Met as a juvenile hormone receptor. *PLOS Genet.* 11, e1005394.  
<https://doi.org/10.1371/journal.pgen.1005394>
- Kamsoi, O., Belles, X., 2019. Myoglianin triggers the premetamorphosis stage in hemimetabolan insects. *FASEB J.* 33, 3659–3669. <https://doi.org/10.1096/fj.201801511R>

- Konopová, B., Smykal, V., Jindra, M., 2011. Common and distinct roles of juvenile hormone signaling genes in metamorphosis of holometabolous and hemimetabolous insects. *PLoS One* 6, e28728. <https://doi.org/10.1371/journal.pone.0028728>
- Kukalová-Peck, J., 1983. Origin of the insect wing and wing articulation from the arthropodan leg. *Can. J. Zool.* 61, 1618–1669. <https://doi.org/10.1139/z83-217>
- Kukalová-Peck, J., 1978. Origin and evolution of insect wings and their relation to metamorphosis, as documented by the fossil record. *J. Morphol.* 156, 53–125. <https://doi.org/10.1002/jmor.1051560104>
- Lancaster, J., Downes, B.J., 2013. *Aquatic Entomology*. Oxford University Press, Oxford.
- Lozano, J., Belles, X., 2014. Role of methoprene-tolerant (Met) in adult morphogenesis and in adult ecdysis of *Blattella germanica*. *PLoS One* 9, e103614. <https://doi.org/10.1371/journal.pone.0103614>
- Lozano, J., Belles, X., 2011. Conserved repressive function of Krüppel homolog 1 on insect metamorphosis in hemimetabolous and holometabolous species. *Sci. Rep.* 1, 163. <https://doi.org/10.1038/srep00163>
- Maiorana, V.C., 1979. Why do adult insects not moult? *Biol. J. Linn. Soc.* 11, 253–258.
- Mora, C., Tittensor, D.P., Adl, S., Simpson, A.G.B., Worm, B., 2011. How many species are there on earth and in the ocean? *PLoS Biol.* 9, e1001127.
- Okude, G., Futahashi, R., Fukatsu, T., 2019. Molecular mechanisms of metamorphosis in dragonflies. *Commun. 4th Int. Insect Horm. Work. (Kolymbari, Crete, Greece)* 43.
- Okude, G., Futahashi, R., Kawahara-Miki, R., Yoshitake, K., Yajima,

- S., Fukatsu, T., 2017. Electroporation-mediated RNA interference reveals a role of the multicopper oxidase 2 gene in dragonfly cuticular pigmentation. *Appl. Entomol. Zool.* 52, 379–387.  
<https://doi.org/10.1007/s13355-017-0489-9>
- Raikhel, A.S., Brown, M.R., Belles, X., 2005. Hormonal Control of Reproductive Processes, in: Gilbert, L I, Iatrou, K, G.S.S. (Ed.), *Comprehensive Molecular Insect Science*. Elsevier, San Diego, California, pp. 432–491.
- Schaefer, C.W., 1975. The mayfly subimago: a possible explanation. *Ann. Entomol. Soc. Am.* 68, 183.
- Si, Q., Luo, J.-Y., Hu, Z., Zhang, W., Zhou, C.-F., 2017. De novo transcriptome of the mayfly *Cloeon viridulum* and transcriptional signatures of Prometabola. *PLoS One* 12, e0179083.  
<https://doi.org/10.1371/journal.pone.0179083>
- Slama, K., Romanuk, M., Sorm, F., 1974. *Insect Hormones and Bioanalogues*. Springer-Verlag, New York and Wien.
- Snodgrass, R.E., 1954. Insect metamorphosis. *Smithson. Misc. Collect.* 122, 1–124.
- Soldán, T., 1981. Secondary sexual characters in mayfly larvae and their evolutionary significance (Ephemeroptera). *Acta ent. bohemoslov.* 78, 140–142.
- Ureña, E., Manjón, C., Franch-Marro, X., Martín, D., 2014. Transcription factor E93 specifies adult metamorphosis in hemimetabolous and holometabolous insects. *Proc. Natl. Acad. Sci. U. S. A.* 111, 7024–7029.  
<https://doi.org/10.1073/pnas.1401478111>
- Weber, H., 1949. *Grundriss der Insektenkunde*. Gustav Fischer, Jena.
- Wingfield, C.A., 1937. Function of the gills of the mayfly nymph,

*Cloeon dipterum*. Nature 140, 27.

Wootton, R.J., Kukalová-Peck, J., 2000. Flight adaptations in Palaeozoic Palaeoptera (Insecta). Biol. Rev. 75, 129–167.

**Table S1.** Primers used to measure expression levels of selected *Cloeon dipterum* by qRT-PVR

Gene	Forward primer	Reverse primer
<i>Actin 5C (Act5C)</i>	AGAAGTTGCTGCCCTCGTT	GACCATCACACCCTGATGC
<i>Broad complex (Br-C)</i>	AGGACTTCGTGGATGTGACC	TGCACATGGGGTACTCTTGA
<i>Ecdysone-induced protein 75B (Eip75 or E75)</i>	CTTCTTCAGGCCTAGCATCC	CAGTACTGGCAACGGTTCCCT
<i>Ecdysone-induced protein 93F (Eip93F, E93 or mblk-1)</i>	CTACGATCGTGACAGCCTGA	CGCTCCTTGACTTTGTACTIONG
<i>Ecdysone receptor (EcR)</i>	GCTGCAAAGGTTTCTTCAGG	CATGTGCGATCTCGCAGTTGT
<i>ftz transcription factor 1 (ftz-f1)</i>	CAGCTGCCATATCGACAAGA	ACATTGGCCCGAATTTATTG
<i>Hormone receptor 3 (HR3)</i>	GCAACAAGAAGTGCCTCGT	GCTGCTTTTTGGACATTCGT
<i>juvenile hormone acid methyl transferase (jhamt)</i>	TACGCGATGTCCAAGTACCA	CCAATGGAGGCAGTAGAAGG
<i>Krüppel homolog 1 (Kr-h1)</i>	TGCGAGTACTGCCACAAGTC	CATTTGTACGGTCGTCCTT
<i>Methoprene tolerant (Met)</i>	ACACAACCTTGACGGTGACA	GAAGGCAGAGGACCCACATA
<i>myoglianin (myo)</i>	TACCCGCTGGTAGTGGACTT	GGAACACATTCTCCAGAGC

Note: Genes manually annotated in *Cloeon dipterum* genome project accessions PRJEB34721. The sequence reads and the genome assembly have been deposited in the European Nucleotide Archive (ENA)

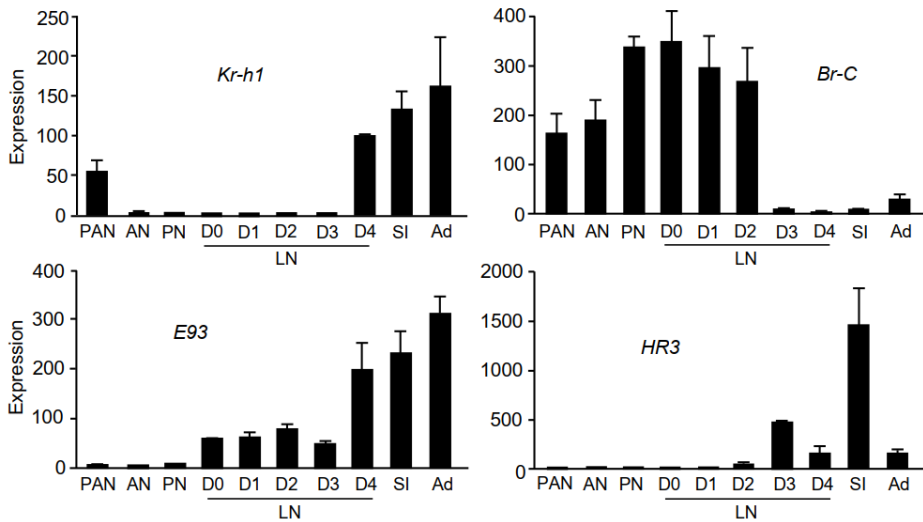


**Figure S1.** Expression of genes relevant for metamorphosis in males of *Cloeon dipterum*. The genes *Krüppel homolog 1 (Kr-h1)*, *E93*, *Broad-complex (Br-C)* and *Hormone receptor 3 (HR3)*, were examined. The expression was measured in males of penultimate nymphal instar (PN), all days of the last nymphal instar (LN, from D0 to D4), the subimago (SI) and the adult (Ad). The results are indicated as copies of the examined mRNA per 1000 copies of CdActin-5c mRNA, and are expressed as the mean  $\pm$  SEM (n=3)

## 4. GENERAL DISCUSSION

The first part of this thesis aimed at further studying the factors regulating metamorphosis in hemimetabolan insects during postembryonic development, using the German cockroach, *Blattella germanica*, as a model. At present, the MEKRE93 pathway is considered the main regulatory axis of insect metamorphosis in both hemimetabolans and holometabolans (Belles and Santos, 2014; Belles, 2019a, 2020). However, the MEKRE93 pathway explains the regulation of metamorphosis that starts with the reduction of juvenile hormone (JH) that occurs in the stage previous to metamorphosis, in the sixth (last) nymphal instar in the case of *B. germanica* (Treiblmayr et al., 2006). Therefore, the next pertinent question is what causes this reduction in the JH in the last nymphal instar? The chapter 3.1. addresses this question for the case of *B. germanica*, and reveals that myoglianin (myo) plays a relevant role in this sense. The study of the role of myo in metamorphosis yielded some data that suggested that the transcription factor E93 could be involved in the degradation of the prothoracic glands (PG) that occurs after molting to the adult stage. This possibility was tested and results are reported in chapter 3.2., which summarizes our observations showing the role of E93 in the degradation of PG, also using *B. germanica* as a model. Finally, we wondered whether the MEKRE93 pathway (which has been validated in polyneopteran, paraneopteran and endopterygote insects) would operate in the early-branching paleopterans. In chapter 3.3, we try to resolve this issue working on the mayfly *Cloeon dipterum*. Using this model has been possible thanks to the continuous laboratory rearing system recently developed by Almudi et al. (2019).

#### 4.1. Myoglianin and the reduction of JH titers in the last nymphal instar

What is the mechanism that regulates the fall of JH at the beginning of the last nymphal instar in *B. germanica*? To answer that question, the chosen candidate gene was *myo*. On the one hand, because previous transcriptomic studies from our laboratory had shown that *myo* expression has a prominent peak in the penultimate nymphal instar (Ylla et al., 2018). In addition, previous research of a Japanese laboratory on the cricket *Gryllus bimaculatus* had revealed that *myo* has an inhibitory effect on JH, via suppressing the expression of the gene *juvenile hormone acid methyl transferase (jhamt)* (Ishimaru et al., 2016), which codes for the enzyme that catalyzes the last step of JH biosynthesis (Belles et al., 2005).

Our results have demonstrated that a high expression of *myo* in the corpora allata in the penultimate nymphal instar is involved in regulating JH production. As occurs in *G. bimaculatus* (Ishimaru et al., 2016), *Myo* suppresses the expression of *jhamt* in the penultimate nymphal instar of *B. germanica*, thus JH production drops at the beginning of the last nymphal instar, which is a prerequisite for metamorphosis. *Myo* might be considered, thus, a first promoter of metamorphosis, as it determines the fall of JH, at least in hemimetabolan insects. But, is this applicable to holometabolan species? *Myo* was discovered in *D. melanogaster*, and its mRNA was detected in adult females, in glia cells in mid-embryogenesis, in developing muscles and cardioblasts (Lo and Frasch, 1999). In *D. melanogaster*, *Myo* plays a crucial role in the remodeling the mushroom bodies during the larva-pupa transition, which is mediated



by the upregulation of the *EcR-B1* gene in neural tissues (Awasaki et al., 2011). No other functions of Myo have been reported in holometabolan insects. Moreover, the expression of *myo* in *D. melanogaster* does not peak in the last nymphal instar or the pupa (Ylla et al., 2018). These data suggest that Myo does not regulate the pre-metamorphic fall of JH in holometabolans. This is not surprising, as in holometabolan species JH must fall twice, first to promote the formation of the pupa, and subsequently to promote the transition from pupa to adult (Belles, 2020). In this context, a mechanism based on a radical inhibition of *jhamt* might be not suitable to modulate a reduction, followed by an increase, and then a further reduction of JH. Therefore, the regulation of the pre-metamorphic suppression of JH in holometabolan species remains to be studied.

Our study has also shown that *myo* dramatically expresses in PG during the transition from the penultimate to the last nymphal instar, which suggests that Myo plays a significant role also in this gland. Indeed, our RNAi experiments showed that the high expression of *myo* in the above transition represses cell proliferation and promotes the expression of ecdysteroidogenic genes in the PG. This is crucial to produce the last and large pulse of ecdysone that triggers metamorphosis in *B. germanica*. In *D. melanogaster*, the activin branch of TGF- $\beta$  pathway also promotes the expression of ecdysteroidogenic genes and results in a developmental arrest prior to metamorphosis (Gibbens et al., 2011). Thus, we can conclude that the stimulating action of Myo upon ecdysteroidogenesis would be conserved in hemimetabolan and holometabolan species, whereas the JH inhibitory action would be ancestral and characteristic of hemimetabolans, but would have been lost in the evolutionary transition to holometaboly. A

side result of RNAi studies suggested that E93 might be involved in the PG degradation that occurs after the adult molt. This side result prompted the works that are summarized in the next section.

The results summarized in this section of the thesis have been published in the FASEB Journal (33: 3659-3669, 2019).

#### 4.2. E93 and the destruction of the PG after the imaginal molt in *Blattella germanica*

Previous studies in *B. germanica* revealed that the histolysis of PG is regulated by 20E signaling via the upregulation of *ftz-fl* mRNA levels in the last day of nymphal life, and the cell death action of FTZ-F1 (Mané-Padrós et al., 2010). However, our studies revealed that the factor that finally determines PG disintegration is E93. The experiments that we report demonstrate that E93-depleted nymphs molt to adults that preserve a functional PG. Thus, the resulting adults are able to molt again. We also observed that FTZ-F1 depletion towards the end of the last nymphal instar downregulates the expression of *E93*, which led to the conclusion that the death of PG induced by FTZ-F1 is mediated by E93. The function of E93 as a cell death effector is not surprising, as in other insects it has been described as a key player in the histolysis of the salivary glands in *D. melanogaster* during metamorphosis (Woodard et al., 1994; Baehrecke and Thummel, 1995; Lee et al., 2000). The action of E93 in promoting cell death has also been reported in the midgut (Lee and Baehrecke, 2001; Lee et al., 2002) and fat body (Liu et al., 2014; Liu et al., 2015) of *D. melanogaster* and the lepidopteran *Bombyx mori*.

The function of E93 as a cell death effector is certainly not surprising, but the fact that E93-depleted adults are able to molt again

has allowed us to study the conditions of the molt in these exceptional circumstances. It seems that molting in E93-depleted adults is not due solely to the high levels of ecdysteroids produced by the active PG, since the ecdysteroid treatments that we carried out in control adults did not trigger any molt, but also because the ecdysone signaling properly operates in their epidermal cells (which would not happen in control adults). Taken together, our observations suggest that the epidermal cells of control adults are submitted to a kind of “adult commitment”, which did not occur in E93-depleted adults. We therefore presume that E93 and FTZ-F1 are be involved in regulating the “adult commitment” of epidermal cells. Whatever the case, the E93-depleted molting adults may be an interesting model in which to investigate the mechanisms determining the adult differentiation of insect epidermal cells, and perhaps find ways to revert this process. Incidentally, our results showing the prominent role of E93 in the PG degeneration afford an additional support to the conjecture that E93 was crucial in the evolutionary innovation of metamorphosis and the last molt (Belles, 2019b).

The publication of the results summarized in this section of the thesis is currently underway in the journal *Development*.

#### 4.3. The regulatory mechanism of metamorphosis in the mayfly *Cloeon dipterum*

In the study of the evolutionary innovation of hemimetaboly, there is a significant lack of information in paleopterans. Very little is known about the regulation of metamorphoses in mayflies and dragonflies, and this is a serious drawback to have the complete picture that would allow evolutionary reconstructions. This lack of information led us to

study the regulatory mechanisms of metamorphosis in the mayfly species *C. dipterum*, by integrating the morphological data and molecular analysis and functional experiments of hormone treatment. The expression patterns of *Kr-h1* and *E93* suggest that metamorphosis takes place in the transition from the last nymphal instar to the subimago. Thus, the subimago would be an instar or phase of the adult stage. This result settles the question of the homology of the subimago, which had been considered equivalent to the pupa of the holometabolan insects (Maiorana, 1979).

The inversely correlated expression pattern of *jhamt* and *Kr-h1* would suggest that Myo inhibits *jhamt* expression, as occurs in *G. bimaculatus* and *B. germanica* (see chapter 3.1). Therefore, the regulation of the fall of JH production by Myo via the repression of *jhamt* expression may be a mechanism conserved in paleopteran and polyneopteran insects. Regarding the MEKRE93 pathway, the dramatic decrease of *Kr-h1* expression from the first day of last nymphal instar until day 3, suggests that a Kr-h1 (JH)-free period is necessary for metamorphosis. Moreover, a peak of HR3 expression in the third day of the last nymphal instar and another one in the subimago suggest that two successive ecdysteroid pulses trigger the respective molts to the subimago and the adult. The fact that in some species, such as *Palingenia fuliginosa*, both subimaginal and adult structures develop nearly simultaneously, overlapping in late last instar nymph (Soldán, 1981) might suggest that a single ecdysone pulse is required for the transition from last nymphal instar to the adult. However, our results indicate that one pulse is required to form the subimago and another to form the adult.

The treatment with the JH mimic methoprene at the beginning of the last nymphal instar increased the expression of *Kr-h1* and prevented the metamorphosis into the subimago. This indicates that *Kr-h1* is a JH-dependent factor, and that it inhibits metamorphosis, as occurs in non-paleopteran insects. Unexpectedly, however, the methoprene treatment did not apparently modify the expression of *E93* and *Br-C*. This would suggest that *Kr-h1* do not repress the expression of these genes in *C. dipterum*, and that the MEKRE93 pathway does not apply in mayflies. However, the measurements were carried out in the whole body, and there is the possibility that *E93* and *Br-C* are expressed in different tissues and their gene products do not interact. We conjectured that *Kr-h1* might be expressed in reproductive organs, whereas the expression of *E93* could concentrate in epidermal tissues and wing pads, playing its typical morphogenetic functions (Belles, 2019a; Ureña et al., 2014). If so, then the results (obtained from the whole body) of *Kr-h1* might reflect the expression in the reproductive system, whereas those of *E93* could come from the epidermis. Regarding *Br-C* expression, and in line with the above conjecture, the most reasonable hypothesis is that *E93*, in the epidermal tissue including the wings, is repressing the *BR-C* expression at metamorphosis, as occurs in other hemimetabolan insects (Belles, 2019a; Ureña et al., 2014). Further experiments of methoprene treatment and measurement of *Kr-h1*, *E93* and *Br-C* expression separately in the epidermis and the reproductive organs are needed to test these hypotheses.

A preliminary manuscript summarizing the results of this section of the thesis has been prepared. However, we await the completion of the results related to the effects of methoprene treatments

in epidermal and reproductive tissues, before writing a definitive manuscript, appropriate for publication.

## 5. CONCLUSIONS

From the results obtained in the present thesis, the following nine conclusions can be inferred. The first six refer to the cockroach species *Blattella germanica* (Insecta, Polyneoptera, Blattodea), whereas the last three refer to the mayfly *Cloeon dipterum* (Insecta, Palaeoptera, Ephemeroptera).

1. In *B. germanica*, myoglianin (myo) depletion in the penultimate nymphal instar triggers the formation of supernumerary nymphs after the last nymphal instar. Molecular analysis indicates that the expression of *juvenile hormone acid methyl transferase (jhamt)* in the corpora allata became upregulated, which led to an increase of *Kr-h1* expression in the last nymphal instar, and a downregulation of *E93*. From these results we can conclude that myo triggers the pre-metamorphosis stage by reducing *jhamt* and, thus, juvenile hormone production. The molecular analysis confirms that the formation of supernumerary nymphs is explained by the MEKRE93 pathway.

2. Myo depletion in the penultimate nymphal instar of *B. germanica* caused cell hyperproliferation in the prothoracic gland (PG). Moreover, myo depletion downregulated the expression of *dacapo (dap)*, a gene coding for a cyclin-dependent kinase involved in regulating cell cycle, and that of *neverland*, *phantom* and *disembodied*, three steroidogenic genes. These results suggest that myo induces the arrest of cell proliferation in PG via the TGF- $\beta$  signaling, which appears to be a prerequisite to stimulate the expression of steroidogenic genes, and to produce the large ecdysteroid pulse needed to promote metamorphosis.

3. Myo depletion prevents the onset of PG degeneration. Our molecular studies have shown that the upregulation of *jhamt* triggered by this depletion increases *Kr-h1* expression and results in an upregulation of the expression of the *inhibitor of apoptosis 1 (iap1)* and a downregulation of the proapoptotic gene *ftz-f1* in the PG. Interestingly, the adult specifying gene *E93* is also downregulated. These findings confirm the important role of JH and *iap1* in preventing PG degeneration, as well as the proapoptotic role of FTZ-F1. Importantly, our findings also suggest that *E93* is involved in the degeneration of PG in *B. germanica*.

4. Depletion of *E93* late in the final nymphal instar triggers the formation of adults that preserve the PG and can molt again in the adulthood. These observations indicate that *E93* plays a major role in eliciting the death of the PG which normally occurs after the imaginal molt in hemimetabolans insects and during metamorphosis in holometabolans insects.

5. Previous studies in the laboratory showed that PG death is induced by FTZ-F1 in *B. germanica*. Our present results have shown that FTZ-F1 depletion downregulates the expression of *E93* specifically in the PG. The above observations strongly suggest that the “classic” proapoptotic role of FTZ-F1 is mediated by *E93*.

6. Treatments in the adult of *B. germanica* with physiological or pharmacological doses of 20-hydroxyecdysone (20E) do not induce a new molt in *B. germanica*. These findings suggest that adult epidermal



cells are subjected to a sort of “adult commitment”, and do not respond to 20E, apparently because they do not transduce the hormonal signal.

7. The expression pattern of *Kr-h1* and that of *E93* intersect in the last nymphal instar of *C. dipterum*, prior to the subimago. This suggests that metamorphosis in mayflies take place at the transition from the last nymphal instar to the subimago, and that it is regulated by the MEKRE93 pathway.

8. Administration of JH mimic methoprene in the last nymphal instar of *C. dipterum* inhibits metamorphosis. The treatment upregulated the expression of *Kr-h1* but did not apparently affect the expression of *E93* and *Br-C*. These results indicate that *Kr-h1* inhibits metamorphosis, as in Neopteran insects. However, the observations do not allow to conclude that *Kr-h1* represses *E93* expression according to the MEKRE93 pathway. Further work, studying the expression of *Kr-h1* and *E93* specifically in epidermal and reproductive tissues, should be needed to assess whether the MEKRE93 pathway operates in mayflies.

9. The expression patterns of *Kr-h1* and *E93* during the last nymphal instars and the subimago indicate that the last nymphal instar of *C. dipterum* is homologous to the last nymphal instar of non-paleopteran hemimetabolan insects (Polyneoptera and Paraneoptera). This leads to conclude that the subimago would be a first phase of the adult stage.



## 6. REFERENCES

- Almudi, I., Martín-Blanco, C.A., García-Fernandez, I.M., López-Catalina, A., Davie, K., Aerts, S., Casares, F., 2019. Establishment of the mayfly *Cloeon dipterum* as a new model system to investigate insect evolution. *Evodevo* 10, 6.  
<https://doi.org/10.1186/s13227-019-0120-y>
- Ashburner M., Chihara C., Meltzer P., A.G.R., 1974. Temporal Control of Puffing Activity in Polytene Chromosomes. *Cold Spring Harb Symp Quant Biol* 38, 655–662.  
<https://doi.org/10.1101/SQB.1974.038.01.070>
- Ashburner, M., 1974. Sequential gene activation by ecdysone in polytene chromosomes of *Drosophila melanogaster*. II. The effects of inhibitors of protein synthesis. *Dev. Biol.* 39, 141–157.  
[https://doi.org/10.1016/S0012-1606\(74\)80016-3](https://doi.org/10.1016/S0012-1606(74)80016-3)
- Ashok, M., Turner, C., Wilson, T.G., 1998. Insect juvenile hormone resistance gene homology with the bHLH-PAS family of transcriptional regulators. *Proc. Natl. Acad. Sci. U. S. A.* 95, 2761–2766. <https://doi.org/10.1073/pnas.95.6.2761>
- Baehrecke, E.H., Thummel, C.S., 1995. The *Drosophila* E93 Gene from the 93F Early Puff Displays Stage- and Tissue-Specific Regulation by 20-Hydroxyecdysone. *Dev. Biol.* 171, 85-97.  
<https://doi.org/10.1006/dbio.1995.1262>
- Belles, X., 2020. Insect metamorphosis. From natural history to regulation of development and evolution. Academic Press, Cambridge, MA.
- Belles, X., 2019a. Krüppel homolog 1 and E93: The doorkeeper and the key to insect metamorphosis. *Arch. Insect Biochem. Physiol.* 103, e21609. <https://doi.org/10.1002/arch.21609>

- Belles, X., 2011. Origin and Evolution of Insect Metamorphosis. eLS 1–11. <https://doi.org/10.1002/9780470015902.a0022854>
- Belles, X., 2010. Beyond *Drosophila*: RNAi In Vivo and Functional Genomics in Insects. *Annu. Rev. Entomol.* 55, 111–128. <https://doi.org/10.1146/annurev-ento-112408-085301>
- Belles, X., 2019b. The innovation of the final moult and the origin of insect metamorphosis. *Philos. Trans. R. Soc. B Biol. Sci.* 374, 20180415. <https://doi.org/10.1098/rstb.2018.0415>
- Belles, X., Martín, D., Piulachs, M.D., 2005. The mevalonate pathway and the synthesis of juvenile hormone in insects. *Annu. Rev. Entomol.* 50, 181–199.
- Belles, X., Santos, C.G., 2014. The MEKRE93 (Methoprene tolerant-Krüppel homolog 1-E93) pathway in the regulation of insect metamorphosis, and the homology of the pupal stage. *Insect Biochem. Mol. Biol.* 52, 60–68. <https://doi.org/10.1016/j.ibmb.2014.06.009>
- Bialecki, M., Alycia S., Fichtenberg, C., Segrave, W.A., T.C.S., 2002. Loss of the Ecdysteroid-Inducible E75A Orphan Nuclear Receptor Uncouples Molting from Metamorphosis in *Drosophila*. *Dev. Cell* 3, 209–220.
- Cruz, J, Martín, D., Pascual, N., Maestro, J., Piulachs, M., Bellés, X., 2003. Quantity does matter. Juvenile hormone and the onset of vitellogenesis in the German cockroach. *Insect Biochem. Mol. Biol.* 33, 1219–1225. <https://doi.org/10.1016/j.ibmb.2003.06.004>
- Cruz, J., Nieva, C., Mane, D., Marti, D., Belle, X., 2008. Nuclear Receptor BgFTZ-F1 Regulates Molting and the Timing of Ecdysteroid Production During Nymphal Development in the Hemimetabolous Insect *Blattella germanica*. *Dev. dynam.* 237,

- 3179–3191. <https://doi.org/10.1002/dvdy.21728>
- Gibbens, Y.Y., Warren, J.T., Gilbert, L.I., O'Connor, M.B., 2011. Neuroendocrine regulation of *Drosophila* metamorphosis requires TGF $\beta$ /Activin signaling. *Development* 138, 2693–2703. <https://doi.org/10.1242/dev.063412>
- Grimaldi, D., Engel, M.S., 2005. *Evolution of the Insects*, Cambridge University Press.
- Hill, R.J., Billas, I.M.L., Bonneton, F., Graham, L.D., Lawrence, M.C., 2013. Ecdysone receptors: from the Ashburner model to structural biology. *Annu. Rev. Entomol.* 58, 251–271. <https://doi.org/10.1146/annurev-ento-120811-153610>
- Huang, J.-H., Lozano, J., Belles, X., 2013. Broad-complex functions in postembryonic development of the cockroach *Blattella germanica* shed new light on the evolution of insect metamorphosis. *Biochim. Biophys. Acta - Gen. Subj.* 1830, 2178–2187. <https://doi.org/10.1016/j.bbagen.2012.09.025>
- Huang, J., Tian, L., Peng, C., Abdou, M., Wen, D., Wang, Y., Li, S., Wang, J., 2011. DPP-mediated TGF signaling regulates juvenile hormone biosynthesis by activating the expression of juvenile hormone acid methyltransferase. *Development* 138, 2283–2291. <https://doi.org/10.1242/dev.057687>
- Ishimaru, Y., Tomonari, S., Matsuoka, Y., Watanabe, T., Miyawaki, K., Bando, T., Tomioka, K., Ohuchi, H., Noji, S., Mito, T., 2016. TGF- $\beta$  signaling in insects regulates metamorphosis via juvenile hormone biosynthesis. *Proc. Natl. Acad. Sci. U. S. A.* 113, 5634–5639. <https://doi.org/10.1073/pnas.1600612113>
- Jindra, M., Palli, S.R., Riddiford, L.M., 2013. The Juvenile Hormone Signaling Pathway in Insect Development. *Annu. Rev. Entomol.*

- 58, 181–204. <https://doi.org/10.1146/annurev-ento-120811-153700>
- Karlson, P., 1996. On the hormonal control of insect metamorphosis. A historical review. *Int. J. Dev. Biol.* 40, 93–96.  
<https://doi.org/10.1387/ijdb.8735917>
- King-Jones, K., Charles, J.P., Lam, G., Thummel, C.S., 2005. The ecdysone-induced DHR4 orphan nuclear receptor coordinates growth and maturation in *Drosophila*. *Cell* 121, 773–784.  
<https://doi.org/10.1016/j.cell.2005.03.030>
- King-Jones, K., Thummel, C.S., 2005. Nuclear receptors - A perspective from *Drosophila*. *Nat. Rev. Genet.* 6, 311–323.  
<https://doi.org/10.1038/nrg1581>
- Lam, G.T., Jiang, C., Thummel, C.S., 1997. Coordination of larval and prepupal gene expression by the DHR3 orphan receptor during *Drosophila* metamorphosis. *Development* 124, 1757–1769.
- Lee, C.-Y.Y., Simon, C.R., Woodard, C.T., Baehrecke, E.H., 2002. Genetic mechanism for the stage- and tissue-specific regulation of steroid triggered programmed cell death in *Drosophila*. *Dev. Biol.* 252, 138–148. <https://doi.org/10.1006/dbio.2002.0838>
- Lee, C.Y., Baehrecke, E.H., 2001. Steroid regulation of autophagic programmed cell death during development. *Development* 128, 1443–55.
- Lee, C.Y., Cooksey, B.A.K., Baehrecke, E.H., 2002. Steroid regulation of midgut cell death during *Drosophila* development. *Dev. Biol.* 250, 101–111. <https://doi.org/10.1006/dbio.2002.0784>
- Lee, C.Y., Wendel, D.P., Reid, P., Lam, G., Thummel, C.S., Baehrecke, E.H., 2000. E93 directs steroid-triggered programmed cell death in *Drosophila*. *Mol. Cell.* 6, 433–443.

- [https://doi.org/10.1016/S1097-2765\(00\)00042-3](https://doi.org/10.1016/S1097-2765(00)00042-3)
- Liu, H., Wang, J., Li, S., 2014. E93 predominantly transduces 20-hydroxyecdysone signaling to induce autophagy and caspase activity in *Drosophila* fat body. *Insect Biochem. Mol. Biol.* 45, 30–39. <https://doi.org/10.1016/j.ibmb.2013.11.005>
- Liu, X., Dai, F., Guo, E., Li, K., Ma, L., Tian, L., Cao, Y., Zhang, G., Palli, S.R., Li, S., 2015. 20-Hydroxyecdysone (20E) primary response gene *E93* modulates 20E signaling to promote *Bombyx* larval-pupal metamorphosis. *J. Biol. Chem.* 290, 27370–27383. <https://doi.org/10.1074/jbc.M115.687293>
- Lo, P. C., and Frasch, M. 1999. Sequence and expression of myoglianin, a novel *Drosophila* gene of the TGF-beta superfamily. *Mech. Dev.* 86, 171–175
- Maiorana, V.C., 1979. Why do adult insects not moult? *Biol. J. Linn. Soc.* 11, 253–258. <https://doi.org/10.1111/j.1095-8312.1979.tb00037.x>
- Mané-Adrós, D., Borràs-Castells, F., Belles, X., Martín, D., 2012. Nuclear receptor HR4 plays an essential role in the ecdysteroid-triggered gene cascade in the development of the hemimetabolous insect *Blattella germanica*. *Mol. Cell. Endocrinol.* 348, 322–330. <https://doi.org/10.1016/j.mce.2011.09.025>
- Mané-Adrós, D., Cruz, J., Vilaplana, L., Nieva, C., Ureña, E., Bellés, X., Martín, D., 2010. The hormonal pathway controlling cell death during metamorphosis in a hemimetabolous insect. *Dev. Biol.* 346, 150–160. <https://doi.org/10.1016/j.ydbio.2010.07.012>
- Massagué, J., Blain, S.W., L., R.S., 2000. TGFb Signaling in Growth Control, Cancer, and Heritable Disorders. *Cell* 103, 295–309.
- Massagué, J., Chen, Y.G., 2000. Controlling TGF-b signaling. *Genes*

- Dev. 14, 627–644.
- Ou, Q., King-Jones, K., 2013. What Goes Up Must Come Down. Transcription Factors Have Their Say in Making Ecdysone Pulses, in: *Current Topics in Developmental Biology*. 103, 35-71. <https://doi.org/10.1016/B978-0-12-385979-2.00002-2>
- Piulachs, M.D., Pagone, V., Bellés, X., 2010. Key roles of the Broad-Complex gene in insect embryogenesis. *Insect Biochem. Mol. Biol.* 40, 468–475. <https://doi.org/10.1016/j.ibmb.2010.04.006>
- Segraves, W.A., Hogness, D.S., 1990. The E75 ecdysone-inducible gene responsible for the 75B early puff in *Drosophila* encodes two new members of the steroid receptor superfamily. *Genes & Dev.* 4, 204–219.
- Soldán, T., 1981. Secondary sexual characters in mayfly larvae and their evolutionary significance (Ephemeroptera). *Acta Entomol. Bohemoslov.* 78, 140–142.
- Sullivan, A., Thummel, C. S., 2003. Temporal Profiles of Nuclear Receptor Gene Expression Reveal Coordinate Transcriptional Responses during *Drosophila* Development. *Mol. Endocrinol.* 17, 2125–2137. <https://doi.org/10.1210/me.2002-0430>
- Talbot, W.S., Swyryd, E.A., Hogness, D.S., 1993. *Drosophila* tissues with different metamorphic responses to ecdysone express different ecdysone receptor isoforms. *Cell* 73, 1323–1337. [https://doi.org/10.1016/0092-8674\(93\)90359-X](https://doi.org/10.1016/0092-8674(93)90359-X)
- Treiblmayr, K., Pascual, N., Piulachs, M.-D., Keller, T., Belles, X., 2006. Juvenile Hormone Titer Versus Juvenile Hormone Synthesis in Female Nymphs and Adults of the German Cockroach, *Blattella germanica*. *J. Insect Sci.* 6, 1–7. <https://doi.org/10.1673/031.006.4301>



- Upadhyay, A., Moss-Taylor, L., Kim, M.J., Ghosh, A.C., O'Connor, M.B., 2017. TGF- $\beta$  Family Signaling in *Drosophila*. Cold Spring Harb. Perspect. Biol. 9, 1–34.  
<https://doi.org/10.1101/cshperspect.a031963>
- Ureña, E., Manjón, C., Franch-Marro, X., Martín, D., Urena, E., Manjon, C., Franch-Marro, X., Martin, D., 2014. Transcription factor E93 specifies adult metamorphosis in hemimetabolous and holometabolous insects. Proc. Natl. Acad. Sci. U. S. A. 111, 7024–7029. <https://doi.org/10.1073/pnas.1401478111>
- Uyehara, C.M., McKay, D.J., 2019. Direct and widespread role for the nuclear receptor EcR in mediating the response to ecdysone in *Drosophila*. Proc. Natl. Acad. Sci. U. S. A. 116, 9893–9902.  
<https://doi.org/10.1073/pnas.1900343116>
- White, K. P., Hurban, P., W.T., Hogness, D.S., 1997. Coordination of *Drosophila* Metamorphosis by Two Ecdysone-Induced Nuclear Receptors. Science. 276, 114–117.
- Woodard, C.T., Baehrecke, E.H., Thummel, C.S., 1994. A molecular mechanism for the stage specificity of the *Drosophila* prepupal genetic response to ecdysone. Cell. 709, 607-615.  
[https://doi.org/10.1016/0092-8674\(94\)90546-0](https://doi.org/10.1016/0092-8674(94)90546-0)
- Ylla, G., Piulachs, M.D., Belles, X., 2018. Comparative Transcriptomics in Two Extreme Neopterans Reveals General Trends in the Evolution of Modern Insects. iScience 4, 164–179.  
<https://doi.org/10.1016/j.isci.2018.05.017>